408

Line fault phenomena and their implications for 3-phase short- and long-line fault clearing

Working Group
A3.19

February 2010

Working Group
A3.19

Line fault phenomena and their implications for 3-phase short- and long-line fault clearing

Members

Anton Janssen (NL), Roy Alexander (US), Don Shoup (US), Denis Dufournet (FR), Heinz Schramm (DE), Mark Waldron (GB), Michel Landry (CA), Jan Weisker (DE), Nicola Gariboldi (CH), Haruhiko Kohyama (JP), Anders Johnson (US), Mauricio Aristizabal (US), John Brunke (US), Sergio A. Morais (BR), Jack Sawada (CA)

ISBN: 978-2-85873-095-7

Acknowledgement

CIGRÉ WG A3.19 would like to thank Prof. Dr. Ir. R.P.P. Smeets from KEMA High Power Laboratory for the information supplied with respect to the dielectric performance of modern circuit-breakers during SLF tests with current-zero measurements.

Contents

Abbreviations

ATP	alternative transient program
BPA	Bonneville Power Administration
BTF	Breaker Terminal Fault
CDV	IEC Committee Draft for Voting
CVT	capacitive voltage transformer
EMTP	electro-magnetic transient program
ITRV	Initial Transient Recovery Voltage (due to travelling waves on busbar)
IWD	CIGRÉ internal working document
JEC	Japanese Electro-technical Committee
L90	SLF with 90% of the rated short-circuit current
L75	SLF with 75% of the rated short-circuit current
L60	SLF with 60% of the rated short-circuit current
Lxx	SLF with xx% of the rated short-circuit current
LIWL	Lightning impulse withstand level
LLF	Long line fault
OP	Out-of-phase current switching test duty
RRRV	Rate of Rise of Recovery Voltage
SIWL	Switching impulse withstand level
SLF	Short line fault (test duty)
SPAR	Single pole auto-reclosing
T100	BTF test duty with 100% of the rated short-circuit current
T100s	T100 with symmetrical short-circuit current
T100a	T100 with asymmetrical short-circuit current (DC offset)
T60	BTF test duty with 60% of the rated short-circuit current
T30	BTF test duty with 30% of the rated short-circuit current
T10	BTF test duty with 10% of the rated short-circuit current
t_1	time value at first reference point of TRV envelope
t_d	time delay at initial part of TRV
TACSR	high temperature aluminium conductor steel reinforced
TRV	Transient Recovery Voltage
U_1	voltage value at first reference point of TRV envelope
U_c	peak voltage

Summary

The TRVs due to three-phase line faults are rather complicated because of the interaction between the phases at power frequency and the high frequency phenomena. To understand the phenomena and to be able to compare different TRVs, the experts involved in the discourse needed some time to communicate carefully all aspects. Special attention was necessary to get a common understanding of the conditions and parameters that are considered not to vary, versus those conditions and parameters that are considered as variables. For instance, by choosing the amplitude of the interrupted current to be equal for the first and the last clearing pole and fixing the short-circuit power at the busbar to correspond to the rated short-circuit current of the circuit-breaker (for three-phase and single-phase faults), a number of other variables are fixed (X_0/X_1 ratio at the busbar, distance to the three-phase and to the single-phase fault). Other choices lead to completely different results, such as comparing three-phase and single-phase faults at the same location but with slightly different currents.

New calculations and simulations confirm the statement in the Master Thesis of Anders Johnson [4], as well the statements published around 40 years ago [5][9][10], that the line-side TRV for the first pole to clear a three-phase SLF is roughly 50% higher than that of the last clearing pole. This statement is made under the assumption that the short-circuit current interrupted by the last pole is equal to that of the first pole which infers that the distance to the three-phase fault on the Overhead line is over 50% larger for the first clearing pole than for the last clearing pole. It is this distance that leads to a higher peak value of the triangular TRV waveshape, while the somewhat lower equivalent surge impedance for the first clearing pole in comparison with the last clearing pole leads to an approximately 10% lower steepness of the triangular waveshape.

The staged tests described in the Master Thesis of Anders Johnson, demonstrate that today's simulation tools for transient phenomena on Overhead lines give results that match quite well with the phenomena in service.

CIGRÉ publications of experts from Japan [1][18] have addressed the phenomenon of Long Line Faults that show high peak values of the line-side TRV due to the travelling waves coming from the interruption of faults at a distance up to 100 km and more. Despite the low steepness, as the interrupted currents are moderate or even low, it is the long travel time that gives the high peak value. This LLF TRV may exceed the peak value of the IEC test duties T30, T10 and OP, especially under conditions of high operating voltages. In Japan special test duties have been specified to cover such LLF conditions. In the meantime IEC has revised Standard 62271-100 [3] and raised the TRV peak value for T10.

The equivalent surge impedance as experienced by the circuit-breaker is a rather complicated parameter that depends on a wide variety of factors including frequency of the phenomena, earth resistance, tower geometry, the operational mode of a second circuit, the status of the other poles, the arrangements of earth wires, the height of the towers and the contraction of bundle conductors. Apart from very high towers with a single circuit (or where a second circuit is open and not earthed) the value of 450 Ω, as specified in the Standards, covers for all cases the equivalent surge impedance in the vicinity of the circuit-breaker of the last clearing pole For Overhead lines with bundled conductors, where bundle contraction is not expected within 100 ms, a value around 330 Ω would be sufficient. If there is another circuit

on the same tower which is either in operation or earthed, this will lead to an even lower equivalent surge impedance. The same is true when the other poles have not (yet) cleared, as, for instance, with SPAR.

The line-side peak factor or excursion factor, d, is twice the ratio between the equivalent high frequency inductance and the equivalent power frequency inductance of the Overhead line. This ratio is about 50% higher for the first clearing pole in comparison to the last clearing pole.

Considering these aspects, and by reducing the short-circuit power at the busbar-side of the circuit-breaker to 80% of the rated short-circuit current of the circuit-breaker, the TRV-waveshape of the first pole clearing a three-phase SLF is covered by the envelopes given in the Standards for the SLF test duties.

From the Standards and from test experience, it is clear that experts regard the RRRV as the most critical parameter for SLF, and therefore they focus on the last clearing pole. Indeed, SLF test duties have been introduced 40 years ago to verify the circuit-breaker behaviour under such steep TRV phenomena. Recent test results, evaluated from a large number of single-phase L90 tests, showed very few re-ignitions (less than 1%) in the latter half of the first line-side TRV excursion, thus confirming the low sensitivity of modern designs to the dielectric stress after the thermal phase of the interruption process.

There is evidence, but no conclusive proof, that a wide variety of circuit-breaker designs inherently can withstand a 50% higher peak value of the TRV at the line-side providing that they have passed successfully the full range of regular type tests.

Furthermore it is important to note that the decision, 40 years ago, to test for single-phase SLF only, has been made on the basis that the probability of occurrence of a three-phase line fault is far less than of a single-phase fault (80% to 90%). In reality, it is not simply the probability of a three-phase fault that must be considered. For critical conditions to occur there must be a combination of a three-phase fault at a critical location along the Overhead line, a high equivalent surge impedance and a short-circuit power at the substation corresponding to the rated short-circuit current of the circuit-breaker (i.e. assuming no contribution from the circuit with the three-phase fault). Considering the circuit-breaker itself, worst case operating conditions as per the type tests should also be considered i.e. lockout pressure of the SF_6 gas and the operating mechanism at minimum operating energy.

Such decisions not to test explicitly for low probability events are often made for the purposes of Standardisation however the acceptability of disregarding such events must be considered by utilities taking into account their national regulations.

In summary, the specified test duties within existing Standards cover all commonly occurring line faults (short and long line faults, as well as single and three-phase) but, by consideration of probability, do not explicitly cover certain specific conditions with a very low probability of occurrence. Utilities for whom this position is unacceptable should request special type tests for the particular conditions.

No recommendations are made within this document for modifications to Standards, since it is clearly integral to the role of Standards development bodies to properly reflect the concerns of users and developments in society's willingness to tolerate risk.

Introduction

1. Introduction

In the Standards for circuit-breakers the most critical line fault clearing condition are covered by the SLF test duties L90, L75 and, when necessary, L60. These test duties simulate interruption of single-phase faults at a short distance from the circuit-breaker when the short-circuit power at the busbar side is equal to the rated short-circuit current of the circuit-breaker. Recent studies in the USA [4] and in Japan [1][18] addressed more severe TRV conditions when clearing three-phase faults, especially at a long distance (the so-called LLF: Long-Line Fault).

In late 2004 CIGRÉ Study Committee A3 (High Voltage Equipment) established WG A3.19 "Implications of three-phase line fault TRV to Standards" to study in detail the phenomena described in recent studies in relation to the Standards. The original scope of WG A3.19 is presented below. During the life of the WG it became clear that, for such a complex topic, it would be inappropriate for WG A3.19 to make specific proposals for adaptation of the Standards which must also consider non-technical aspects such as "market relevance". This document reflects this and presents only technical and risk based considerations.

The study of WG A3.19 generated much correspondence and debates between experts in order to understand precisely all aspects of the three-phase phenomena and the mutual interaction between the phases. The connection between the results from modern simulation techniques and the analytical approach of the early days has been investigated intensively in order to look for potential new insights as well as new judgements.

The objective of this Technical Brochure is to present and review the results of the comparisons in two ways. The first is the description of all phenomena that are relevant in order to get a deeper understanding of the TRVs that appear when clearing three-phase line faults. The second focuses more upon the conditions that lead to a more severe TRV than recognised in the Standards and of the consequences of such TRV values. The first aspects has a more tutorial character whilst the second offers users the tools and information to judge whether potentially rather extreme conditions may prevail in their network leading to a risk that has to be assessed in greater detail.

This Technical Brochure contains three main parts and three appendices which contain details of specific simulations and calculations. The phenomena related to three-phase line faults are described in Part I "Line fault phenomena". By different approaches the phenomena are analysed and compared. Part I can be regarded as the tutorial level, necessary to get a deeper understanding of the mutual influence between the phases.

The information required to judge the severity of TRVs that may appear at clearing three-phase line faults is given in Part II "Implications for short line faults" and in Part III "Implications for long line faults". In contrast to Part I where purely factual information is presented, the information in Part II and Part III is both factual and subject to interpretation. As such, in some areas, differing points of view are presented in a balanced manner.

The original scope of WG A3.19 is as follows:

- Preliminary work on 3-phase line fault Transient Recovery Voltages (TRV's) has been undertaken by the line TRV Task Force of WG A3.13. It has been confirmed that the first peak of a 3-phase line fault TRV is definitely of a significantly higher magnitude, although a slightly longer time to peak occurs (slower rate of rise), than the present TRV standards require. (The present "short line fault" TRV requirements in standards are based on single-phase to ground faults.) If 3-phase line faults are to be considered, proper circuit-breaker application demands that the 3-phase line fault TRV values may be included within the standard TRV envelope. Another topic to be considered is the so-called long line fault (3-phase and 1-phase), based on field measurements by BPA and a Japanese publication at the CIGRE SC 13 Session 2002 and the contribution of the authors.

- For 3-phase line faults, the magnitude and time to first peak of the Transient Recovery Voltage (TRV) will be investigated for various rated voltages, short circuit currents, and line configurations. These values will be compared to the existing standard TRV envelopes for each condition. The appropriate surge impedance and amplitude "d" factor will be determined for the 3-phase fault TRV's. In addition, the probability of 3-phase line faults at each voltage will be assessed based on operating experience. The knowledge collected four decades ago will be taken into account. Commentary as to the seriousness of possible delayed fault clearing of 3-phase faults at each voltage level will be developed. Finally, investigation will be made into the validity of combining the TRV from traditional short line fault with the TRV from terminal faults to form a composite TRV envelope.

Note: throughout the document the expression "three-phase fault" is used without specifying whether the three-phase fault is grounded or ungrounded. As will be explained in Part I, especially in section 4.1.4, for the high frequency phenomena (travelling waves) at the terminals of the clearing pole of the circuit-breaker it is not relevant whether the fault is grounded or not. But for the power frequency phenomena, e.g. the amplitude of the interrupted short-circuit current, it is important to know whether the three-phase fault is connected to earth or not. However, often in this document the amplitude of the short-circuit current (at the busbar or at the fault location) is assumed to be equal to that of the single phase short-line fault, in which case it is not necessary to know the earthing condition of the fault. So, in general by the expression "three-phase fault" both grounded and ungrounded faults are meant.

2. Background

At the CIGRÉ SC 13 Session in 2002, Report 13-103 [1] was presented by experts from Japan. The publication dealt with a number of TRV topics and one of them was termed Long Line Fault (LLF). This has similarities with Short-line Faults (SLF) in the sense that the short-circuit power at the busbar side of the circuit-breaker is assumed to correspond to its 100% rated short-circuit current, whilst the TRV at the line-side consists of a damped triangular waveshape, caused by travelling waves. For SLF the distance between circuit-breaker and fault is rather limited (some km), leading to an overall short-circuit current close to 100% of the rated short-circuit current. Conversely, for LLF the distance is quite long (e.g. 100 km or more), leading to much lower percentages of the rated short-circuit current (e.g. 10%). This means that the steepness of the line side TRV (rate of rise of recovery voltage) is much higher for SLF than for LLF but that the peak value of the triangular TRV is small at SLF and very high at LLF since the travelling waves along long distance steadily build up a high peak value for the TRV. In summary, the critical stress parameter is RRRV for SLF and the TRV peak value for LLF.

In Report 13-103 for LLF, TRV parameters beyond the values specified in the Standards were found, especially when considering the test duties T10, T30 and OP. However, since then Amendment 1 of IEC 62271-100 [2] has been accepted including a change to the specified TRV envelope for the T30 test-duty to a 2-parameter envelope that almost covers the LLF parameters calculated by the experts from Japan. Nevertheless, the topic of LLF was taken seriously by CIGRÉ WG A3.13 ("Changing Network Conditions and System Requirements"). In a further development IEC SC17A has prepared a second edition of IEC 62271-100 (IEC document 17A/815/FDIS[3]) that has been approved at the FDIS stage (Final Draft International Standard), and in which the specified parameters of the T10-duty have changed to values that cover the LLF-parameters calculated by the experts from Japan.

In 2003, experts from BPA (USA) performed a staged fault test on a 550-kV Overhead line. The purpose of the test was to verify computer simulations of transients on Overhead lines, as well as to assess the TRV parameters for series compensated lines. The staged fault tests were performed with and without by-passing the series capacitor banks. When the capacitor banks are bypassed, the faults look like a LLF, as the distance from the substation to the fault was around 125 km. The results from the measurements on a real line matched very well with the computer simulations, and were published at the end of 2003 in the Master Thesis of Anders Johnson [4], who compiled the computer model. In common with the experts from Japan, the Master Thesis concluded that LLF could lead to TRV peak values beyond the values specified in the Standards.

The experts from Japan and the experts from BPA considered three-phase line faults, while SLF type test defined in the Standards address the single-phase fault case. In his Master Thesis, Anders Johnson paid much attention to the difference between three-phase and single-phase tests and concluded that three-phase SLF are not covered by the present Standards. As the three-phase versus single-phase aspects of SLF were beyond the scope of WG A3.13, first a task force and later a new CIGRÉ WG A3.19 was established in 2004 to study three-phase SLF and (single/three-phase) LLF.

The conclusions in the Master Thesis were based on the value of 450 Ω for the equivalent surge impedance of the last clearing pole, as specified in the Standards. As the particular 550-kV line of BPA showed a much lower equivalent surge impedance, WG A3.19 requested

other experts to calculate and/or simulate the equivalent surge impedance of the Overhead lines in their countries such that the conclusions could be based on a wider experience than the value from the Standards and the Overhead line of BPA. In order to understand the phenomena reported and their relevance the members of WG A3.19 made new calculations and simulations for comparison with those of Anders Johnson who became a corresponding member of WG A3.19. In addition, historical information on the IEC/IEEE/CIGRÉ decisions to introduce a single-phase SLF instead of a three-phase fault was collected, including publications from time when this decisions was originally taken, where the same phenomena have been addressed analytically.

A study of Short-line faults was first made in the 1960's by CIGRÉ Study Committee A3 (then SC3) and the results were transmitted to IEC Subcommittee 17A in August 1963. AT this time IEC SC17A was revising its standard for high-voltage circuit-breakers, IEC 56, and intended to standardise ratings and testing for short-line fault conditions [5]. The preliminary conclusions of the CIGRÉ Study Committee were as follows:

> *"Having in mind the complexity of the problem, judging and testing of circuit-breakers regarding short-line faults should, for the time being, be based on the case of single-phase-to-ground faults only, because this type of fault is the most frequent and the most important one".*

This recommendation was justified in the report in the following way:

> *"Taking into account all above considerations, it seems quite reasonable to establish type testing according to combination B, that is to consider single-line to ground faults, in order to avoid unjustified increases in circuit cost, just to face extremely unlikely conditions (three-phase short-line fault at the critical distance, with 100% short-circuit capacity on the supply side)."*

It is interesting to note that when this recommendation was made, the Study Committee had a detailed knowledge of TRVs related to single-phase and three-phase SLF, in particular of the magnitude of the first peak of TRV seen by the-first-pole-to-clear during three-phase SLF interruption. Based on this study, IEC SC17A standardised the requirements and testing for SLF in IEC 56, using single-phase SLF as the basis for rating.

The argument that was presented by CIGRÉ in 1963 is still valid today as will be shown in the following chapters. With the knowledge and experience that was gained on SLF interruption by circuit-breakers with different technologies, some additional justifications can be added that support the choice of single-phase SLF as basis for rating.

It should be pointed out also that when SLF ratings and type tests were introduced, the aim was to cover the thermal phase of interruption that was not yet properly tested by the existing type tests. It is clear from the correspondence of the time that the decision to base the rating on the most severe case, with the full short-circuit power of the source and the most aggressive conditions in terms of di/dt and RRRV was taken intentionally. Nevertheless, and as recognised in the past, when three-phase line faults, other than SLF, are considered, different stresses can exist from those associated with thermal phase of interruption as demonstrated by the SLF (single-phase) type tests.

Amongst the technologies that are (and were) used for high-voltage circuit-breakers, those based on oil or vacuum as an interrupting media are known to be insensitive to the high rate-of-rise of TRV (RRRV) associated with SLF. Air blast circuit-breakers are particularly sensitive to such high RRRV but are able to interrupt SLF when equipped with opening resistors due to the RRRV being reduced by a factor $\frac{R}{R+Z}$ where R is the resistor value and Z the line surge impedance.

In the case of SF_6 circuit-breakers, studies made using arc modelling and experience gained during more than 30 years of development and testing have shown that the decisive parameters for interruption are the current slope before current zero (di/dt) and the RRRV. The amplitude of the first peak of the TRV has generally been found to be of secondary importance, with the success of interruption being decided during the first microseconds that follow the passage of current through zero. Any decrease in the RRRV leads to an increase in the performance of an SF_6 circuit-breaker as can be seen with the following equation that gives the relation between the interrupted current (di/dt) and the RRRV [29]:

$$di/dt = \frac{K}{RRRV^{a}} \qquad \text{with} \quad 0.4 < a < 0.5$$

As the RRRV associated with three-phase SLF is lower or, at worst equal to, the value for single-phase SLF, it follows that the single-phase SLF presents the most severe condition for known technologies of circuit-breakers that are sensitive to SLF conditions.

Part I

Line fault phenomena

3. Three-phase Short Line Fault versus single-phase Short Line Fault

3.1 Basis of short-line fault rating in the present standards: single-phase fault

The short-line fault rating is presently based on the last-pole-to-open for a three-phase-to-ground fault or the single pole that clears a single-phase-to-ground fault. For a given magnitude of fault current, this results in the highest rate of rise of recovery voltage (RRRV) since the surge impedance for the last clearing pole is the highest (to be shown later). When the fault current is near full rating (90% or more), it is necessary to test the thermal breaking capability power of the circuit-breaker when the highest RRRV is applied. This is well recognized as a paramount factor in the current interruption process. Also, the phase-to-ground fault is the most likely fault occurring on transmission systems and therefore it becomes logical to define a test for the thermal breakdown regime. As lower percentages, such as 75% and 60%, give less thermal stress but a higher TRV peak at the line side, type tests are performed at a lower than 90% current levels also.

The "standard" line surge impedance for last-pole-to-open, on which testing is based, is 450 Ω. This is higher than most actual system conditions and assumes bundled conductors at the higher system voltages have clashed; an effect which increases the surge impedance as well as affecting the power frequency impedances and the fault current and associated di/dt at current zero. For lower fault currents, this clashing certainly does not occur and therefore the standard value of 450 Ω introduces some margin in the application compared to testing.

The speed of the transient for the line travelling waves is taken as the speed of light at which the electro-magnetic wave is propagating through air (or vacuum). At the higher frequencies of the TRV transients, the ground modes are coupled tightly into the ground wires and the speed is approaching typically 95% of the speed of light. Therefore, the slower ground modes do not need special consideration.

At the moment of clearing a 90% short line fault, the impedance at the line side of the circuit-breaker is 10% of that at the source side, while the source side impedance corresponds to the rated short-circuit current of the circuit-breaker. The power frequency voltage at both sides of the circuit-breaker is 10% of the rated voltage. After clearing, the voltage at the busbar side will respond with a waveshape corresponding to 90% of the rated TRV and corrected for the first-pole-to-clear factor. According to the Standards during type tests an RRRV of 90% of 2.0 kV/μs has to be applied, showing that surge impedances have a different relationship to ground than power frequency entities. At the line side, after clearing, the electrical charge corresponding to the voltage profile along the Overhead line (10% at the breaker terminal to 0% at the fault location) is released and the line will be discharged into the fault by means of travelling waves between circuit-breaker terminal and fault location. At the circuit-breaker terminals, a slowly damped triangular waveshape will appear with an initial overshoot with respect to the initial 10% voltage value. The overshoot, caused by the reflection of the travelling waves against the open circuit-breaker, is less than the theoretical maximum of 2.0. In the Standards, the overshoot accounted for by the application of a "d"-factor, that is presently specified as 1.6 for all rated voltage classes.

The "d" factor is simply the ratio of the peak of the line-side voltage excursion to the instantaneous power frequency line-to-ground voltage at the point of interruption. It is not a damping or loss factor in the classic sense of a decaying oscillatory transient. The "d" factor is calculated under the assumption of "no loss", but it relates a travelling wave phenomenon

to a power frequency voltage. The major influence on the "d" factor is the variation of the line impedance (mainly inductance) that changes from the power frequency impedance to that of the high-frequency TRV transient. The variation mainly in inductance is predictable and is a result of the high-frequency transients being tightly coupled to the ground wires and the surface of the earth versus the penetration of the power frequency currents deeper into the earth. Calculations are generally done as per Carson's earth return formulae.

Impedances of the SLF test circuit are calculated according to the specified fault current. As a result, the testing is done at a factor "M" times the circuit-breaker rating and the following derives the results based on that factor.

> Note: The standards deal with ratings and the TRV parameters are modified according to the short-circuit current value for a given voltage class. The following analysis uses the same short-circuit current as the main reference for the purposes of comparison. For a phase-to-ground fault, the impedance of the line per unit distance is higher than the impedance for a three-phase-to-ground fault. Therefore, for the same fault current, the distance to the fault is different for the two fault types.

For the phase-to-ground fault case, the standards are based on a source that has the same fault current magnitude as the circuit-breaker rating which is assumed to be the same as the three-phase fault current. In reality this may not be the case where there is a significant contribution of fault current from lines where $\mathbf{X_0}$ my be 2 to 3 times larger than $\mathbf{X_1}$, while transformers may have an $\mathbf{X_0}$ which is less than $\mathbf{X_1}$. The fault current is determined by the phase-to-ground voltage $\mathbf{V_{ph}}$, the source impedance $\mathbf{X_s}$, and the line impedance $\mathbf{X_{1line}}$.

The source impedance is based on circuit-breaker rating: $\mathbf{X_s = V_{ph}/I_{sc}}$. The line reactance per metre for a phase-to-ground fault is based on the positive ($\mathbf{X_1}$) and zero sequence ($\mathbf{X_0}$) power frequency reactances for a length of line $\mathbf{l_1}$: $\mathbf{X_{1line} = (⅔X_1 + ⅓X_0)\times l_1}$. The short-circuit current is the phase-to-ground voltage divided by the sum of the source and line reactances using these expressions:

$$\mathbf{I_{1SLF}} = \frac{\mathbf{V_{ph}}}{\frac{\mathbf{V_{ph}}}{\mathbf{I_{SC}}} + \frac{(2\mathbf{X_1} + \mathbf{X_0})\mathbf{l_1}}{3}} \qquad (3.1)$$

Solved for the line length up to the single-phase fault, this gives:

$$\mathbf{l_1} = \frac{\frac{\mathbf{V_{ph}}}{\mathbf{I_{1SLF}}} - \frac{\mathbf{V_{ph}}}{\mathbf{I_{SC}}}}{\frac{2\mathbf{X_1} + \mathbf{X_0}}{3}} \qquad (3.2)$$

with $\mathbf{V_{ph}/I_{1SLF}}$-$\mathbf{V_{ph}/I_{sc}}$, when multiplied by $\mathbf{I_{1SLF}}$, being the power frequency line-to-ground voltage (rms) at the instant of interruption, at the location of the circuit-breaker.

The rate of rise of recovery voltage for the last clearing pole, $\mathbf{RRRV_{last}}$ for the line side voltage based on the effective surge impedance for the last pole to open $\mathbf{Z_{last}}$, evaluated at the high TRV frequency, and the rate of change of current at the current zero is given by:

$$\mathbf{RRRV_{last}} = \omega\sqrt{2} \times \mathbf{I_{1SLF}} \times \mathbf{Z_{last}} \qquad (3.3)$$

The peak of the transient voltage would be the RRRV multiplied by twice the travel time to the fault at distance $\mathbf{l_1}$. Substituting for $\mathbf{RRRV_{last}}$ and using the speed of light **c** to calculate

the travel time across twice the distance $\mathbf{l_1}$, the TRV peak at the line side for the last pole or the single pole $\mathbf{E_{line1}}$ gives:

$$\mathbf{Eline1} = \omega\sqrt{2} \times \mathbf{I1SLF} \times \mathbf{Zlast} \times \frac{2}{\mathbf{c}} \times \frac{\frac{\mathbf{Vph}}{\mathbf{I1SLF}} - \frac{\mathbf{Vph}}{\mathbf{I_{SC}}}}{\frac{\mathbf{2X_1 + X_0}}{\mathbf{3}}} \qquad (3.4)$$

Recognizing that $\mathbf{V_{ph}/I_{1SLF}}$-$\mathbf{V_{ph}/I_{sc}}$ multiplied by $\mathbf{I_{1SLF}}$ and $\sqrt{2}$ is the line-to-ground voltage, $\mathbf{E_0}$ (momentary or peak value) at the instant of interruption, the d-factor is simply:

$$\mathbf{d1} = \frac{\omega \times \mathbf{Zlast} \times \frac{2}{\mathbf{c}}}{\frac{\mathbf{2X_1 + X_0}}{\mathbf{3}}} \qquad (3.5)$$

3.2 First-pole-to-clear, three-phase fault

The same steps can be used for the first pole to clear a three-phase fault at the same magnitude of fault current (same M factor, for instance 0.90).

The source impedance $\mathbf{X_s}$ is the same as above. The line reactance for a three-phase to ground fault is based on the positive power frequency reactance for a length of line $\mathbf{l_3}$: $\mathbf{X_{1line} = X1 \times l_3}$. The short-circuit current is the phase-to-ground voltage divided by the sum of the source and line reactances using the expressions above:

$$\mathbf{I3SLF} = \frac{\mathbf{Vph}}{\frac{\mathbf{Vph}}{\mathbf{I_{SC}}} + \mathbf{X_1 \times l3}} \qquad (3.6)$$

Solved for the line length up to the three-phase fault gives:

$$\mathbf{l3} = \frac{\frac{\mathbf{Vph}}{\mathbf{I3SLF}} - \frac{\mathbf{Vph}}{\mathbf{I_{SC}}}}{\mathbf{X_1}} \qquad (3.7)$$

with $\mathbf{V_{ph}/I_{3SLF}}$-$\mathbf{V_{ph}/I_{sc}}$, when multiplied by $\mathbf{I_{3SLF}}$, being the power frequency line-to-ground voltage at the instant of interruption.

Calculating the $\mathbf{RRRV_{first}}$ for the line side voltage based on the effective surge impedance for the first pole to open $\mathbf{Z_{first}}$, evaluated at the high TRV frequency, and the rate of change of current at the current zero:

$$\mathbf{RRRV_{first}} = \omega\sqrt{2} \times \mathbf{I_{3SLF}} \times \mathbf{Z_{first}} \qquad (3.8)$$

The peak of the transient voltage would be the RRRV multiplied by twice the travel time to the fault at distance $\mathbf{l_3}$. Substituting, the TRV peak at the line side for the first pole $\mathbf{E_{line3}}$:

$$\mathbf{Eline3} = \omega\sqrt{2} \times \mathbf{I3SLF} \times \mathbf{Zfirst} \times \frac{2}{\mathbf{c}} \times \frac{\frac{\mathbf{Vph}}{\mathbf{I3SLF}} - \frac{\mathbf{Vph}}{\mathbf{I_{SC}}}}{\mathbf{X_1}} \qquad (3.9)$$

Recognizing the line-to-ground voltage at the instant of interruption, the d-factor is simply:

$$\mathbf{d3} = \frac{\omega \times \mathbf{Zfirst} \times \frac{\mathbf{2}}{\mathbf{c}}}{\mathbf{X_1}} \qquad (3.10)$$

This is the "d" factor for the first pole to clear a three-phase fault (grounded or ungrounded) remote on the line.

The d ratio of the first pole to clear a three-phase to ground fault versus the last pole to clear or the single pole to clear a single-phase to ground fault with the same fault current is:

$$\frac{\mathbf{d3}}{\mathbf{d1}} = \frac{\mathbf{2X_1 + X_0}}{\mathbf{3X_1}} \times \frac{\mathbf{Zfirst}}{\mathbf{Zlast}} \qquad (3.11)$$

and the RRRV ratio (Eqs 3.3 and 3.8) is:

$$\frac{\mathbf{RRRV_{first}}}{\mathbf{RRRV_{last}}} = \frac{\mathbf{Z_{first}}}{\mathbf{Z_{last}}} \qquad (3.12)$$

when evaluated at the same fault current levels.

3.3 Effective surge impedances for the first and last clearing poles

The effective surge impedances for first and last poles can be calculated from the circuit shown in Fig. 3.1. This analysis uses positive and zero sequence components. The more complete approach would be to use modal analysis and derive the impedances for specific conductors but the positive and zero sequence analysis yields a reasonably accurate analysis and effectively explains the effects of the first and last pole and the ground impedances. The method uses a current injection across the contacts of the pole of the circuit-breaker that is opening with all other sources shorted (method of superposition). The voltage across the open pole is the transient recovery voltage since the voltage across the pole when closed is zero in the steady state. The voltages to ground are the "transient" voltages which, when added to the steady state voltages, result in the total voltage at that point.

The source is represented by the surge impedances of "n" parallel lines connected to the source. The inductances of supply transformers is not shown since they are best represented as open circuits during the first part of the TRV. Since the RRRV is determined by the surge impedance of the lines at the source side, all sources look "grounded" because the lines have a significant "ground-mode" surge impedance. The debate over the first-pole-to-clear factor for grounded or ungrounded sources or grounded or ungrounded faults is erroneous for the RRRV phenomena, which form the more critical parameter of the TRV.

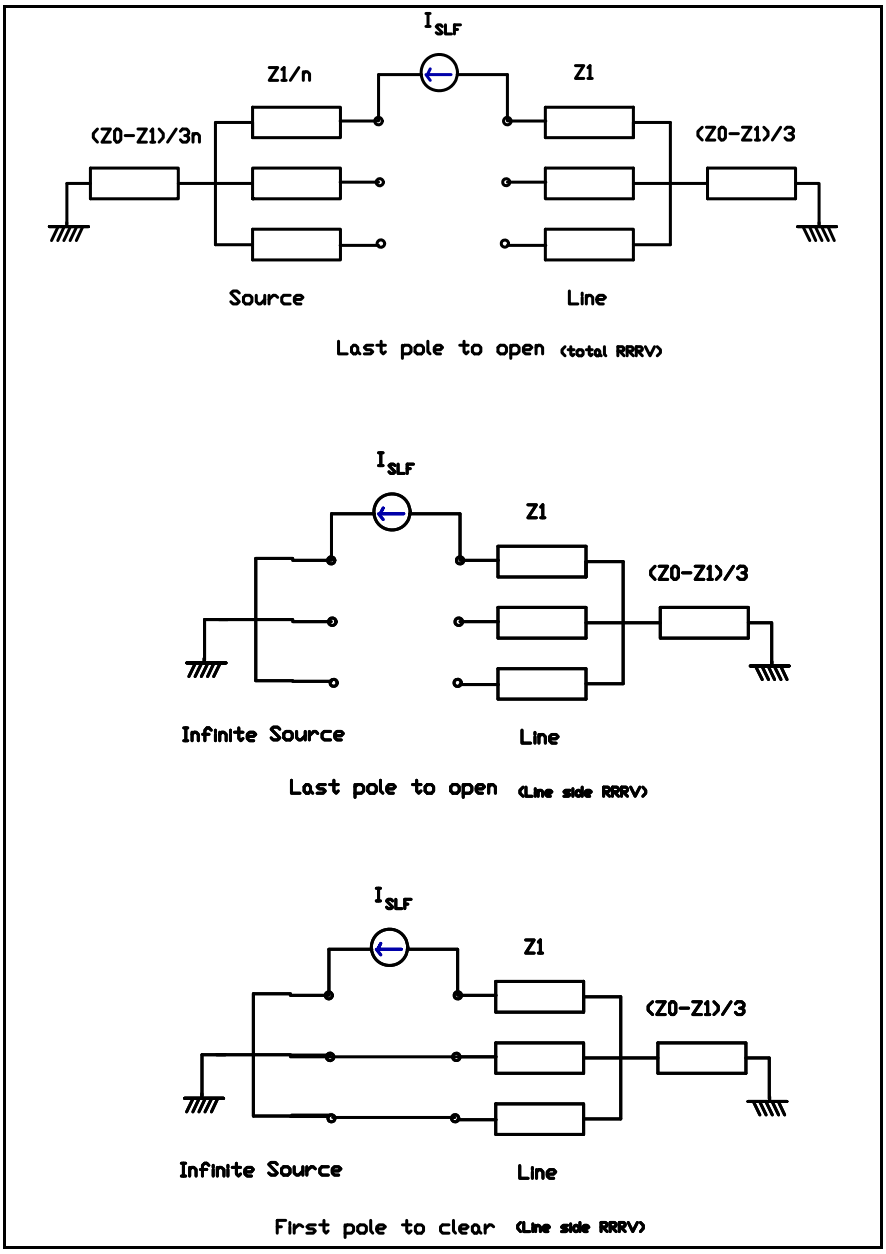

Figure 3.1: RRRV-schemes for the last and first clearing poles

The line can be represented as a simple resistance of the positive and zero sequence surge impedances until the first reflection returns. The circuit-breaker is subject to the RRRV from both the line and source side as shown at the top scheme of Fig.3.1. On the assumption that the source side lines have the same surge characteristics as the faulted line, they are represented as "n" lines in parallel. The nature of the fault is not represented since the fault is not "seen" until the first reflection returns to the circuit-breaker once the current is interrupted. Therefore, this represents the last pole to open for a phase to ground fault or for a three-phase ungrounded or grounded fault. The nature of the source (grounded or ungrounded) or the fault is not a factor other than dictating the fault current to be interrupted.

For the purposes of evaluating the RRRV from the line side, the source can be represented as an infinite source as shown in the middle scheme of Figure 3.1 from which the equivalent surge impedance for the last clearing pole can be derived:

$$\mathbf{Z_{last}} = \frac{\mathbf{2Z_1 + Z_0}}{\mathbf{3}} \qquad (3.13)$$

For the first clearing pole, the neutral resistance and two of the other phases are in parallel, as shown in the bottom scheme. Reducing the connection and adding $\mathbf{Z_1}$ results in the effective surge impedance for the first pole:

$$\mathbf{Z_{first}} = \frac{\mathbf{3Z_0 \times Z_1}}{\mathbf{Z_1 + 2Z_0}} \qquad (3.14)$$

The application of this approach to the case of the BPA transmission line which was subject to the fault test is shown below.

Example of a BPA 500-kV transmission line
Twin bundled conductors, Chukar conductors, 50 and 78 feet high spaced 40 feet apart, with two ground wires 100 feet high space 24 feet apart, no bundle clashing, segmented conductors.

(Note: ground wires are grounded only at first tower outside substation resulting in slightly higher surge impedance for the first 2 microseconds which is not accounted for in the RRRV.)

$\boldsymbol{X_1}$ *= .5868 Ω/mile and* $\boldsymbol{X_0}$ *= 2.185 Ω/mile for the positive and negative reactance at 60 Hz.*

$\boldsymbol{Z_1}$ *= 279 Ω and* $\boldsymbol{Z_0}$ *= 487 Ω for the sequence Surge Impedances evaluated at 600 kHz.*

$\boldsymbol{c}$ *= 297 m/μs for the travelling wave velocity.*

$\boldsymbol{Z_{last}} = \boldsymbol{⅔Z_1 + ⅓Z_0}$ *as the effective surge impedance for the last clearing pole .*

$\boldsymbol{Z_{first}} = \boldsymbol{3Z_1 \times Z_0 / (Z_1 + 2Z_0)}$ *as the effective surge impedance for the first clearing pole in case of a three-phase fault.*

$\boldsymbol{Z_{last}}$ *= 348 Ω and* $\boldsymbol{Z_{first}}$ *= 325 Ω*

The ratio of RRRV first pole to RRRV last pole is simply the ratio of the surge impedances:
$\boldsymbol{Z_{first} / Z_{last}}$ *= 0.934*

The "d" factor for the first and for the last pole to clear on a three-phase fault (grounded or ungrounded) remote on the line are:

$\boldsymbol{d_3}$ *= 2.26 and* $\boldsymbol{d_1}$ *= 1.27*

The ratio of the TRV excursion on the line side for the first pole versus the last pole to clear is: $\boldsymbol{d_3 / d_1}$ *= 1.78.*

3.4 Peak values for three-phase and single-phase faults

The effect of the somewhat lower RRRV and higher d-factor for the first pole to clear a three-phase short line fault is shown in the figures 3.2 and 3.3, where the source side as well as the line side parts of the transient recovery voltage are compared.

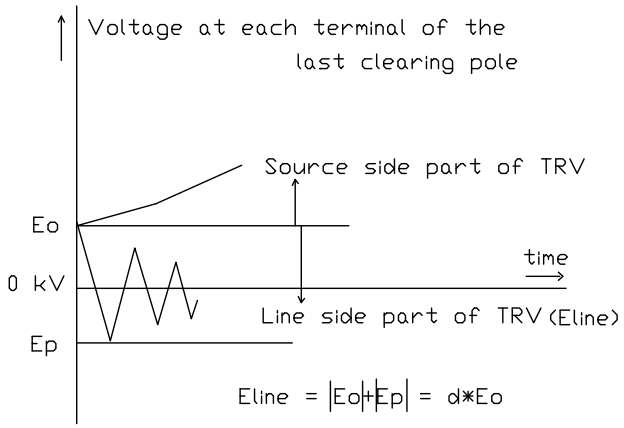

Figure 3.2: Line and source side parts of TRV for 1-phase SLF (or last clearing pole for 3-phase SLF)

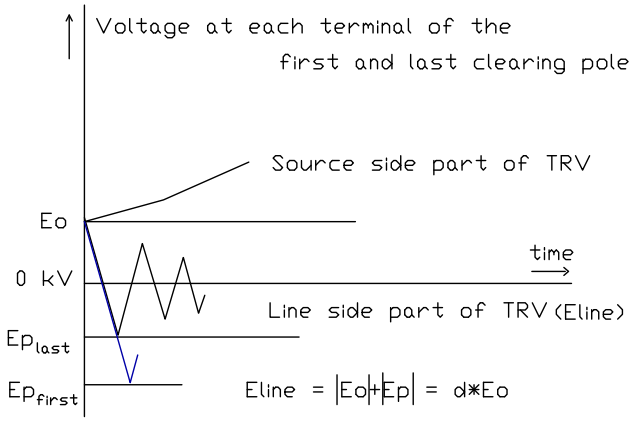

Figure 3.3: Line and source side parts of TRV for the first and last clearing pole

In the above comparisons between single and three-phase faults, it is assumed that both fault currents are equal and that the equivalent source impedances up to the circuit-breaker are equal ($\mathbf{X_0} = \mathbf{X_1}$). As the positive and zero sequence impedances of the line are not equal, the equivalent reactance per length is actually higher for the single-phase than for the three-phase fault. This implies to a larger distance between circuit-breaker and fault location for the three-phase fault and thus to a longer travelling time and longer time to the TRV-peak at the line side (Fig. 3.3).

Within the framework of the Standards where the circuit-breaker performance is specified for certain levels of short-circuit current, such an approach is understandable. However, from a utility point of view it is more logical to compare the effects of faults at a certain location, giving the same time to peak for single and three-phase faults, but a somewhat higher three-phase current (at L90 about 3% higher, at L75 about 9% higher and at L60 about 15% higher). It should be noted that the surge impedance for the first pole the clear compared to the last are not all that much different (within 5 to 15%), giving, in the case of faults at the same location, rather comparable RRRVs, and consequently comparable peak values of the line-side TRV as shown in figure 3.4.

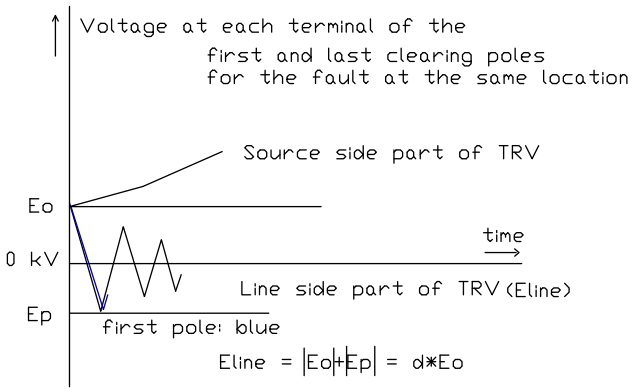

Figure 3.4: Line and source side parts of the TRV for the first and last clearing poles with the three-phase and single-phase fault at the same location

Moreover, in real networks, the $\mathbf{X_0/X_1}$ ratio at the source side of the circuit-breaker may vary over a wide range and may even be below 1.0, such that the rating of the circuit-breaker has to be based on the single-phase fault current rather than on the three-phase fault current. The combination of all these parameters can be such that the outcome in terms of TRV peak values is larger, equal or smaller for single-phase in comparison to three-phase faults.

Further, as will be discussed in the next chapter, the SLF surge impedance of 450 Ω, as specified in the Standards, covers these cases with margins. When bundle conductor clashing is not a factor, the 450 Ω is over-specified and previous editions of the Standards incorporated surge impedances in the range of 325 to 360 Ω, assuming no clashing. Also the standard d- factor for SLF of 1.6 for single-phase faults covers distribution lines but it is an over-specification for the bundled conductor transmission lines.

3.5 Effect of mutual inductance on the d-factor

In a simple linear RLC circuit and assuming an ideal switch, it can be mathematically demonstrated that the overshoot factor, i.e. the d-factor, is always lower than 2. For three-phase short-line faults (3ϕ SLF), the d-factor of the line TRV is greater than 2 due to the mutual inductances between phases. The mutual inductance between two phases i and j can be evaluated by equation 3.15.

$$\mathbf{M_{ij}\ (in\ H/m) = \frac{\mu}{2\pi} \ln \frac{1}{D_{ij}}} \qquad (3.15)$$

where

$\boldsymbol{\mu}$ = air permeability = $4\pi \times 10^{-7}$ H/m

$\mathbf{D_{ij}}$ = centre-to-centre spacing between conductors i and j, in metres

For example, for $\mathbf{D_{ij}}$ = 10m, the mutual inductance between the two conductors would be equal to 0.46 μH/m.

As an example we can use the circuit topology of figure 3.5 for which the source is isolated, giving a first-pole-to-clear factor of 1.5 and analyse the case in which the first-pole-to-clear is the central pole (B) of a 3ϕ SLF. The analysis of the mutual inductance effect is simplified in this circuit since there is no 60-Hz short-circuit current circulating in the ground path. Therefore, only the mutual inductances between phases must be taken into account. During

the three-phase fault, these mutual inductances provide a parallel path for the short-circuit currents, thus increasing short-circuit current amplitudes. After current interruption by the first pole and during line TRV build-up, an induced voltage ($\mathbf{V_{ind}}$, Eq. 3.16) would be generated by the high short-circuit current still circulating through the two other phases. In fact, this induced voltage will be superimposed on the line TRV of the interrupted pole.

$$\mathbf{V_{ind}} = \mathbf{M_{ab}} \frac{\mathbf{dI_a}}{\mathbf{dt}} + \mathbf{M_{cb}} \frac{\mathbf{dI_c}}{\mathbf{dt}} \tag{3.16}$$

For the purposes of the example the source parameters are:
- Rated voltage: 315 kV
- Power frequency: 60 Hz
- Short-circuit current amplitude: 32 kA (80% of 40 kA)
- TRV slope: 2.6 kV/µs
- TRV amplitude factor: 1.46

The line parameters are:
- Line length: 4.28 km
- Line model: frequency-dependent line model
- Distance between conductors: 10 m
- SLF test duty: In the vicinity of L60

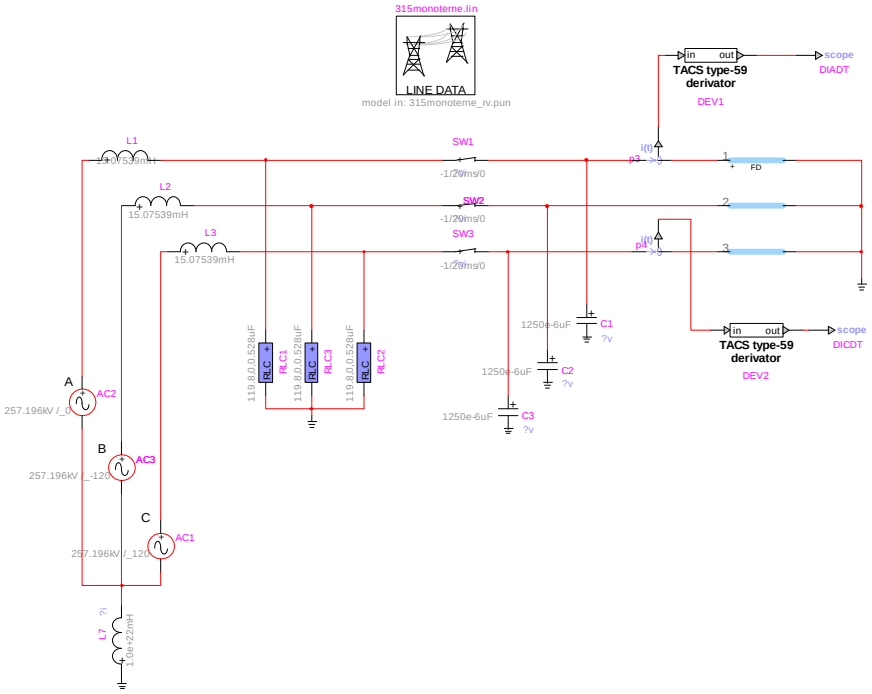

Figure 3.5: EMTP circuit for simulating the induced voltages generated by the high short-circuit currents circulating through the last two poles

Figure 3.6a shows the interrupted current of the first pole ($\mathbf{I_b}$= 25.3 kA rms) and the short-circuit currents circulating through the last two poles ($\mathbf{I_a}$ and $\mathbf{I_c}$). Figure 3.6b depicts the corresponding current derivatives ($\mathbf{dI_a/dt}$ and $\mathbf{dI_c/dt}$). These derivative signals have been filtered since it is well known that the derivative calculation introduces noise.

By applying equation 3.15, the value of the mutual inductances ($\mathbf{M_{ab}} = \mathbf{M_{bc}}$ = 1.97 mH (0.46 µH/m x 4280 m)) can be calculated. However, since the line model is a frequency-dependent model, mutual inductances should be evaluated using the EMTP output file *.lig. In our case

study, and considering that the frequency of the current slope (**dI_a/dt** and **dI_c/dt**) is in the range of 1.3 kHz, the mutual inductance **M_{ab}** and **M_{bc}** is equal to 1.55 mH.

The induced voltage on the first interrupted pole can therefore be assessed. Figure 3.6c shows the actual line TRV (blue line) and the calculated induced voltage (red line). It can be seen that the line TRV exhibits a low-frequency oscillation that closely matches the induced voltage waveshape.

Finally, to retrieve the line TRV without the influence of the mutual inductances (Fig. 3.6d), the induced voltage can be subtracted from the actual line TRV (blue curve of Fig. 3.6c). Figure 3.7 depicts expanded views of the line TRV. Note that the d factor is decreased from 2.37 to 1.81 by eliminating the influence of the mutual inductances.

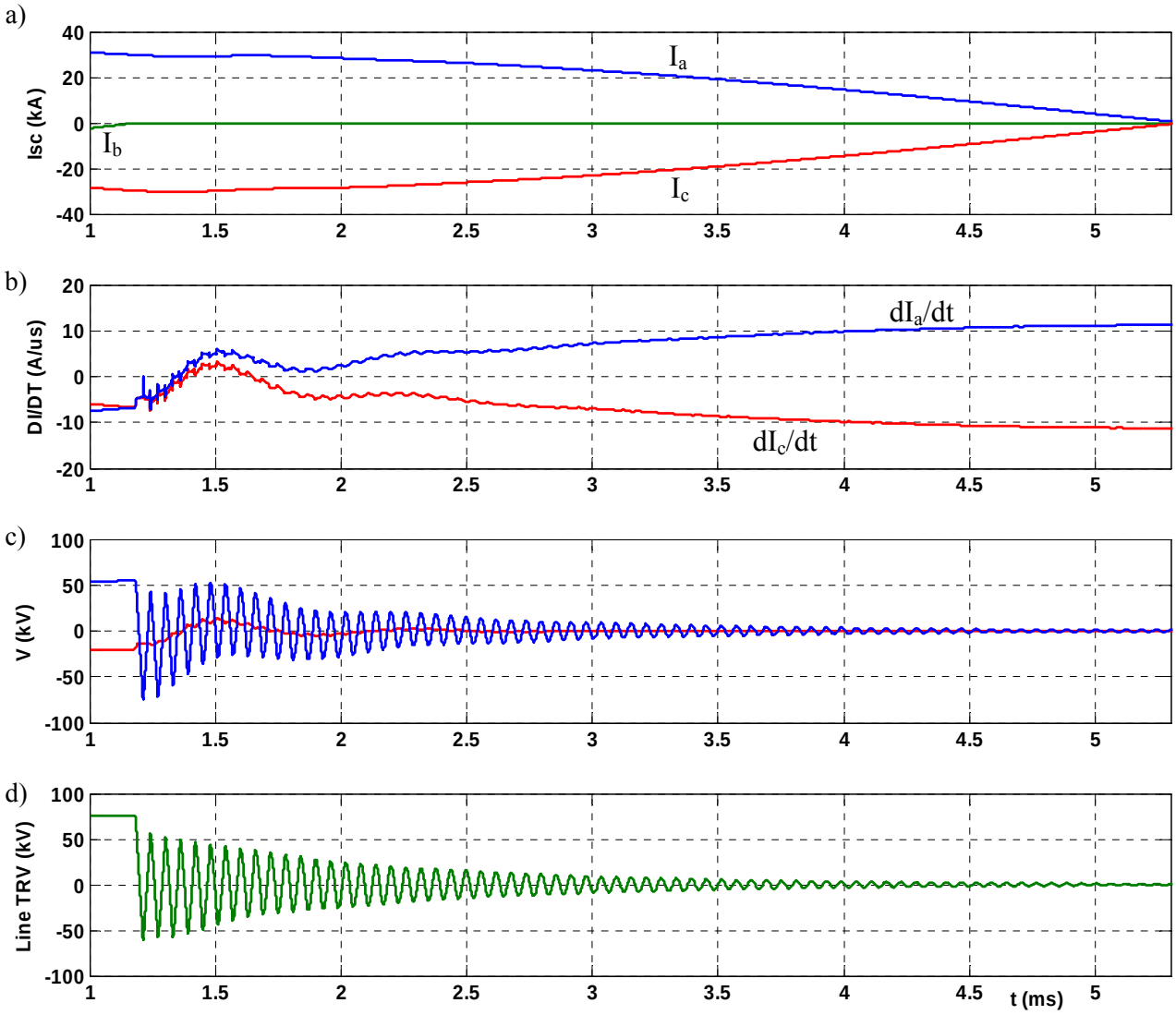

Figure 3.6: Graphs of the induced voltage generated by the high short-circuit currents circulating into two other phases in the case of the first-pole-to-clear factor of 1.5
*a) Short-circuit currents (**I_a, I_b, I_c**)*
*b) Current derivatives (**dI_a/dt, dI_c/dt**)*
c) Induced voltage (red curve) and actual line TRV (blue curve)
d) Actual line TRV minus the induced voltage (green curve)

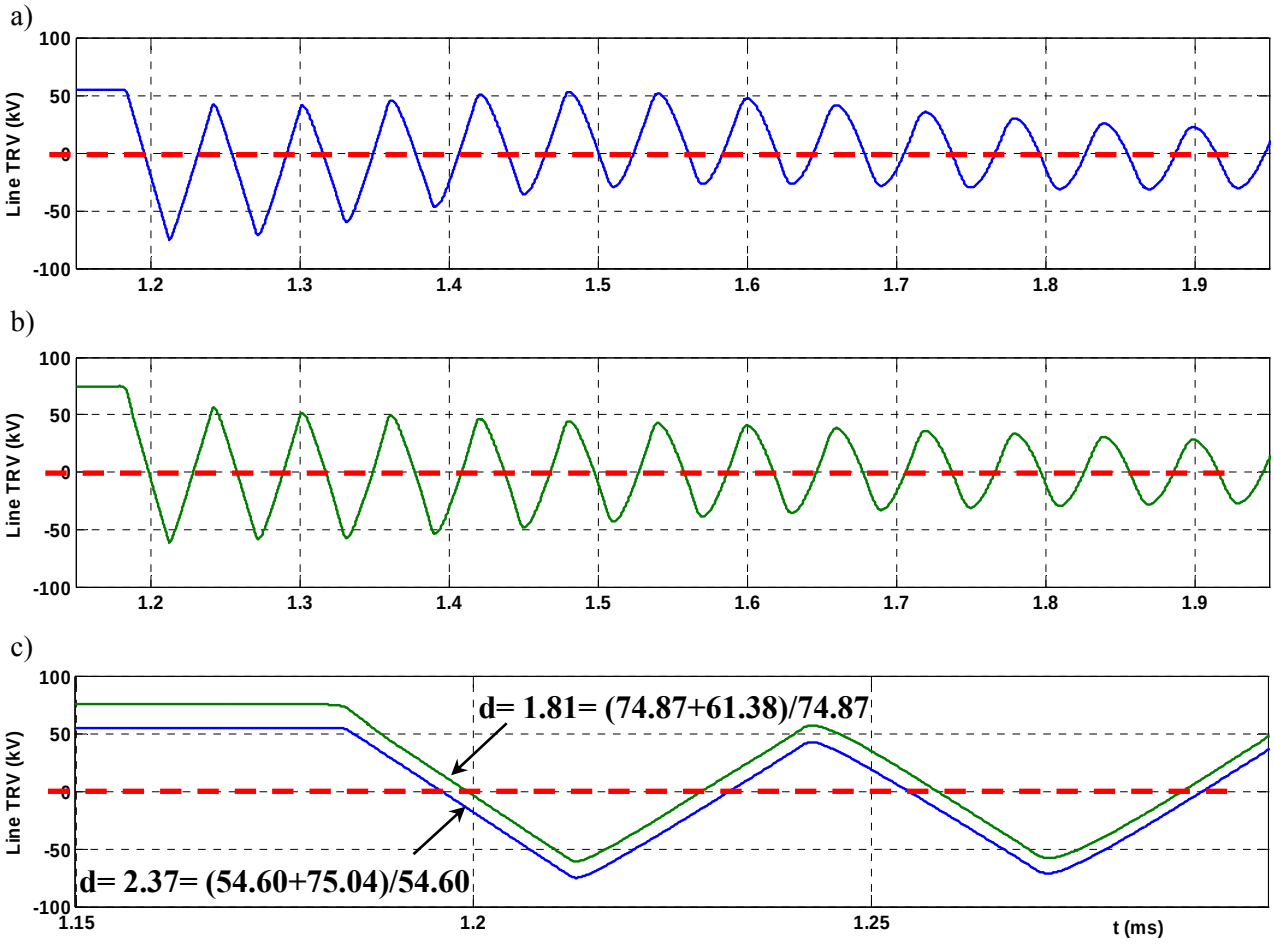

Figure 3.7: Expanded views of the line TRV
a) Line TRV for a time span of 0.8 ms
b) Line TRV minus the induced voltage for a time span of 0.8 ms
c) Superposition of curves a) and b) for a time span of 150 μs

The simplified modal analysis shows the relationship between the d-factor, that may reach values above 2.0, and the damping factor of travelling waves, that must be lower than 2.0. It is the initial jump of the voltage induced by the second and third clearing phase that causes the higher d-factor. The initial jump appears as the **dI/dt** of the second and third clearing phases suddenly changes following interruption of the first phase current. The initial jump generates a transient induced voltage where the system natural frequency is visible. Without the induced voltage the line-side TRV with its travelling waves behaves as expected and disappears. A similar voltage jump with transient phenomena is experienced in the two other phases as they couple the system natural frequency into the first clearing phase.

As detailed in section 3.2, formula (3.11), and section 3.3, figure 3.1, $\mathbf{d_3/d_1}$ is proportional to

$$\mathbf{(2*X_1+X_0)/(3*X_1) = (2*L_1+L_0)/(3*L_1).}$$

With $\mathbf{Lm = \tfrac{1}{3}L_0 - \tfrac{1}{3}L_1}$ (figure 3.1):

$$\frac{\mathbf{d_3}}{\mathbf{d_1}} = (\mathbf{1} + \frac{\mathbf{Lm}}{\mathbf{L_1}}) \times \frac{\mathbf{Z_{first}}}{\mathbf{Z_{last}}} \tag{3.17}$$

where **Lm** is typically represented in the part influenced by the other phase currents, as shown in Figs 3.6 and 3.7.

For different circuit topologies, similar results could be obtained. For example, for a first-pole-to-clear factor (K_{pp}) of 1.0 (i.e. $X_0/X_1=1$) and for different SLF test duties, Table 3.1 gives typical d factor values for the three poles as obtained by ATP simulations (Appendix A). In this case, mutual inductances between phases and ground would have to be considered since a significant power frequency current, as a result of the unbalanced three-phase circuit, is circulating in the ground path following the interruption of the first pole. It should be emphasized that the d-factor for the SLF TRV at the third-pole interruption is always lower than 2 since any mutual effect between phases vanishes at the instant of the 2nd pole interruption, thus leaving alone the 3rd pole that will interrupt without any short-circuit currents circulating in the two other phases.

Table 3.1- Typical d factor values as obtained by ATP simulations
Rated I_{SC}= 63 kA, f_r= 50 Hz, Source TRV parameters: RRRV= 2 kV/μs, K_{af}= 1.40

U_r (kV)	K_{pp}	SLF test duty	d factor		
			1st pole	2nd pole	3rd pole
420	1.0	L90	2.50	1.93	1.58
		L75	2.47	2.02	1.54
		L60	2.52	2.20	1.58

4. Parameters affecting line fault TRV waveshapes

A number of parameters that have a major influence on the TRV waveshape are considered below. Firstly, considering surge impedance, this is the proportionality factor representing the ratio between the voltage related travelling wave and the current related travelling wave. Based on the Maxwell equations, the theory of travelling waves leads to a linear relationship, that is expressed in Ω, i.e. as an impedance. At the moment of interruption of the short-circuit current due to a line fault, the voltage distribution between circuit-breaker terminal and fault location is dissipated by travelling waves which give rise to a steep rising voltage at the open terminal. The ramp function dU/dt can be seen as the line response to the discontinuity of dI/dt or the superposition of an injected negative dI/dt. It can be deduced that the relationship between dU/dt and dI/dt is the same impedance, Z.

4.1 Surge impedances

Previously several surge impedances (positive and zero sequence, equivalents for the first/last clearing poles, self and mutual surge impedance) have been addressed. Here, in this section, a number of aspects related to these surge impedances are dealt with.

4.1.1 Literature

The phenomena associated with the first and last clearing poles of a short-line fault have already been described in the 1960's and 1970's. In 1963 the then Chairman of CIGRÉ SC 3 advised IEC regarding "Preliminary conclusions concerning short-line faults in three-phase systems" [5] and a more detailed article was presented in Électra 17 entitled "Surge impedance of overhead-lines with bundle conductors under short-line faults". First and last clearing pole phenomena have already been addressed at this time [8].

The comparison between first and last clearing pole equivalent surge impedance calculations and CEGB field measurements in combination with some field tests has, for example, been presented in the IEE Proceedings on Power, Volume 120 (1973): "Overhead-line parameters for circuit-breaker application" by E. Bolton, e.a. [9]. In common with other publications, it has been stated that the surge impedances, as "seen" by the circuit-breaker do not contain any information about the type of fault (single, double or three-phase fault, grounded or ungrounded) and that it is after the reflection of the travelling waves that such information is of relevance. Of course the power frequency short-circuit currents per phase contain such information, including information about the neutral treatment (Xo/X_1 ratio) of the source side.

Another important statement in this respect is that the surge impedances as "seen" by the circuit-breaker contain information about the status of the other circuit-breaker poles (open or closed). In summary the equivalent surge impedance is not influenced by the type of fault (single-phase or three-phase), but whether the other poles are still closed or already open or both. In other words: the last clearing pole in case of a three-phase fault does not "see" the same equivalent surge impedance as the pole that clears a single-phase fault, unless that pole happens to be the last pole under a three-pole tripping condition. Modal analysis with its more precise simulation of all involved conductors leads to a similar conclusion as described in greater detail below.

Results from this IEE publication have been presented by M.B. Humphries at a symposium on "Current interruption in HV networks" in Baden (1977) [10]. Parameters discussed in the

publication as well as in the presentation are the effects of: earth wires, earth resistivity, the presence of a second circuit, last versus the first clearing pole, high frequency caused by the travelling waves versus the power frequency parameters, conductor clashing, tower height, earth resistance of the substation and distance to the fault in relation to the X_0/X_1 ratio in the substation. These topics are addressed in the following sections.

4.1.2 The effect of the earth wires

The effect of earth wires, as of any conductor running in parallel and connected in some way between source side and fault side, is to reduce the surge impedances. Depending on the mutual coupling, a rather moderate reduction can be experienced when earth wires are applied; for instance about 8%.

4.1.3 The effect of the earth resistivity

For a single conductor the surge impedance is given by the simple formula:

$$\mathbf{Z = 60\sqrt{\frac{2h}{r}}} \qquad (4.1)$$

with **h** as the equivalent height (depending on the earth resistance) and **r** the equivalent radius.

For high frequencies, occurring with faults at a short distance, the earth resistivity is of less importance but for lower frequencies and power frequencies the impact of a high earth resistivity cannot be neglected. An increase of the resistivity from 10 Ωm to 300 Ωm, leads to a few percent increase in the surge impedances, but to an approximately 8% increase in power frequency inductances. In combination with the frequency an increase of ρ/ω from 100 to 10,000 gives, for instance, an increase of 3% in the surge impedance for the last pole to clear [9] (See also Appendix C).

4.1.4 The effect of the neutral

So far not much attention has been paid to whether the three-phase fault is grounded or not. The reason for neglecting this difference is that it is unimportant for the surge impedances, i.e. for the ratio between the travelling voltage waves and the travelling current waves. The same applies for the neutral treatment of the system: it does not influence the surge impedances. Of course the neutral treatment and whether the fault is grounded or not has an influence on the power frequency currents, and therefore on the amplitudes of the travelling waves, but not on the ratio.

There is another aspect that has to be mentioned, as this aspect may give the impression that the neutral treatment of the system and the connection of the fault to earth have an influence on the surge impedance. This has to do with the measuring method of the surge impedances during field tests as well as from simulation results. Especially for TRV calculations and verifications, the equivalent surge impedance is measured from the voltage response to an injected current, based on the relationship $\mathbf{dU/dt = Z \times dI/dt}$. Knowing **dI/dt**, **dU/dt** is measured from the voltage plot by drawing a straight line between the points where the voltage response is 10% and 90% of the peak value, coming from the travelling wave. In reality damping, distortion and minor reflections give a voltage response that is not exactly linear and create small deviations from the ideal surge impedance. Due to this effect for the

simulation of different cases, small differences between surge impedances, that in fact are identical, may also appear in Appendices A and B of this Technical Brochure.

4.1.5 The effect of a second circuit

Like the earth wires, the phase conductors of another circuit on the same towers will lead to a reduction of the surge impedances. The reduction depends on whether the conductors are connected to the busbar, disconnected or even earthed. As an indication, without a second circuit or with the second circuit disconnected, the surge impedances will be roughly 10% higher in comparison with a second circuit normally connected to the busbar.

4.1.6 The effect of the last versus the first clearing pole

As explained in the former Chapter, based on symmetrical components the equivalent surge impedance as experienced by the first clearing pole is different from that of the last clearing pole:

$$\mathbf{Z_{first} = 3\ Z_0 * Z_1/(Z_1 + 2Z_0)} \text{ and } \mathbf{Z_{last} = \tfrac{2}{3}Z_1 + \tfrac{1}{3}Z_0}$$

The symmetrical components in fact give average values based on the different self and mutual surge impedances as can be calculated (and measured) for each individual phase conductor. But within a certain accuracy these average values are acceptable. Further, the difference between the equivalent surge impedances is moderate in comparison to the differences in equivalent power frequency reactances. As an indication, the surge impedance of the last clearing pole is about 10% larger than that of the first clearing pole.

From modal analysis it is clear that the surge impedances “seen” by the circuit-breaker are not influenced by the situation at the location of the fault, but they are influenced by the situation of the involved conductors in the vicinity of the circuit-breaker. The mutual effects are depending on whether the other (phase) conductors are connected or not (can conduct or not), as the surge impedances (self, mutual, positive sequence, zero sequence, earth wire, etc.) are only determined by their relative positions and spacings, and not by the short-circuit currents flowing. To determine the surge impedances, it is not relevant whether the fault is a single-phase, double phase, three-phase, grounded or ungrounded fault. In that sense, a single pole operation to clear a single-phase fault (for instance by SPAR: single pole auto-reclosing) gives the same equivalent surge impedance as the first pole clearing a three-phase fault current.

4.1.7 The effect of the high frequency

The higher the frequency of the travelling wave oscillation, the more efficient is the earth as a return conductor. The frequency mainly has an impact on the zero sequence inductances and far less on the positive sequence inductances. As the frequency is depending on the distance to the fault, the zero sequence surge impedance will vary with the distance. However, for the equivalent surge impedances the effect of the frequency is modest: from power frequency up to very high frequencies the equivalent surge impedance will roughly decrease by 5%.

Another effect of the frequency is that, at high frequencies, the rounding of the triangular waveshape due to capacitance close to the circuit-breaker may prevent the TRV from forming a straight section that is proportional to the surge impedance and dI/dt (See also subsections 4.1.4 and section 4.4).

4.1.8 The effect of conductor clashing

One of the phenomena that has a major impact on the value of the equivalent surge impedance is the contraction of bundle conductors, as may happen due to large short-circuit currents. Important questions as whether the bundle will contract and how fast, have already been investigated some decades ago. Figure 4.1, taken from an Électra publication in 1971, gives the twin bundle time-to-clash in seconds as a function of the short-circuit current value.

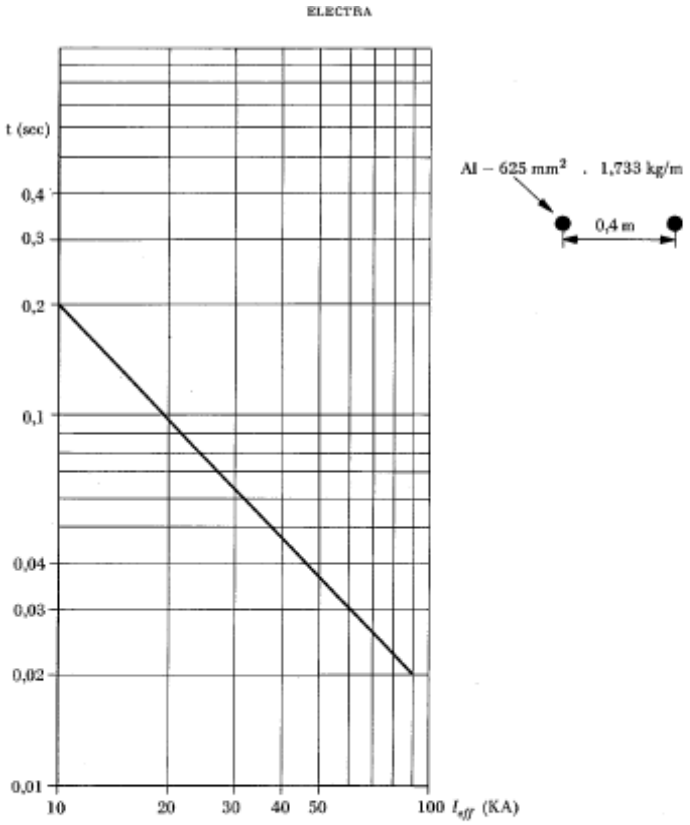

Temps de rapprochement en fonction du courant de court-circuit dans le cas de deux conducteurs par faisceau (exemple calculé)

Time to clash in fonction of the short-circuit current in case of two conductors per bundle (calculated example).

I_{eff} (kA) Courant de court-circuit symétrique (valeur efficace) en kA.

I_{eff} (kA) *Symmetrical short circuit-current in kA r.m.s.*

t (sec.) Temps de rapprochement en seconde.

t Time to clash in sec.

D'après « Brown Boveri » SE 414 091-1

According to "Brown Boveri" SE 414 091-1

Figure 4.1: Twin bundle time-to-clash [8]

If the short-circuit current is large enough the sub-conductors of a bundle will attract and possibly clash. Due to the smaller radius of a contracted bundle, the surge impedance will increase, leading to an equivalent surge impedance that is about 30% higher than that of a bundle in its normal state.

In [8], it is reported that twin conductors show a complete attraction within 100 ms at short-circuit currents between 15 and 20 kA and within 40 ms for currents between 35 and 50 kA (Fig. 4.1). Bundles with 4 sub-conductors are reported to clash between 120 and 450 ms at a short-circuit current of 20 kA and between 60 and 160 ms at 40 kA. In an appendix of [8],

test results from short-circuit tests at KEMA are given for twin conductors: complete attraction after 78, 62 and 31 ms at currents of 18, 26 and 40 kA respectively are reported.

A lot of detailed studies have also been performed theoretically and experimentally by C. Manuzio [11] and others [12][13][14][15], and the clashing condition is now understood quite clearly. Examples of experimental studies using the model line shown in figure 4.2 [15] are given. The clashing time from short-circuit current initiation to sub-conductor impact is summarized in the figures 4.3 to 4.6 for the cases of 2, 4 and 6-bundle conductors of the type TACSR at a power frequency of 50 Hz.

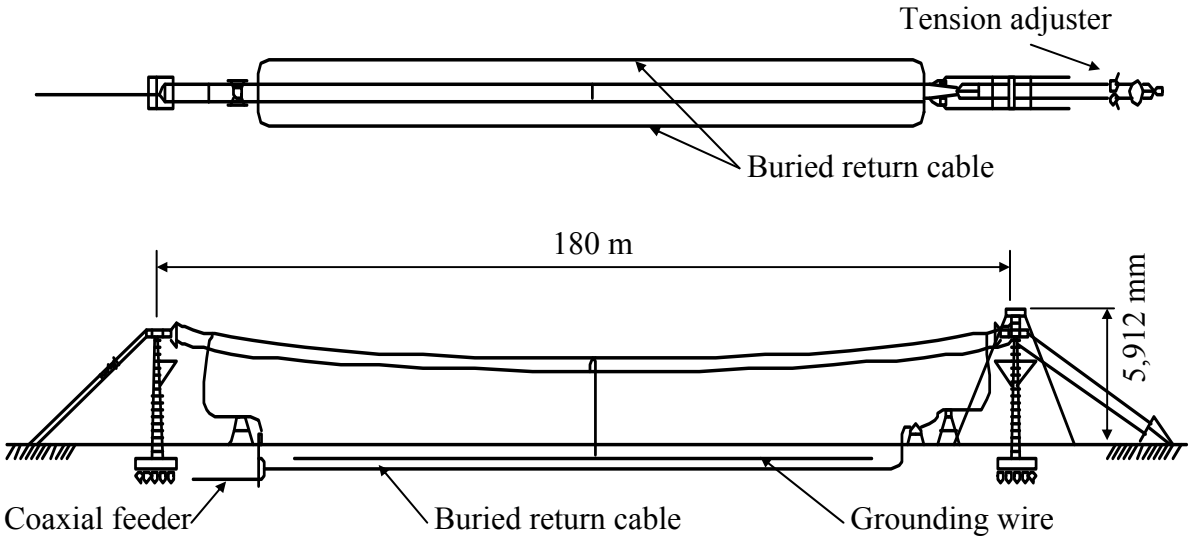

Figure 4.2: Model line for sub-conductor clashing in short-circuit condition

Twin bundle

As clashing of sub-conductors was observed around 2.5 to 3.0 cycles after short circuit current initiation, circuit-breakers would normally clear the faults after sub-conductor clashing. Though a surge impedance at clashed condition is calculated as around 390 to 410 ohms, the surge impedance of 450 ohms specified in IEC is adequate as non-bundled conductor may also be applied for some ratings. The 10% difference of surge impedance will not give significant impact considering the time delay of line side.

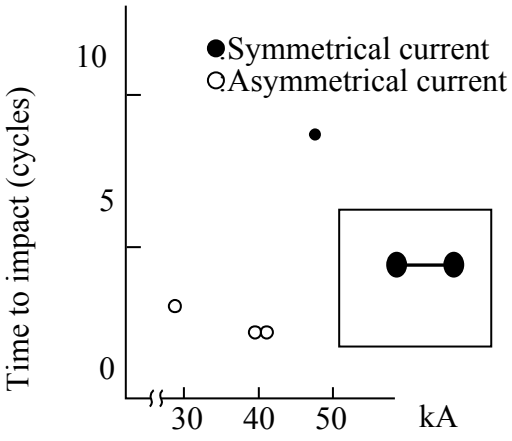

Figure 4.3: Time to impact for twin bundle (Tension :35 kN)

Quad bundle

In this case, conductor clashing was observed 5 to 10 cycles after short circuit current initiation because of higher tension of conductor than the case of a twin bundle. Recent high-speed protection relays and 2-cycle circuit-breakers will offer fault clearing before conductors clashing. The surge impedance at single-phase ground fault of a quad bundle without clashing is calculated as:

$$Z = (Z_0 + 2 Z_1) / 3 = 333 \text{ ohms}$$

where, $Z_1 = 250$ ohms and $Z_0 = 500$ ohms

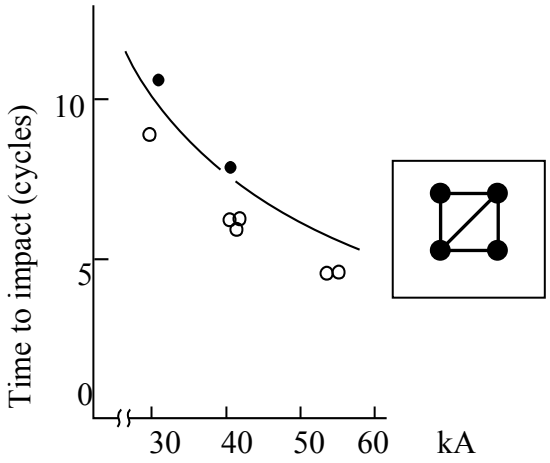

Figure 4.4: Time to impact for a quad bundle (Tension :50 kN)

6-conductor bundle

Slightly shorter clashing times were observed in the case of 6-conductor bundle because of lower tension, but they were still 4 cycles and longer. No clear difference was observed between hexagonal and rectangular arrangement of conductor.

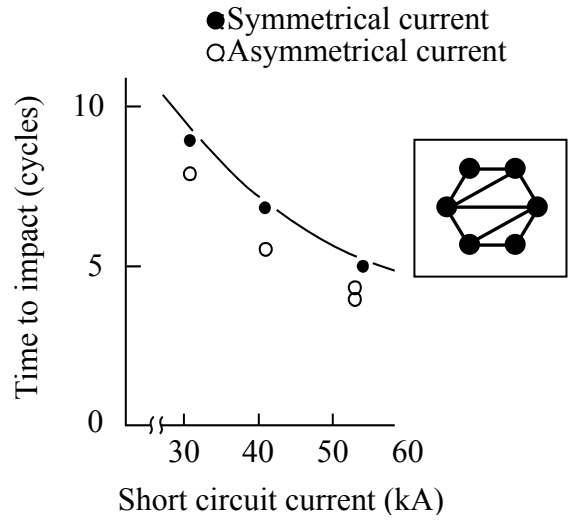

Figure 4.5: Time to impact for 6-conductor bundle (hexagonal), tension 35 kN

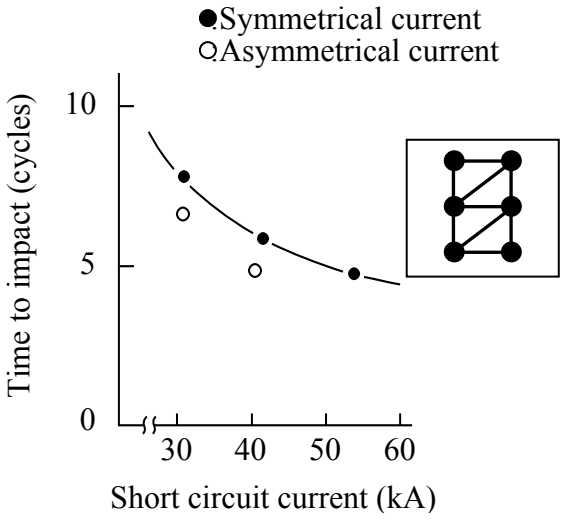

Figure 4.6: Time to impact for 6-conductor bundle (rectangular), tension 35 kN

The theoretical and experimental studies show that it is necessary to consider conductor clashing in the analysis of line side TRV in the case of a twin bundle, but that no conductor clashing was observed for within 4 cycles for 4- and 6-conductor bundles. This means that 450 ohms of line surge impedance is adequate for 275 kV and lower voltage system, where single or twin-bundle conductors are typically applied, but that lower surge impedance could be applied for the higher voltage system by consideration of conductor arrangement, tension, short-circuit current rating and so on.

Of course, the power frequency inductances and stray capacitances will also change due to the bundle contraction. The positive sequence components will change to a higher degree than the zero sequence components. The effect on the short-circuit current will be limited, as for the higher values of the short-circuit current, the line impedance is a small part of the

overall impedance. For instance, at a distance corresponding to L90, a 25% increase of the line impedance will lead to an overall increase of the impedance of only 3%.

4.1.9 The effect of high towers

Towers with higher than normal geometry will give higher surge impedances, as well as higher power frequency inductances. An increase in height of about 10m has an effect of only a few percent, but very high towers, as used for river crossings, may experience an increase in surge impedances of 10 to 20%. At the same time the top phase conductors, that normally show the highest surge impedance of the three phases, will give the lowest surge impedance because of the stronger coupling with the earth wires.

4.1.10 The effect of the earthing resistance in the substation

As the earth return mode of the travelling waves has to pass the earthing resistance of the substation where the circuit-breaker is located, this resistance has an influence on the equivalent surge impedance as well. For substations with a normal earth resistance of only a few ohms the impact will be negligible, but resistances up to 100 Ω may cause increases in equivalent surge impedances of 10 to 20%.

4.1.11 Summary of parameters influencing the surge impedance

The largest impact on the value of the surge impedances is from bundle conductor contraction; this will give a surge impedance for the last clearing pole of up to 450 Ω. Single conductors will also show also a surge impedance close to 450 Ω but a value around 330 Ω is more realistic for a bundled conductor system.

The first clearing pole will face an equivalent surge impedance that is about 10% less and the presence of another circuit on the same towers gives a further 10% reduction of surge impedance. Conversely, lower frequencies due to substantially longer distances to the fault will lead to an increase of several percent, as will a higher earth resistivity. The lack of earth wires lead to a higher equivalent surge impedance (for instance +8%) as does the use of extra high towers such as those used for river crossings (about +15%).

The equivalent surge impedance of the last clearing pole clearing a three phase fault is not the same as that of the pole clearing (as with SPAR) since the other poles that are still conducting have an impact on the equivalent surge impedance. Single pole operation in case of a single-phase to earth fault (or the first pole clearing a single-phase fault) gives an equivalent surge impedance equal to the equivalent surge impedance of the first pole to clear a three-phase fault.

4.2 The effect of the distance to the fault at SLF

The distance to the fault has an influence on the travelling time of the travelling waves and thus on the frequency of the line side TRV, as discussed above. The distance to the fault also has an impact on the amplitude of the short-circuit current, as the line impedance up to the fault will lead to a reduction of the short-circuit current, taking a busbar fault as the reference for the short-circuit current.

The ratio between a single-phase short-circuit current and a three-phase short-circuit current depends on the X_0/X_1 ratio at the busbar and the X_0/X_1 ratio of the involved line. The ratio for a line does not vary much and a factor of three is normally used but the X_0/X_1 ratio at a substation can vary substantially. The lines that supply a part of the short-circuit current will

show the ratio of about three while local sources fed through transformers may show a ratio less than one. A substation with 70% local contribution to the short-circuit current and 30% through overhead lines will, based on the factors 3 and 0.8, give an overall X_0/X_1 ratio close to 0.9. In such a case the single-phase short-circuit current at the busbar is higher than the three-phase short-circuit current. Many utilities experience in their substations single-phase short-circuit currents larger than the three-phase short-circuit currents.

Since, for an overhead line, X_0 is larger than X_1, at a certain distance to the fault the single-phase fault current and the three-phase short-circuit current become equal and beyond that distance the three-phase short-circuit current will always be larger than the single-phase current. As an exercise to estimate where this break-even point may be located, it is assumed that at the busbar the single-phase short-circuit current is 5% larger than the three-phase short-circuit current, corresponding to the X_0/X_1 ratio 0.88, given above. The equilibrium can be found at a distance that corresponds to a reduction of the three-phase short-circuit current of 6%. For single-phase short-circuit currents at the busbar as large as 125% of the three-phase short-circuit current, the equilibrium is found at a distance corresponding to a 12% reduction of the three-phase short-circuit current. In both cases this location is close to that of L90.

It is noteworthy that for SF_6 gas technologies, L90 is widely recognized as the (single phase) SLF test duty at the most critical current/distance with criticality being judged in the sense of RRRV = 450 Ω * dI/dt. With this in mind, three-phase SLF conditions may be compared with single phase SLF, under the assumption of an equal RRRV, an equal distance to the busbar or an equal dI/dt. With the 100% short-circuit power at the busbar and a X_0/X_1 ratio of 1.0 at the busbar, the three cases lead to locations of the three-phase fault in comparison to single phase L90, that correspond to:

1. Equal RRRV: L99 (three-phase)
2. Equal distance: L93 (three-phase)
3. Equal dI/dt: L90 (three-phase).

4.3 The excursion factor

The excursion factor or d-factor (called peak factor k to IEC) has been discussed in a former Chapter, but some particularities are further illustrated here, starting with the case of the last clearing pole. The d-factor has been defined as the ratio of the first peak of the TRV at the line side (due to the travelling waves) to the initial voltage at the circuit-breaker terminals. The initial voltage is given by $\mathbf{L_L(lf)\times dI/dt}$ with $\mathbf{L_L(lf)}$ being the inductance of the line between circuit-breaker and fault location, determined at power frequency (low frequency: lf).

The first peak of the TRV at the line-side is given by $\mathbf{Zeq\times dI/dt\times 2\, l_L/c}$ with $\mathbf{l_L}$ being the line length between circuit-breaker and fault. As $\mathbf{Zeq = \sqrt{(L'/C')}}$ and $\mathbf{c = 1/\sqrt{(L'C')}}$, with $\mathbf{L'}$ the equivalent inductance per metre and $\mathbf{C'}$ the equivalent capacitance per metre then $\mathbf{Zeq/c = L'}$ and $\mathbf{2\, l_L\times L' = 2\, L_L(hf)}$, i.e. the inductance of the Overhead line determined at the high frequency of the oscillating travelling waves. The ratio of first peak of the TRV and the initial voltage is thus:

$$\mathbf{d = 2\, L_L(hf)/L_L(lf)} \qquad (4.2)$$

For faults at a further distance, the high frequency inductance will increase and approach the power frequency inductance, while for shorter distances the difference is substantial. The positive sequence inductance is decreasing only a few percent, but the zero sequence inductance will decrease by several tens of percent, giving a decrease of the equivalent inductance of about 20% for faults at a distance of a few km. In such a case, the excursion factor becomes less than 1.6.

In this analysis the damping of the travelling waves has not been taken into account. A damping effect may also result from the difference in propagation speed between the zero sequence waves and the positive sequence waves, although for higher frequencies both velocities approach the speed of light c.

In the IEEE Application Guide C37.011 (2005) [16], it is stated that a conservative estimation of the d-factor is by the formula (A29):

$$\mathbf{d = 0.4\ (2 + Z_0/Z_1)} \qquad (4.3)$$

Equation 4.2 can be rewritten in sequential components:

$$\mathbf{d} = 2 \times \frac{2L_L1(hf) + L_L0(hf)}{2L_L1(lf) + L_L0(lf)} \qquad (4.4)$$

As the positive components are hardly influenced by the frequency, the formula becomes:

$$\mathbf{d} = 2 \times \frac{2 + \dfrac{L_L0(hf)}{L_L1(lf)}}{2 + \dfrac{L_L0(lf)}{L_L1(lf)}} \qquad (4.5)$$

And, with $\mathbf{L_L0(lf)}$ being about 3 times $\mathbf{L_L1(lf)}$:

$$\mathbf{d} = 0.4 \times \left(2 + \frac{L_L0(hf)}{L_L1(lf)} \right) \qquad (4.6)$$

Knowing that the wave propagation is approximately **c**, the speed of light, and that **c** is therefore equal to $\mathbf{1/\sqrt{(L_L0(hf) \times C0)}}$ as well as to $\mathbf{1/\sqrt{(L_L1(lf) \times C1)}}$, the ratio $\mathbf{Z_0/Z_1}$ can be transformed into $\mathbf{(Z_0/c)/(Z_1/c) = L_L0(hf)/L_L1(lf)}$, thus making both formula 4.3 and 4.6 approximately equal to each other.

For the first clearing pole, essentially the same formula for the excursion factor is applicable, $\mathbf{d_3 = 2 \times L_L(hf)/L_L(lf)}$, but $\mathbf{L_L(hf)}$ and $\mathbf{L_L(lf)}$ are made up of other sequential components such that:

$$\mathbf{L_L(hf) = 3\ \{L_L0(hf)\}/\{1 + 2L_L0(hf)/L_L1(hf)\}} \qquad (4.7)$$

$$\mathbf{L_L(lf) = L_L1(lf) = L_L1(hf)} \qquad (4.8)$$

$$\mathbf{d_3 = 6\ \{\kappa/(1 + 2\kappa)\}} \qquad (4.9)$$

with $\mathbf{\kappa = L_L0(hf)/L_L1(hf)}$ (4.10)

A ratio of $\kappa = 2$, gives $\mathbf{d_3} = 2.4$. An excursion factor that is about 50% higher for the first clearing pole than for the last clearing pole is also found with the calculations and simulations discussed in a later chapter. Further, $\mathbf{d_3} = 2.4$ is exactly 50% higher than the value d = 1.6, as specified in the Standards. Note that where $\mathbf{L_L0(lf)}$ is about $\mathbf{3\times L_L1(lf)}$, for high frequency yields: $\mathbf{L_L0(hf)}$ is about $\mathbf{2\times L_L1(hf).}$

4.4 The time delay

The distributed capacitances and inductances of the overhead line lead to the well-known travelling waves and their relationships expressed by surge impedances. Lumped capacitances, as may appear at the line entrance, interfere with the linear triangular patterns of the travelling waves in the sense that they are delaying the initial parts of each reflection. The time delay **C×Z** leads to some rounding of the triangular waveshape, as shown in figure 4.7, that has been taken from Fig. 9 of CIGRÉ Technical Brochure 305 [17].

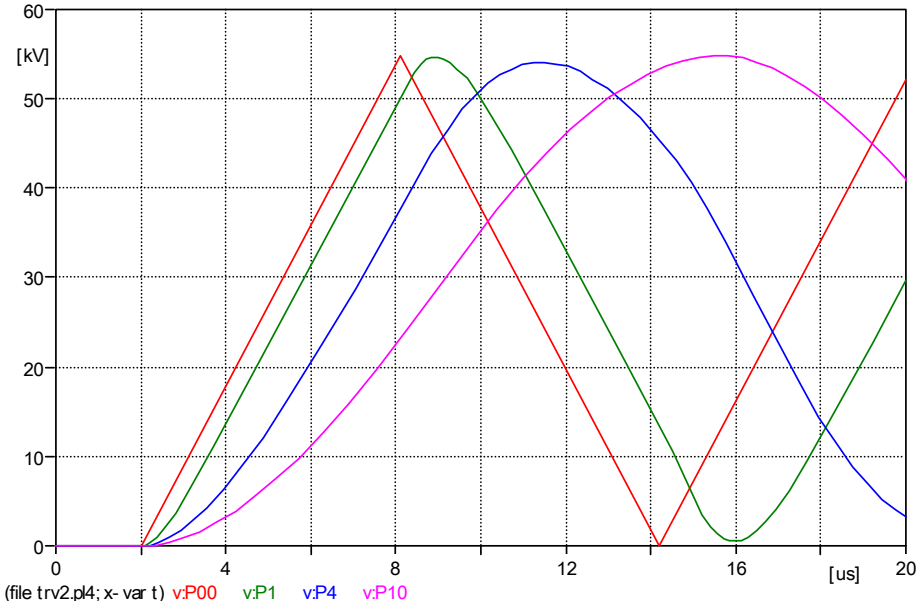

Figure 4.7: Effects of Capacitor Size on the Short-line Fault Component of Recovery Voltage for a fault 915 m from circuit-breaker. Parallel capacitance C = 0, 1.11, 4.44, and 11.1 nF

As explained in subsection 4.1.4, the value of the equivalent surge impedance can be determined by measuring **dU/dt**. The procedure described in the Standards prescribes to use the 10% and 90% values of the recovery voltage to determine the equivalent surge impedance. By following this procedure to determine the equivalent surge impedance, the effect of an additional capacitance is that the surge impedance may appear to become smaller. The higher the frequency of the triangular waveshape, the more dominant this effect will be.

In some designs of high-voltage circuit-breakers, additional capacitors are applied to the circuit-breaker in order to improve their SLF performance. Such capacitors are installed either across the arcing chamber(s) or between one terminal and earth. Between these two possible applications there is a difference in the impact on the initial part of the TRV waveshape, as explained in section 5.4.2.4 of [17]. Neither application will show a difference between the single-phase SLF performance and three-phase SLF performance of the circuit-breaker. This is obvious for application across the arcing chambers, but applies also for

additional capacitors to earth. This is due to the fact that for the very initial part of the TRV, only the capacitances of dedicated apparatus have to be taken into account (CVTs, bushings, additional capacitance), all of which show only a capacitance to earth. Thus, in all cases, the positive sequence capacitance C_1 is equal to the zero sequence capacitance C_0, and consequently no difference is experienced by the first clearing pole in comparison to the last clearing pole.

4.5 The effect of distance to the fault at LLF

While SLF tests were originally introduced to verify the interrupting capability in the thermal region of the extinction process, long-line fault phenomena typically address the dielectric recovery of the contact gap of a circuit-breaker. Long-line faults (LLF) are faults far away from the circuit-breaker that, nevertheless, give a triangular waveshape of the line-side TRV. For LLF the short-circuit current is relative low, for instance 10% to 30%, meaning that the RRRV is much lower than that for SLF. On the other hand, the long distance to the fault implies that the travelling time forwards and backwards gives a slow but steady increasing TRV value that can reach values beyond the peak value of T30, T10 or even OP.

As shown in section 4.3, the peak value or excursion factor, d, can be expressed as twice the ratio between the high frequency and power frequency inductance of the line. In case of LLF, the frequency is rather low and the ratio will be close to 1.0. Therefore the line-side peak can approach: $\mathbf{2\ X_L \times I_{LLF}}$. As $\mathbf{I_{LFF} = E/(Xs + X_L)}$, the line-side peak value depends on the ratio between the equivalent line reactance up to the fault and the source reactance up to the busbar:

$$\mathbf{Eline} = \mathbf{E} \times \frac{\mathbf{2X_L}}{\mathbf{Xs} + \mathbf{X_L}} \qquad (4.11)$$

Examples in the next Chapter will show that the resulting peak may reach values higher than TRV peak values corresponding to type test with similar short-circuit currents. In Part III, Chapter 12, the implications of this will be discussed and the potential influence of travelling waves at the source side will be addressed as these may lead to an additional TRV stress.

4.6 The arcing window

Although not directly of influence to the TRV waveshape, attention has to be paid to the arcing window, as the required arcing window may be different for clearing single-phase faults and for clearing three-phase faults. For single-phase faults the arcing window that has to be covered corresponds to almost 180° (180° -18º = 162º according to IEC).

For three-phase faults the arcing window for the first clearing pole has to be almost 60°, as afterwards another pole will act as the first clearing pole. But, in order to cover also the last clearing pole, single-phase test conditions for three-phase fault simulation require a maximum arcing time of 60° plus a further 90° or 120° for systems with non-effectively and effectively earthed neutral, respectively. So, depending on the neutral treatment of the system, three-phase SLF requires an arcing window of almost 150° (150º– 18º= 132º) instead of 180°, as required for single-phase SLF (See Table 4.2).

Table 4.2: Required minimum interrupting window for each pole to clear in the case of a three-pole circuit-breaker during SLF interruption

Type of fault and system	First clearing pole	Second clearing pole ° (el. degree)	Third clearing pole ° (el. degree)	Interrupting window ° (el. degree)

	° (el. degree)			
Three-phase fault in systems with non-effectively earthed neutral	0 - 42	90 - 132	90 – 132	132
Three-phase fault in systems with effectively-earthed neutral*	0 - 42	77 - 119	120 – 162	162
Single-phase fault in systems with solidly earthed neutral	0 - 162	NA	NA	162

* : in addition, the neutral must be solidly earthed to have the required SLF conditions.

5. Simulations and calculations of line fault TRVs

Within WG A3.19 line fault TRVs were assessed with ATP and EMTP simulation software. Several tower geometries of overhead lines from Germany and Canada with different rated voltages were simulated and both 100% and 80% of the rated source short-circuit power were taken into account. Simulation results are presented in Appendices A and B. Besides the calculation of actual equivalent surge impedances for all clearing poles of a three-phase fault, some parameters have been varied in order to get an understanding of their impact on the TRV waveshape. TRV parameters have been evaluated for short-line fault (SLF) and long-line fault (LLF).

5.1 EMTP simulation model

Figure 5.1 shows a typical circuit diagram that was used for the EMTP simulations: single circuit line for U_r= 230 kV, k_{pp}= 1.5 (Fig. 5.1a) and double-circuit line for U_r= 230 kV, k_{pp}= 1.5 (Fig. 5.1b).

For 100% of the rated short-circuit current, the source parameters are:
- First-pole-to-clear factor, k_{pp}= 1.5 or 1.3 by changing the source neutral impedance: infinite value for k_{pp}= 1.5, X_N= 0.75 X_1 for k_{pp}= 1.3.
- TRV parameters: RRRV= 2.0 kV/μs, k_{af}= 1.4 with the appropriate RC branch for adjusting the TRV parameters

For 80% of the rated short-circuit current, the source parameters are:
- First-pole-to-clear factor k_{pp}= 1.5 or 1.3
- TRV parameters: RRRV= 2.5 kV/μs, k_{af}= 1.4 with the appropriate RC branch for adjusting the TRV parameters

A local capacitance C_0 is added in order to represent some measuring equipment at the line terminal. The line model is built by providing the following information:
- a complete geometry of the conductor wires (single or bundled conductor, phase numbering, wire diameter, horizontal distance between phase conductors, vertical height of each phase conductor, etc.
- line length to be adjusted according to the amplitude of the required short-circuit current;
- DC resistance of the conductor wires (Ω/km);
- a skin effect correction factor of 0.36;
- selection of a frequency dependent (FD) line model, thus simulating the true nature of a transmission line by modelling the line parameters as distributed and frequency dependent;
- selection of the "Real T_i" matrix option, thus allowing EMTP to automatically calculate the optimum frequency (Model frequency) at which to evaluate this real constant transformation matrix;
- ground return resistivity of 100 ohm.m;
- for the double line circuit, the three-phase line fault was applied on one circuit line while the other circuit line is carrying a typical load current;
- power frequency = 60 Hz;
- non-transposed line;
- the three-phase fault was regarded as having no arc resistance and no resistance to earth.

5.2 ATP simulation model

Figure 5.2 shows typical circuit diagram that was used for the ATP simulations: double circuit line for U_r= 145 kV, k_{pp}= 1.5 (Fig. 5.2a) and double-circuit line for U_r= 420 kV, K_{pp}= 1.0 (Fig. 5.2b).

The same simulation parameters as described in section 5.1 for EMTP software were used, except the following ones:

- First-pole-to-clear factor (k_{pp}= 1.5, 1.3 and 1.0)
- power frequency= 50 Hz
- JMarti model based on infinite long lines which is also a frequency dependent model;
- transposed line.

5.3 Calculated values

In the tables of Appendices A et B, the following parameters are given:

- rated voltage (U_r);
- short-circuit current amplitude (I_{SC}) and the corresponding SLF test duty (L60, L75, L90) or LLF fault current percentage (L10, L30);
- for Canadian overhead lines, line TRV parameters are also given for a SLF fault current percentage of 95% (L95);
- line length adjusted for the required short-circuit current amplitude;
- line TRV parameters for the three poles (Appendix A) and for the first-pole-to-clear (Appendix B) comprising: line residual voltage (u_0), line TRV peak ($\hat{U}_L$), line TRV time-to-peak (t_L), d factor and line TRV slope (S_L);
- TRV parameters across breaker terminals (line + source) of the first peak of the first-pole-to-clear including: TRV peak (u_p), TRV time-to-peak (t_{LS}) and TRV slope (S_{LS});
- current slope (di/dt);
- line surge impedance (Z_L) as seen by the first-pole-to-clear (Appendix B) and calculated by dividing the line TRV slope (S_L) over the current slope (di/dt).

The TRV slopes were calculated by taking the best straight line (10%-90% method) that can be traced on the simulated TRV waveforms. This evaluation method causes some scattering in the surge impedance value, as can be observed in the calculated Z_L (last column, Appendices A and B).

5.4 Simulation result analysis

In section 6 below, simulated TRVs for which parameters are given in Appendices A and B are compared with Standardised values. It is relevant here to focus on two key line TRV parameters: the d factor or excursion factor and the line surge impedance. For the d factor or excursion factor, the following conclusions can be drawn from the simulation results in Appendices A and B:

- for the first-pole to clear, the excursion factor varies from 2.2 to 2.5, being roughly 1.4 to 1.5 times the excursion factor for the last clearing pole;

- the excursion factor is higher on the first-pole-to-clear than on the second-pole-to-clear since the induced voltage contribution is reduced on the second pole while a short-circuit current only remains in the third pole when the second pole interrupts;
- the excursion factor on the third pole corresponds to the Standard value, i.e. as in the case of the short-circuit current interruption of a single-phase short-line fault;
- the first-pole-to-clear factor (k_{pp}= 1.5, 1.3 or 1.0) does not have any influence on the excursion factor since the latter is dictated by the induced voltages generated by the mutual inductances between phases and short-circuit amplitudes;
- the distance to the fault (L90, L75, L60, L30, L10) does not have a significant influence on the excursion factor;
- as in the simulations the fault location is kept the same for the first, second and last clearing pole, the short-circuit current per interrupting pole is slightly different, as can be seen in Appendix A. The time to the line-side peak value of the TRV has therefore to be identical for all three poles. Thus, the total voltage jump $\mathbf{(u_0+\hat{U}_L)}$ is almost identical for the three phases but, for the same three poles, the initial voltage $\mathbf{(u_0)}$ is different, due to the mutual effect, and therefore $\mathbf{d = (u_0+\hat{U}_L)/u_0}$ is differing.

For the line surge impedance which is directly linked to the line TRV slope, the simulation results reveal that:

- the calculated line surge impedance is generally lower than the Standard value of 450 Ω with a lower limit of roughly 300 Ω and an upper limit approaching 430 Ω. However bundle contraction has not be taken into account. The values close to the upper limit appear only for lines with a single conductor per phase.

a)

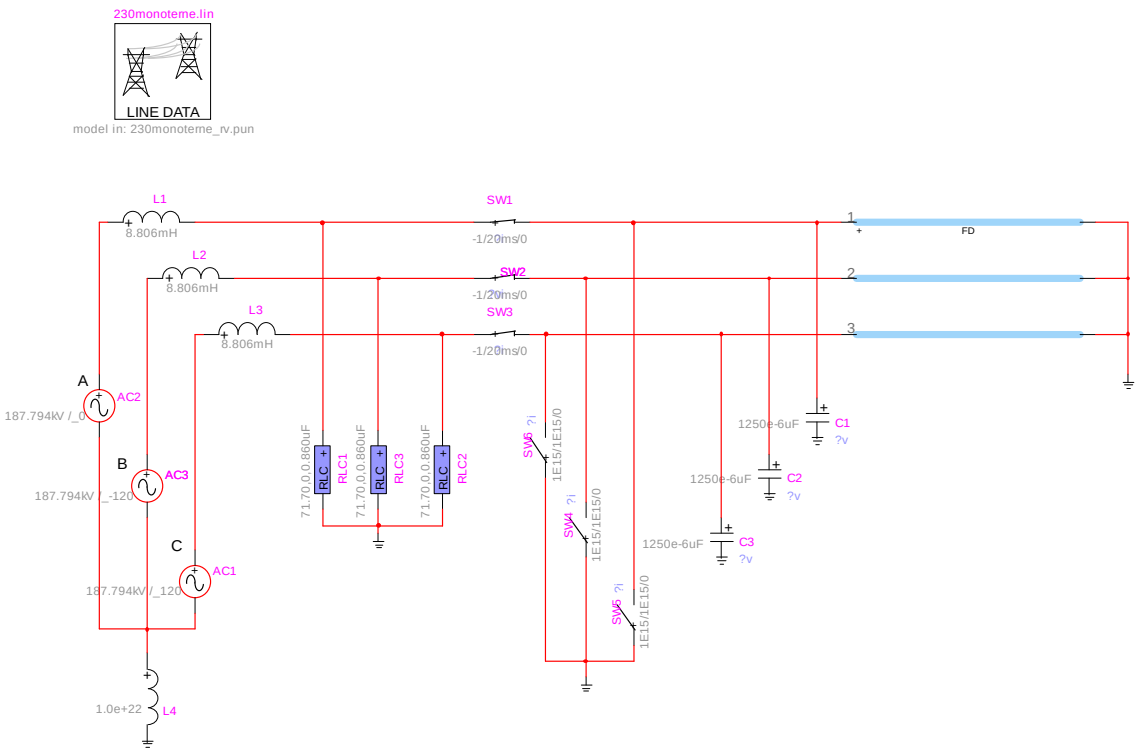

b)

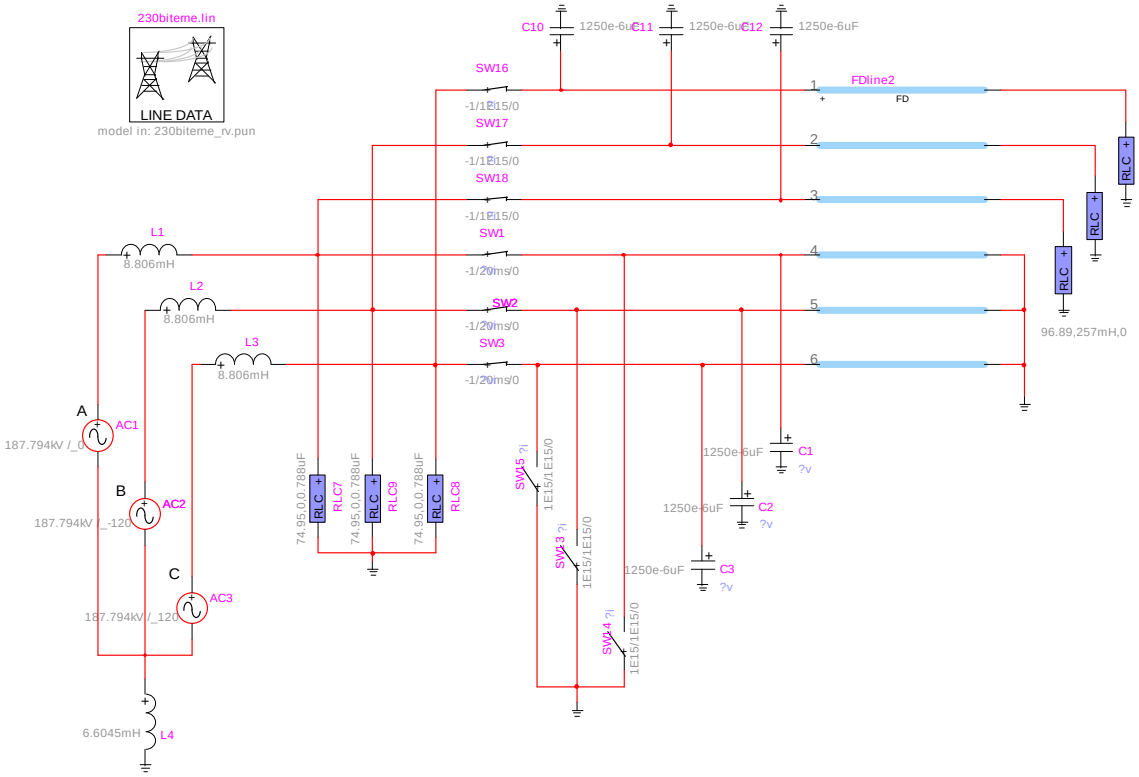

Figure 5.1: Typical EMTP circuit diagram used for calculating the line fault TRVs
a) Single circuit line, U_r= 230 kV, f_r= 60 Hz, , source I_{Sc}= 40 kA k_{pp}= 1.5
b) Double circuit line, U_r= 230 kV, f_r= 60 Hz, source I_{Sc}= 40 kA, k_{pp}= 1.3

a)

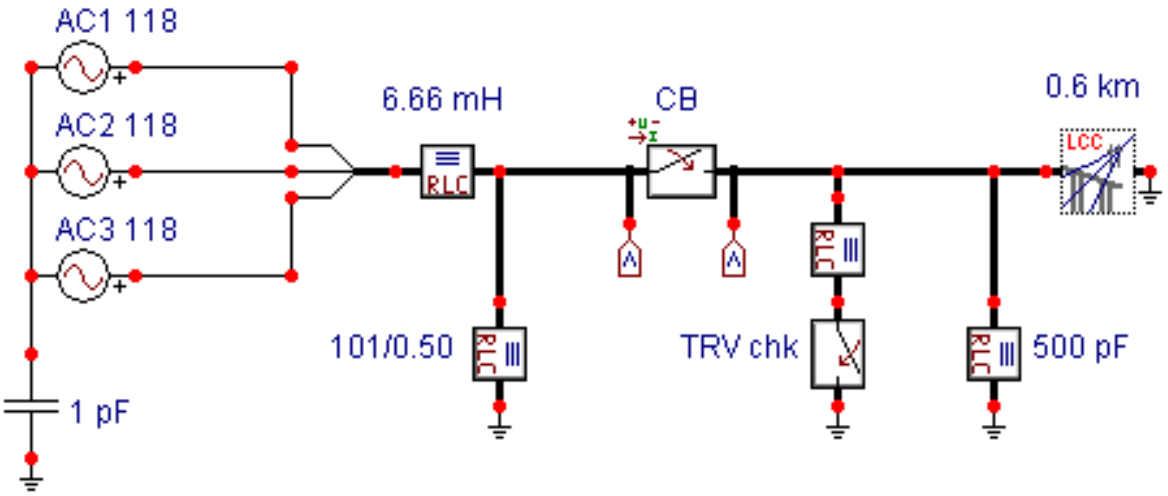

b)

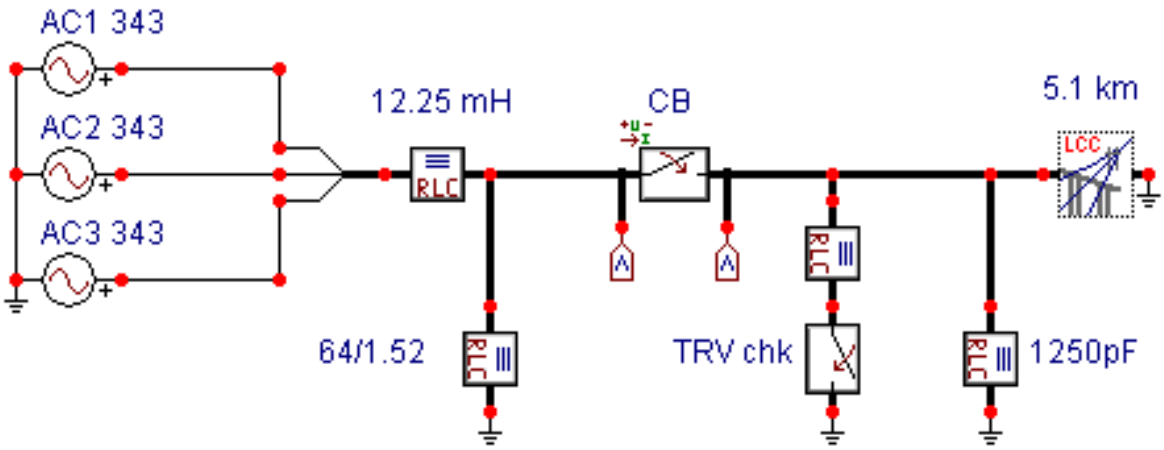

Figure 5.2: Typical ATP circuit diagram used for calculating the line fault TRVs
a) Double circuit line, U_r= 145 kV, f_r= 50 Hz, source I_{SC}= 40 kA, k_{pp}= 1.5
b) Double circuit line, U_r= 420 kV, f_r= 50 Hz, source I_{SC}= 63 kA, k_{pp}= 1.0

6. Comparison with the Standard TRV values

In the following diagrams, three typical cases are considered and the calculated TRV values are compared with the IEC standard values:

- 420kV, 63kA, 50Hz, $k_{pp} = 1.3$
- 245kV, 50kA, 60Hz, $k_{pp} = 1.3$
- 145 kV, 40kA, 50Hz, $k_{pp} = 1.5$

The comparison has been divided in two groups of line faults:

- 3-phase SLF
  - the IEC TRVs for short-line fault (L90, L75 and L60) have been considered as reference.
  - additionally the T100 and T60 TRV profiles are shown.
  - from the calculation, only the 1st voltage peak has been considered at clearing 90%, 75% and 60% of the rated short-circuit current.
  - the comparison is done for 100% and 80% of the source short-circuit power
- LLF
  - the IEC reference values are the TRVs for T30, T10 and OP.
  - from the calculated cases, 1st TRV peak and maximum peak (when higher than the 1st peak) are shown together and connected by a (dashed) line.
  - the comparison is done for 100% and 80% of the source short circuit power (in Chapter 9 attention will be given to a lower short-circuit power at the busbar).
  - for every fault case, the values of the 1st and the 3rd pole-to-clear are considered.

Note that the compared TRV values are those across the breaker terminals, i.e. source-side TRV minus the line-side TRV. The reference values are taken from:

- TRV Calculation for Short Line Fault according to ANNEX A (IEC62271-100 Ed.1.2, 2006-07)
- TRV Specification according to IEC 62271-100 Ed. 2.1, for the revised edition [3].

TRV calculations also show in all cases that when clearing three-phase short-line faults, the TRV waveshapes give higher peak values at the line-side than specified in the Standards for single phase faults. For one case (420 kV, 63 kA, 50 Hz, L30), the peak value for a long line fault is a little beyond the TRV envelope as specified in the Standards for the terminal fault test duties T30 and T10, and for the out-of-phase test duty OP, but may be regarded as covered by the combination of T30 and OP.

So far, from many cases calculated, the results confirm the trends observed in the early days as well as observed by Anders Johnson in his Master Thesis [4], and published in Report 13-103 at the CIGRE SC 13 Session 2002 [1].

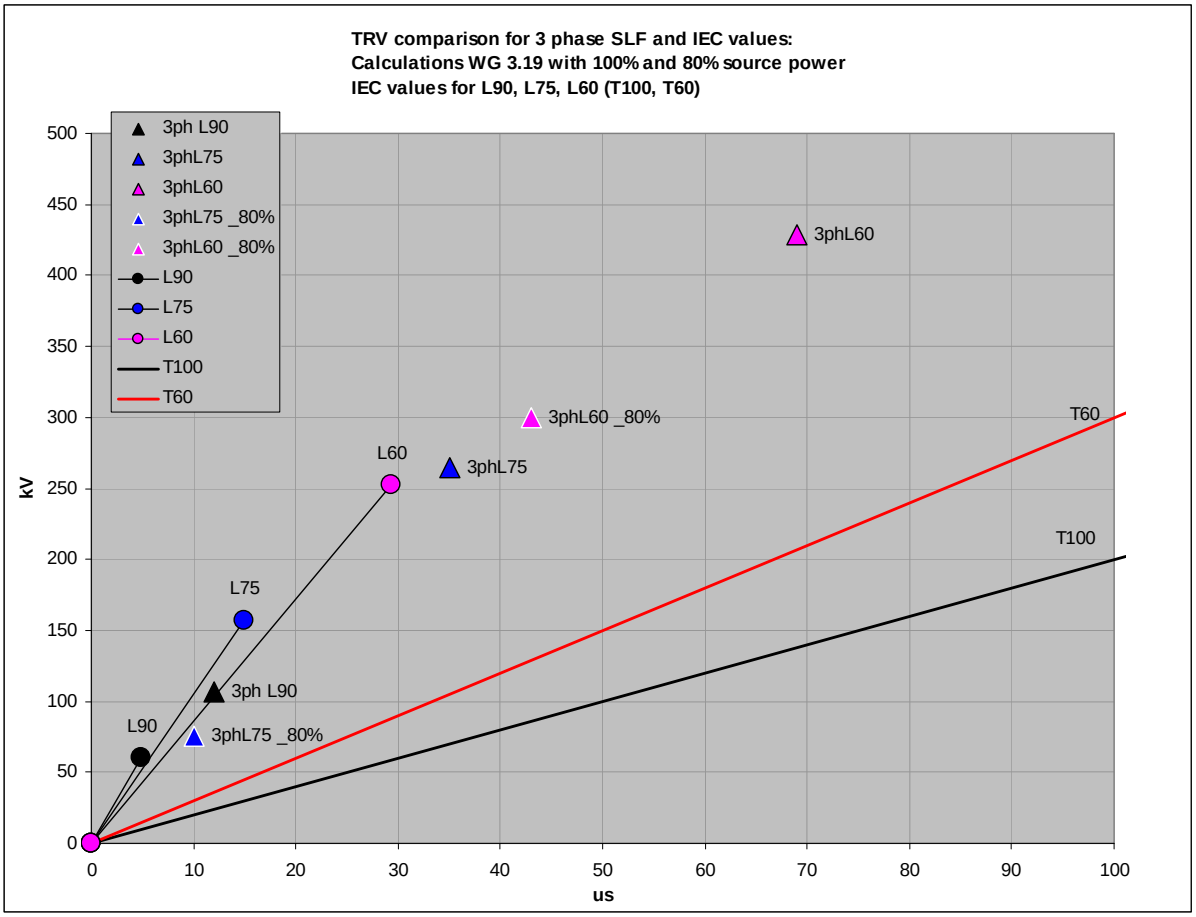

Figure 6.1: 3 ph SLF, 420kV, 63kA, 50Hz, 100% and 80% of the source short circuit power

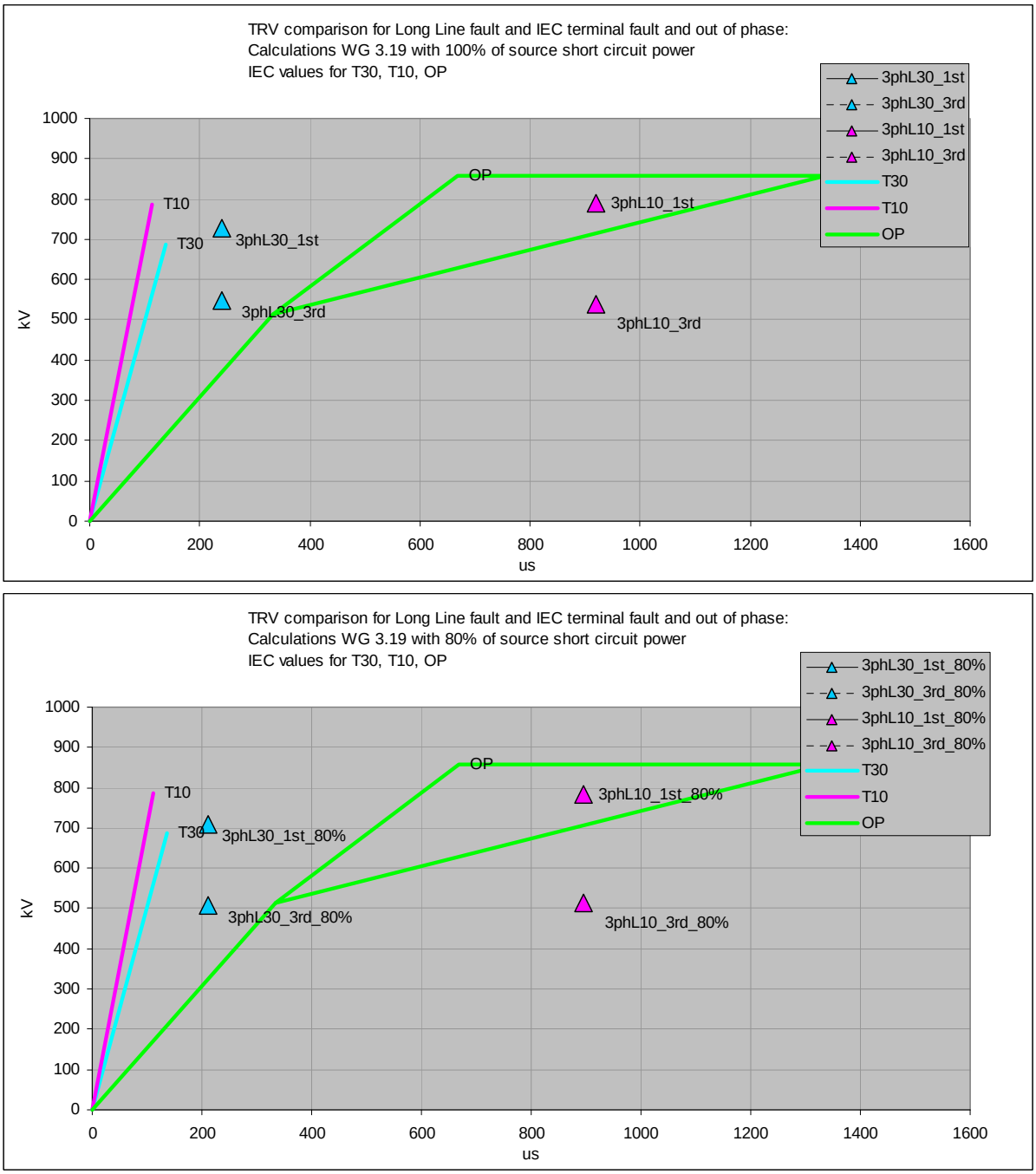

Fig. 6.2: Long line fault 420kV, 63kA, 50Hz, 100% and 80% of the source short circuit power

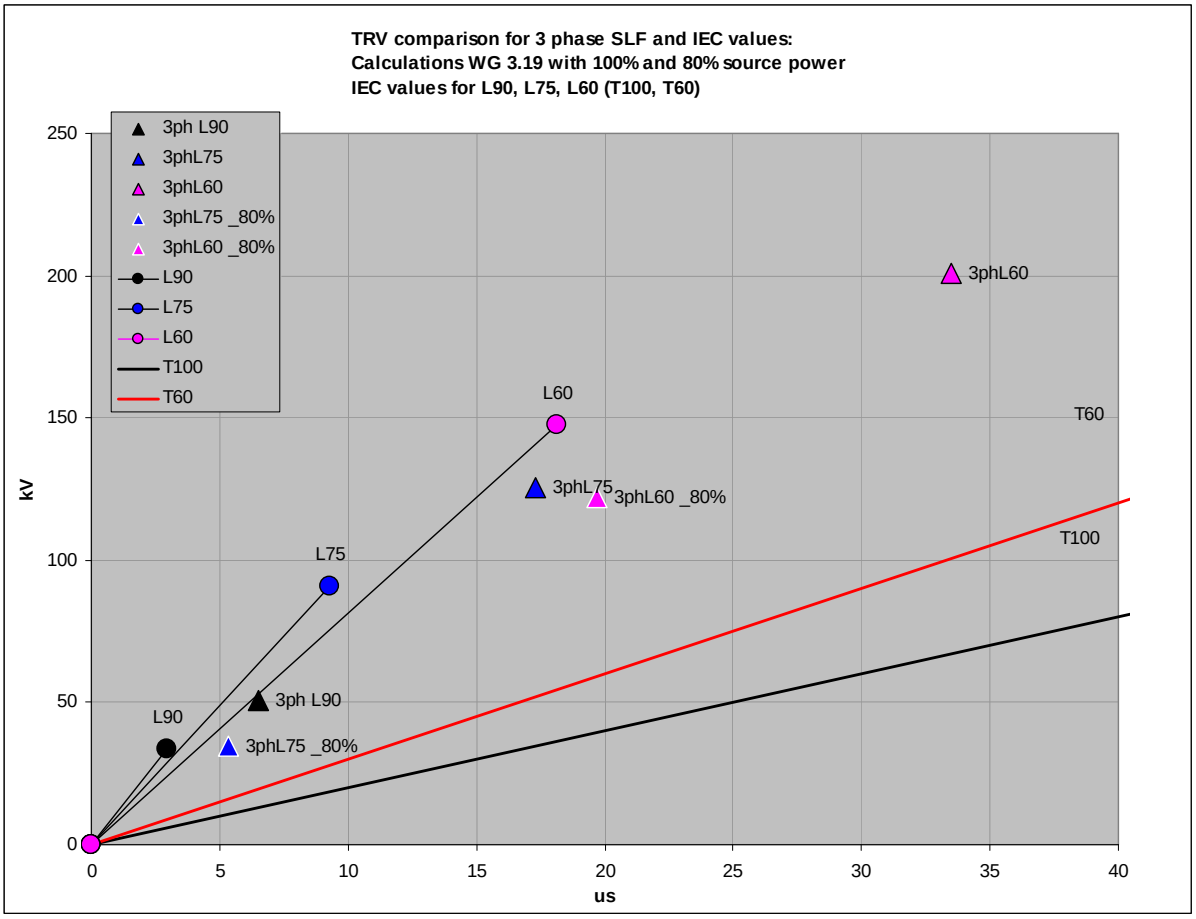

Figure 6.3: 3 ph SLF, 245kV, 50kA, 60Hz, 100% and 80% of the source short circuit power

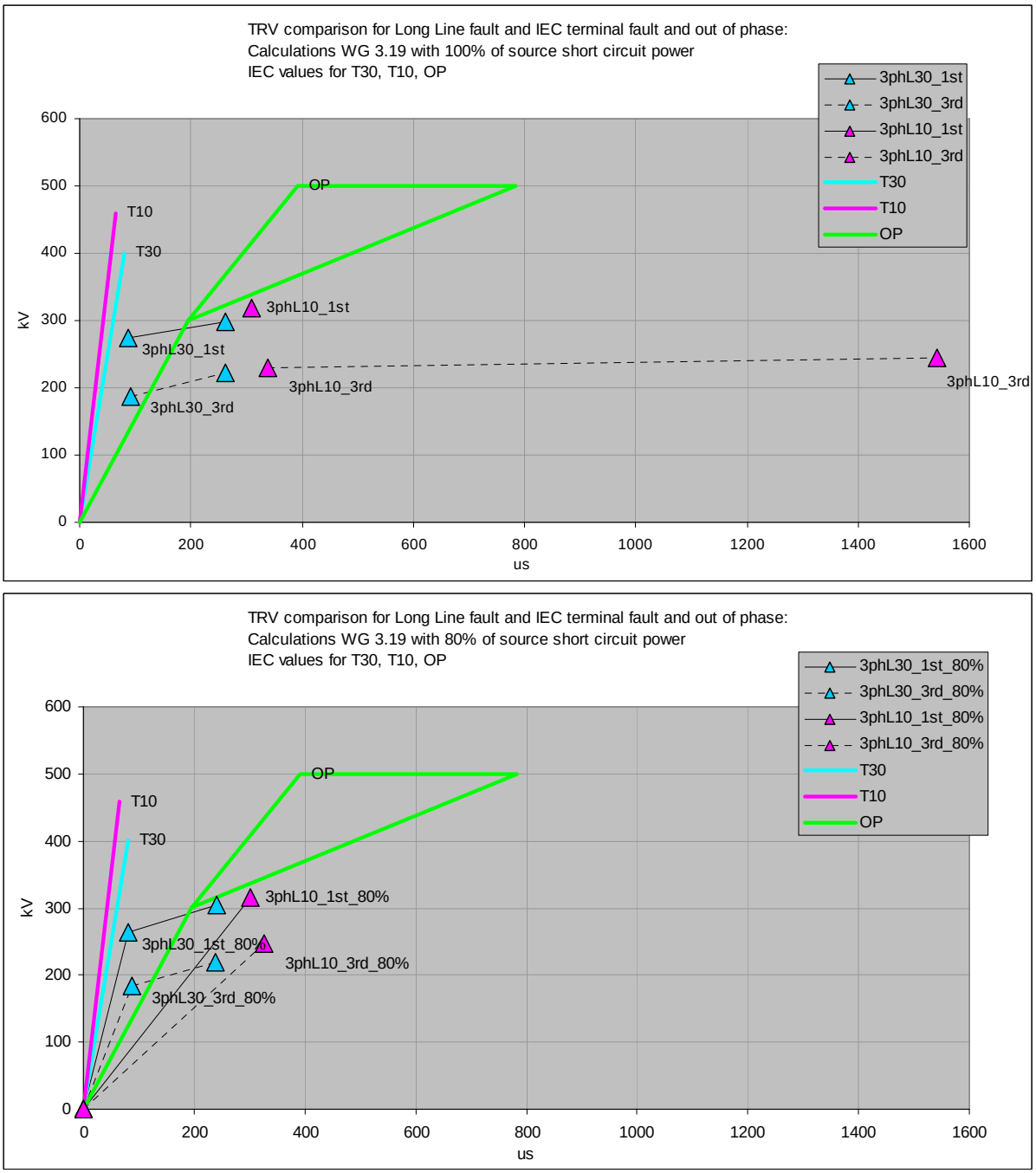

Fig. 6.4: Long line fault 245kV, 50kA, 60Hz, 100% and 80% of the source short circuit power

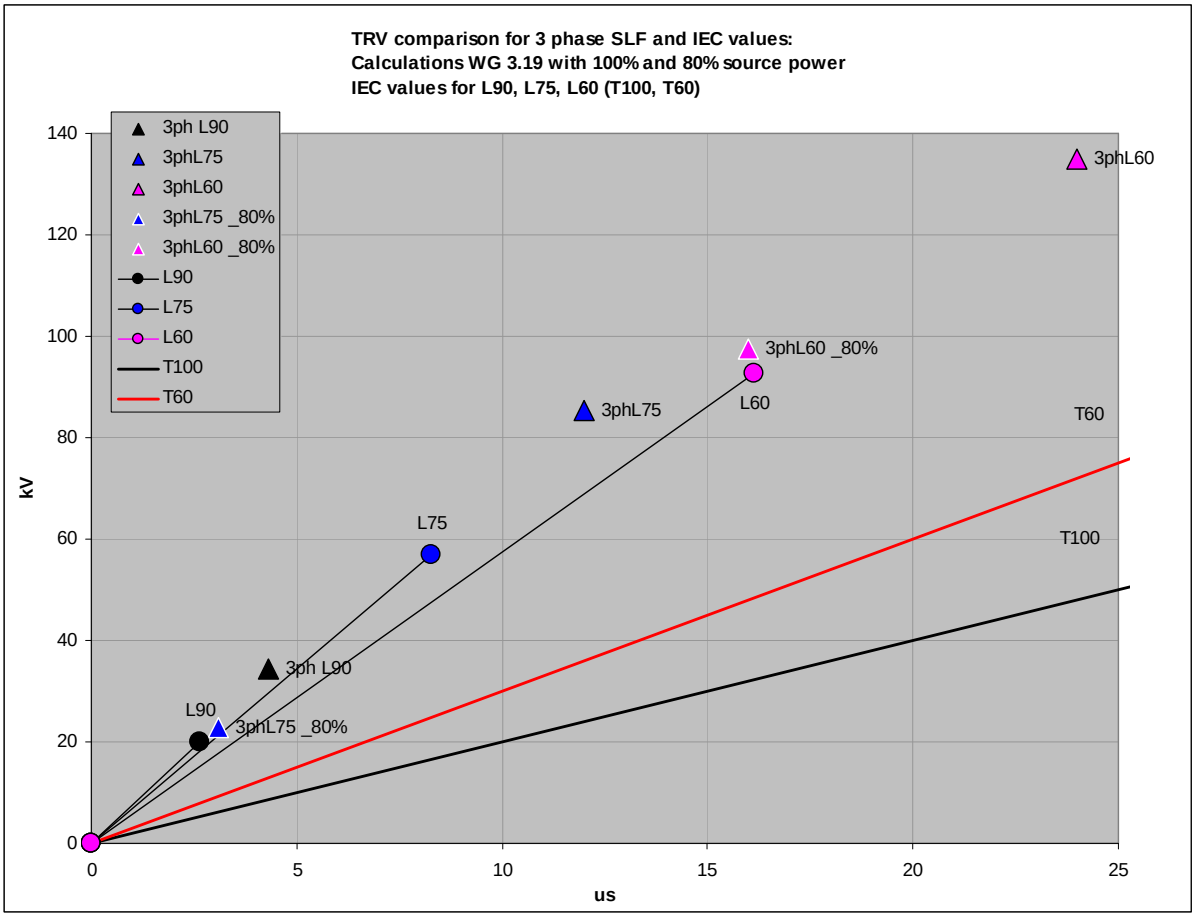

Figure 6.5: 3 ph SLF, 145kV, 40kA, 50Hz, 100% and 80% of the source short circuit power

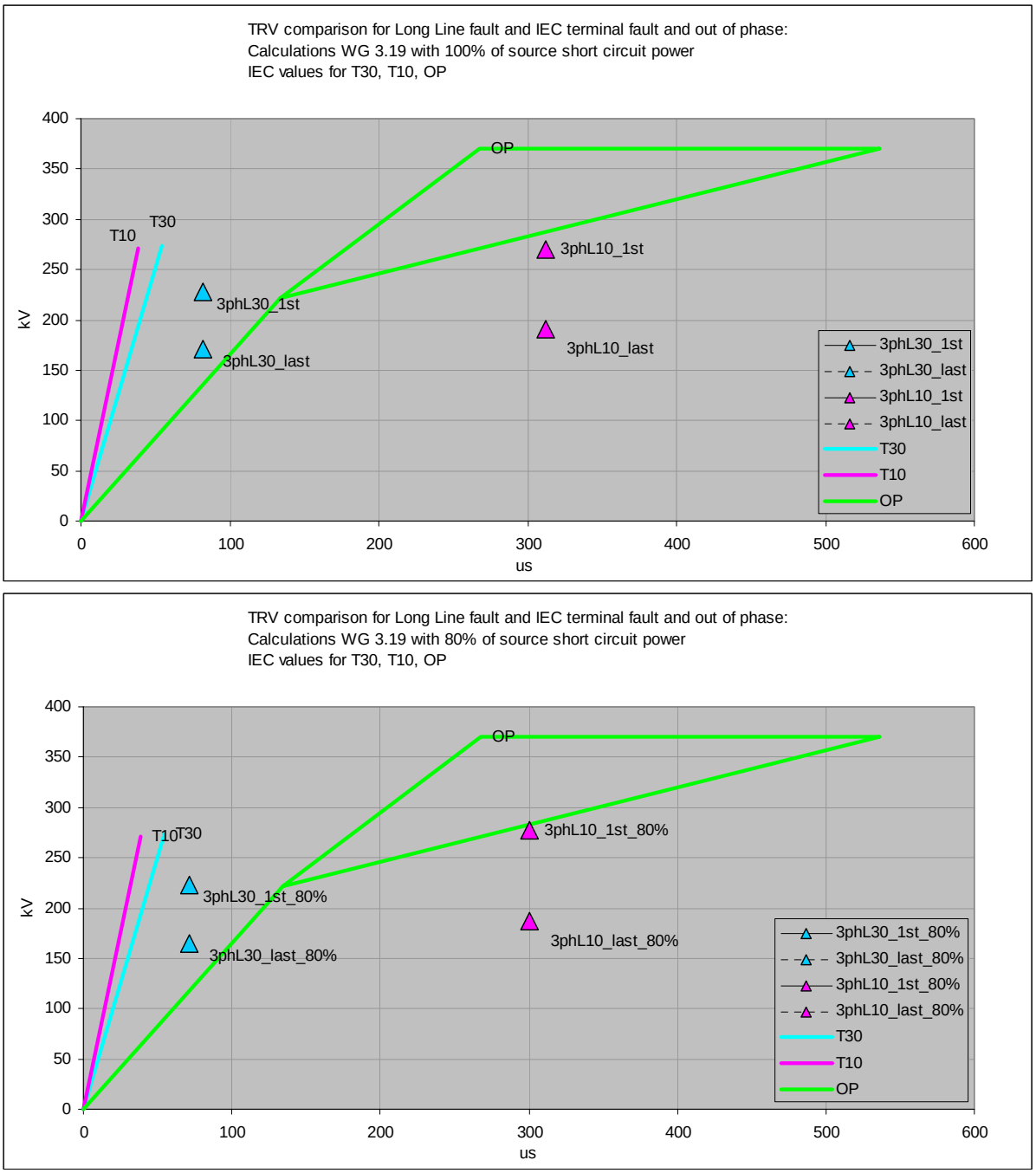

Fig. 6.6: Long line fault 145kV, 40kA, 50Hz, 100% and 80% of the source short circuit power

7. Standardisation of line fault interruption

Circuit-breakers are called upon to perform a wide variety of functions and are subject to a range of type tests to provide confidence in their abilities to carry out these functions safely. Considering the case of fault interruption, International Standards require circuit-breakers to be able to make and break all values of short-circuit current (including line fault current), up to and including the rated value of the circuit-breaker. Clearly it is not practical to test explicitly every condition that may occur in service and hence a representative set of test conditions are specified in the standards. For circuit-breakers, the interrupting performance for all conditions is presently considered to be covered by the combination of terminal fault breaking tests (10%, 30%, 60%, 100% of the rated I_{SC}), SLF breaking tests (L90, L75 and L60 in certain circumstances), out-of-phase switching, capacitive switching, etc. This extrapolation/interpolation of test information to cover untested cases relies heavily upon the definition of the "standard" system on which the test requirements are based and also upon an understanding of the circuit-breaker technologies in use or likely to be in use in the foreseeable future. Standards should be applicable independent of technology, however it is quite conceivable that presently un-foreseen interruption technologies may exhibit very different sensitivities to those presently in use and on which current standards are based. Today, the philosophy applied in the Standards is considered to be independent from the circuit-breaker technology and applies to puffer type, self-blast, other arc/current assisted and even vacuum technologies. Many of these have very complex relationships between contact parting time, current phase at contact part time, pressure build up from current/ablation effects, and the resulting gas mass flow and nozzle arc zone flushing and rinsing. However, the standards have been developed by making certain, experience based, assumptions and generalizations about critical performance factors.

Another critical assumption is that circuit-breakers are able to withstand lesser stresses than those applied during the testing. The intention is to create a situation where testing in accordance with the standard alleviates the user from the need to be concerned about design aspects such as critical currents, gaps in the arcing window, arc phenomena and the behaviour of the circuit-breaker under various interrupting and drive conditions. One could imagine, for instance, that for certain designs there may exist critical currents for the combination of a SLF with a limited short-circuit power at the busbar. Such a design specific criticality cannot easily be catered for within a standardisation framework and is effectively ignored on the basis of its low probability.

Account must also be taken of the environment in which standards are produced where decisions need to be taken, and requirements defined, on the basis of the best information available even if all technical aspects are not totally proven to the satisfaction of all technical experts. In this environment, very low probability events may be disregarded as being of insufficient relevance to be standardised.

It is also important to remember that standards are developed taking into account the vast majority, but not 100%, of system applications meaning that a small minority of system applications are expected to result in potential conditions which fall outside the coverage of the standards.

Considering aspects which are of particular relevance to demonstration of line switching capability, the following can be highlighted:

- Clause 8.103.2 of IEC 62271-100 (Selection of TRV-values) requires that the actual TRV in service will not cross the 2-parameter or 4-parameter envelope as specified for type testing. For SLF conditions in service it is required that the equivalent surge impedance and the peak factor at the line side are smaller than the values specified in the Standard (i.e. 450 Ω and 1.6 respectively) and the time delay larger. However, even if these specific conditions are not met, the actual calculated line-side TRV waveshape in service may fall within the specified test values and be regarded as covered.

- Multi-part testing is allowed by the standards. If all TRV requirements for a given test duty cannot be met simultaneously, the test may be carried out in two or more successive parts between which the test object may be re-conditioned. The first part, for instance, covers the initial part of the TRV up to u1/t1 (initial time delay, RRRV, maybe ITRV), while the second part covers the peak value Uc/t2. The arcing times applied during both parts may not differ more than ± 1 ms. By this logic, it is acceptable within existing standards to cover duties such as three-phase SLF by a combination of several test duties.

- With respect to SLF tests a typical illustration of the philosophy in the Standards is that a proof of the L60 capability is not required if L90 and L75 are passed successfully and the minimum arcing time at L75 is less than the minimum arcing time of L90 plus a quarter cycle. Thus, even when the minimum arcing time of L75 is (considerable) longer than that of L90, indicating that L75 with its lower RRRV gives somewhat higher stresses, it is not considered necessary to prove that L60 can be withstood. The implication of this is that L75 and/or L60 are primarily intended to identify and test "critical current" behaviour rather than cater for the higher line-side peak values associated with these duties.

From the foregoing, the assumptions and basis for the present approach to standardisation of line fault interruption can be clearly seen. This is clearly based on the stated assumption (itself based on considerable test experience) that for today's interrupting technologies, RRRV is the critical parameter to be verified.

The RRRV is highest for the last clearing pole and hence the single phase SLF forms the basis of line fault interrupting tests. Considering specific conditions:

- L90 (three-phase) can be regarded as covered by the single phase L90 in the same way as the single phase L90 and L75 are considered to cover all other percentages (from over 95% to under 50%). Formally, L90 (single phase) covers the thermal stresses of the first pole clearing a three-phase 90% SLF and L90/L75 (single phase) cover the dielectric stresses of a single phase 85% SLF and thus the dielectric stresses of the first pole clearing a three-phase 90% SLF (i.e. at the same location as the 85% fault). Additional support for today's technologies can be derived from the common experience that the contact gap at minimum arcing time for the type test L90 (single phase) is larger than the contact gap at minimum arcing time for the type test T100s (see Chapter 10).
- L60 (three-phase) can be regarded as covered by the single phase L90 and L75 using the present standardisation philosophy described above. Additional support can be derived from the type test for T60 for which the value of t2 is planned to be halved in the IEEE Standard such that the steepness of the TRV waveshape after U1/t1 will be higher than shown in figure 10.4.

- L30 (three-phase LLF) can be regarded as covered by T30 as well as OP2, as the RRRV of T30 is 5 kV/μs. To put this in context, with s = 0.2 kV/μs/kA or 0.24 kV/μs/kA for 50 or 60 Hz respectively, 5 kV/μs corresponds to I30 = 25 kA or I30 = 20 kA respectively, and thus to a full rated current of 80 kA or 70 kA respectively. Moreover, during type tests, it is normal for the time delay applied for T30 and OP2 to be smaller than required due to test station limitations.
- L10 (three-phase LLF) can be regarded as covered by OP2 (non-mandatory), when for t2 the shortest time in the range as specified in the Standards is used. Moreover, it will also be covered by T10, as the first-pole-to-clear factor is raised from the 1.3 to the 1.5 or alternatively when an amplitude factor of 1.76 is specified with kpp=1.3, as included in the revised edition 2.1 of IEC 62271-100 [3]. To ensure that T10 will cover all single-phase and three-phase long line fault conditions, the interrupting window must be 162°.

The ongoing validity of the assumptions, outlined above, on which the present standardisation is based remains an issue for standardisation bodies.

Part II

Implications for short-line faults

8. Probabilities

One of the arguments for the specification of a SLF test duty based on a single-phase fault was the low probability that a three-phase fault could occur on an overhead line. This low probability has been confirmed by a number of national and international surveys, for instance that of the former CIGRÉ WG 13.08, that concluded the probability of three-phase faults on lines to be 10% for the lower transmission voltages and a few percent only or even less for the higher transmission voltages (i.e. 420 kV and above).

Taking a wider view of probabilities, other parameters and variables have to be regarded as well. Type tests to the Standards combine a number of extreme conditions, each of which hampers the circuit-breaker's performance. Releasing one of the requirements may drastically improve the capabilities of the circuit-breaker. To get a three-phase fault corresponding to L90, as specified in the Standards, the following conditions have to be met:

- The system voltage has to be the rated voltage of the equipment i.e. normally the maximum voltage of the system
- The equivalent surge impedance has to be 450 Ω
- The equivalent capacitance at the line side, determining the time delay, has to be rather small, corresponding to the small time delay given in the Standards
- At the supply side an ITRV has to exist (for non-GIS circuit-breakers with a rated voltage of 100 kV and above)
- The fault has to be three-phase
- The distance to the fault has to be critical with respect to the first clearing pole (presumable corresponding to a fault location that gives a short-circuit current of 90%)
- The $\mathbf{X_0/X_1}$ ratio at the busbar has to be critical with respect to the first clearing pole
- The short-circuit power at the busbar has to correspond to the rated short-circuit current of the circuit-breaker. Here it should be noted that this power, at that very moment, has to be based on a situation without the short-circuit current contribution from the line with the three-phase fault.

For the worst conditions for the circuit-breaker to perform, the following conditions have also to be met:

- The auxiliary power and/or pressure has to be the lockout values
- The SF_6 gas pressure has to be the lockout pressure

The probability that all these severe conditions will be met simultaneously is so low that the original decision deserves some credits. When some particular conditions are not met, such as the surge impedance (being for instance 330 Ω) or the SF_6 gas density (being about the rated pressure) or the short-circuit power (corresponding to 80%) or the distance (being in the non-critical area, which is the large part of the line), then successfully type tested designs can be expected to clear the three-phase SLF without difficulty.

Despite the low probability of three-phase faults, examples are known of three-phase faults at the higher system voltages and some utilities cannot neglect them. Further the other conditions mentioned are not regarded as statistical variables, but as conditions specified in

the Standards, that under service conditions offer some margin to the users. How utilities may assess the risks involved will be addressed in Chapter 11.

Although to the textual explanation of the latest edition of the IEC Standard 62271-100 three-phase line faults can be regarded as covered (see Chapter 7), users may want to have more technical or physical evidence that modern circuit-breakers can indeed withstand a somewhat higher peak value of the line-side part of the TRV. In Chapter 10, information is given that points in this direction, but forms no real proof.

The short-circuit power at the busbar is an important variable that may lead to a higher peak value than specified in the Standards (under the condition of equal short-circuit currents for the first and last clearing pole and under the condition of $\mathbf{X_0=X_1}$ at the busbar). Utilities normally have a good idea about the short-circuit power in their substations and therefore in Chapter 9 the influence of a reduced short-circuit power is further elaborated. Chapter 9 starts with the probability of occurrence of a short-circuit power larger than corresponding to a certain percentage of the rated short-circuit current of the circuit-breaker.

9. Source side short-circuit power reduction to 80%

This chapter deals with the effect of the source side short-circuit power reduction on the line-side TRVs. The first section focuses on CIGRE survey results along with other data gathered by electrical utilities about the maximum short-circuit currents that are actually recorded in service. The second section shows simulation results, when comparing a 100% source with an 80% source, and the third section presents analytical equations that were derived for a better understanding of the line TRV variations when source short-circuit power varies. It is shown that the source short-circuit power significantly affects the line TRV peak, time-to-peak and d factor. In the last section, the final results of the analysis are given in graphical form.

9.1 CIGRÉ WG13.08 Survey and other more recent surveys

Calculations performed by WG A3.19 and presented in this report indicate that the first TRV peak is below the IEC standard requirements as long as the short-circuit power available from the grid does not exceed 80%. This means that the TRV peak of a three phase line fault are covered by the IEC standard values as long as the ratio between the maximum short circuit current in the grid and the rated short circuit current of the circuit-breaker installed does not exceed 0.8. In order to support this hypothesis data has been collated from various electrical stress surveys.

Looking at the information collected, it is possible to claim that 90% of the grids have a ratio between the predicted short circuit fault current and the rated short circuit current of the circuit-breaker installed that is below 0.8. Table 9.1 gives a summary of the outcomes coming from different sources.

Table 9.1 – Summary of maximum short-circuit current from various data sources

Data source	(Maximum fault current) / (Rated short-circuit current of circuit-breaker)		
	Average	**90th percentile**	**95th percentile**
Cigre 13.08 [21]	0.4-0.6	0.7-0.8	
CIGRE A3-205 (Japan) [24]	0.189	0.364	
Hydro-Quebec [28]	0.13 - 0.53	0.29 - 0.72	
CIGRE 13-304 (Germany) [25]			123kV → 0.89 245kV → 0.80 420kV → 0.76

9.1.1 CIGRE 13.08 survey

CIGRE WG 13.08 conducted an international survey on electrical stresses in service for circuit-breaker in high voltage systems, particularly those connected to overhead lines.
The outcomes are presented in the [21] and are summarized in [22][23]. Thirteen countries from four continents participated in the international survey on electrical stresses in service by means of 18 independent answers.

The data collection covered voltages of 63kV and above with a total population of 900,000 circuit-breaker years and 70,000 overhead line years and includes:

- Number of short-circuit per 100 km*year of overhead line

- Average line length
- Number of short-circuit per overhead line
- Number of phases involved in fault
- Percentage of transient and permanent failure
- Maximum expected value of short-circuit current in relation to the rated short-circuit current of the installed breaker
- Actual short-circuit current in service.

Focusing on the last two points, only two utilities were able to supply information regarding the actual short-circuit current experienced in service (Fig. 9.1a) which is even less than the predicted values as follows:

- average value: 0.20 of the rated short-circuit current
- 90th percentile value: 0.30 to 0.40

Much more information was available regarding the maximum expected short-circuit current in the grid. From the information given by the utilities it can be concluded that the maximum expected value of short-circuit current in relation to the rated short circuit current of the installed breaker for most utilities (Fig. 9.1b) is as follows:

- average value: 0.40 to 0.60
- 90th percentile value: 0.70 to 0.80

This means that more than 90% of the circuit-breakers in service are installed in systems where the maximum possible short-circuit current is lower than 0.80 of the rating of the circuit-breaker. It should be remembered that, according to the 90th percentile IEC rule, Standards are intended to cover 90% of the known cases.

a)

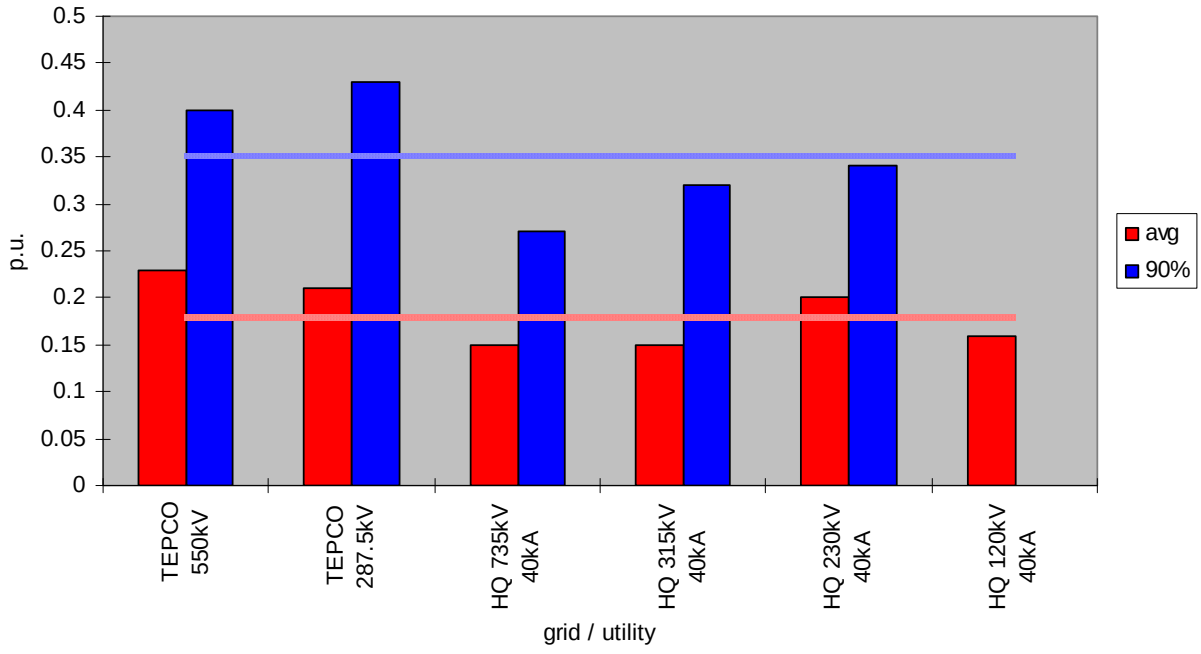

b)

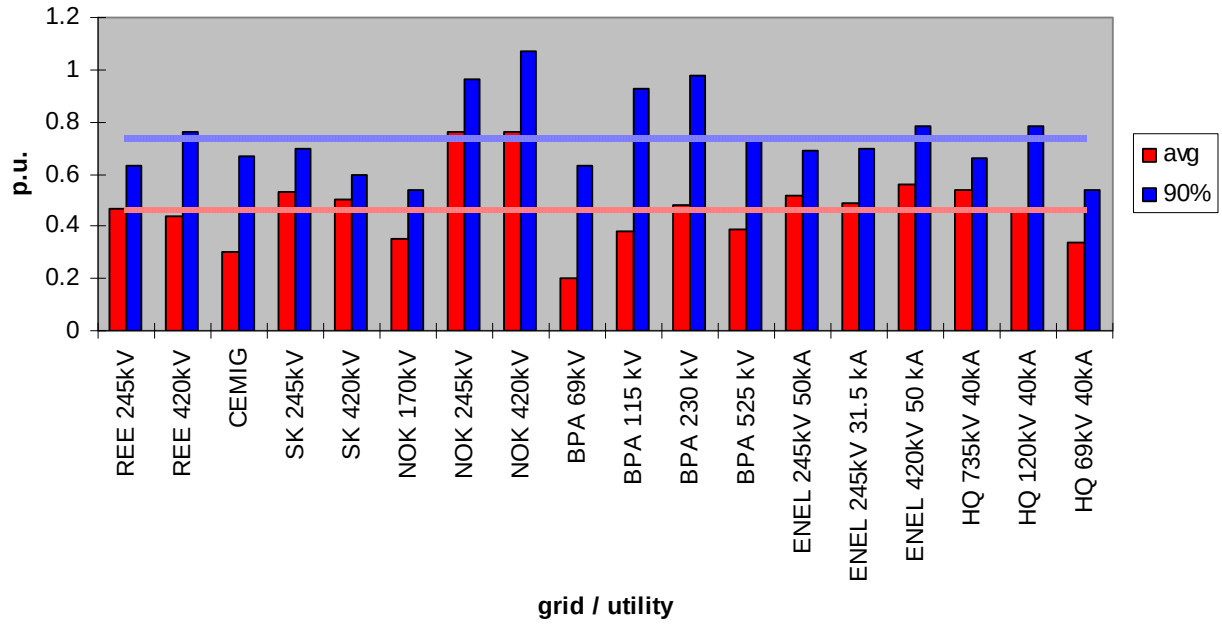

Figure 9.1: a) Actual short-circuit current in service (from Table 8. 3 of 97(SC)31 IWD)
b) Maximum expected I_{SC} in the substation divided by the actual rated I_{SC} (from Table 7. 3 of 97(SC)31 IWD)

9.1.2 Reliability and Electrical Stress Survey on High Voltage Circuit-breakers in Japan

Ten utilities in Japan participated in this survey and have accumulated field data from 2004 [24]. Normalized short-circuit current shows an average of 0.189 with a maximum of 0.844 (Fig. 9.2). The 90th percentile value of the normalized short-circuit currents are below 0.364 and most faults can be covered by the duty T30.

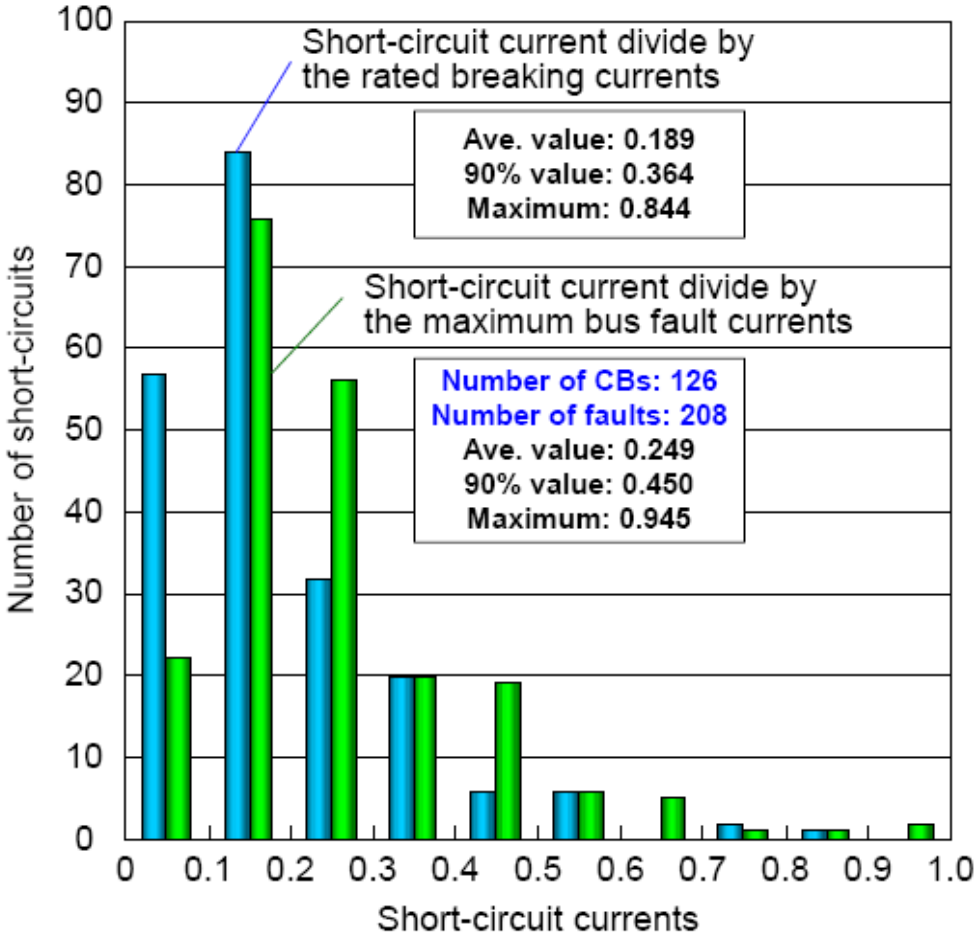

Figure 9.2: Short circuit current urvey results of ten Japanese Utilities

9.1.3 Stress of High Voltage Circuit-Breakers in German Networks

The following information relates to a population of more than 2000 pieces of 123, 245 and 420-kV circuit-breakers (Fig. 9.3) [25] installed within two German utilities. All switching stresses including normal and short-circuit switching were addressed.

For investigation of short-circuit stresses, the highest fault current, normally the three-phase terminal fault, is related to the rated short-circuit current. The 95th percentile of the frequency distribution is at 0.89 of the rated short-circuit current at 123 kV and at 0.80 and 0.76 at 245 and 420 kV respectively.

Table 9.2- 95th percentile and maximum value of the single-phase and three-phase terminal fault current I_{k1TF} and I_{K3TF} respectively related to rated breaking current I_{rb}

Rated voltage	Number of breakers	95th percentile		Maximum value	
		I_{k1TF}/I_{rb}	I_{K3TF}/I_{rb}	I_{k1TF}/I_{rb}	I_{K3TF}/I_{rb}
123kV	591	-	0.89	-	1.04
245kV	543	0.67	0.80	0.85	0.95
420kV	207	0.63	0.76	0.74	0.86

I_{k1TF}: Single-phase terminal fault current
I_{k3TF}: Three-phase terminal fault current
I_{rb}: Rated breaking current

9.1.4 Additional data from Hydro Quebec

Data was collected from 1980 to 2002 for 330 kV circuit-breakers connected to 48 lines at 330 kV, with 3 circuit-breakers per line. Some additional data has also been made available from IEC Maintenance Team 40 working on the revision of the IEC 62271-310 [28]. In this case, the actual measured short-circuit fault was available.

The data was split on the basis of circuit-breakers intended to be use under normal electrical endurance conditions (E1) and those intended for extended electrical endurance condition (E2). Besides the average and 90th percentile value, the 99th percentile is also given.

Table 9.3 – Hydro-Quebec's data related to fault currents

Breaker class	I_{fault} / I_r		
	Average	90th percentile	99th percentile
E1	0.13	0.29	0.53
E2	0.53	0.72	0.84

a)

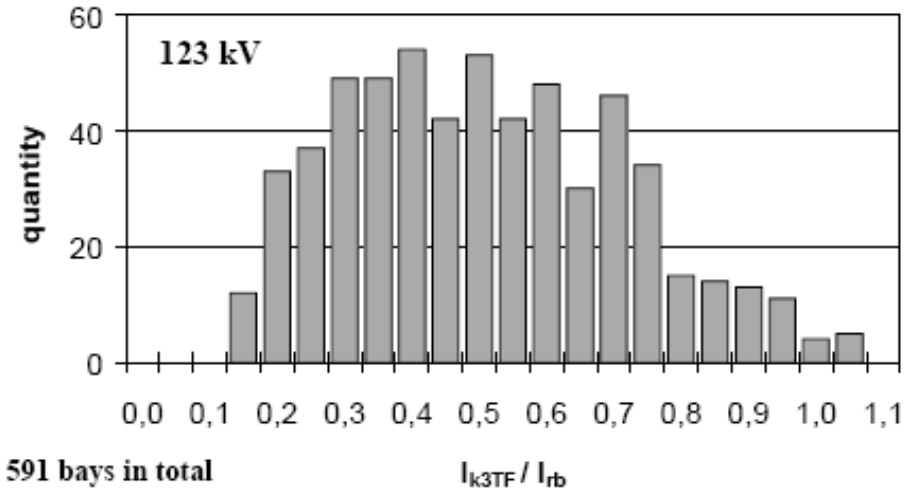

b)

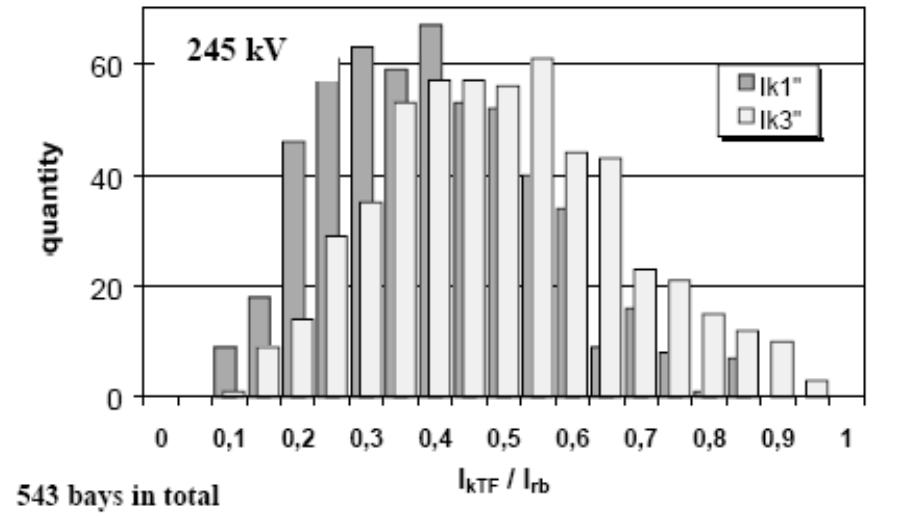

c)

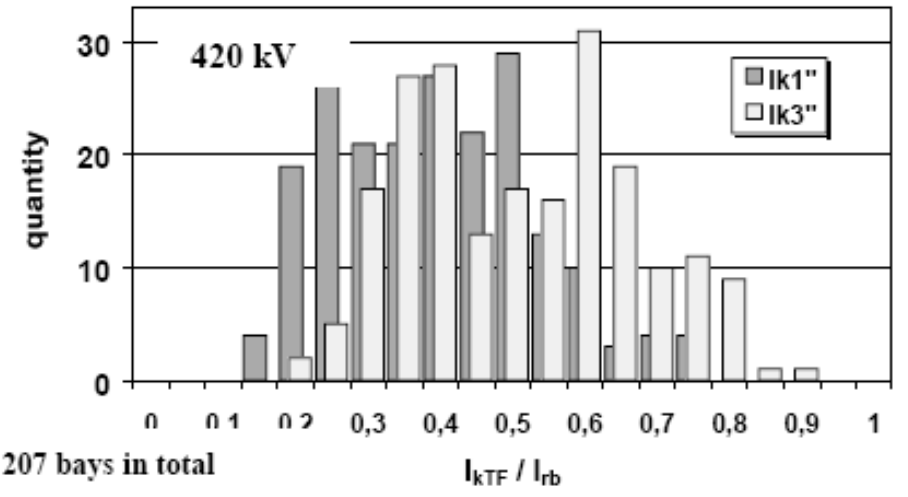

Figure 9.3: Frequency distribution of terminal fault currents related to rated breaking current
a) 123-kV system, three-phase terminal fault currents (I_{k3TF})
b) 245-kV system, single-phase (I_{k1TF}) and three-phase terminal fault currents (I_{k3TF})
c) 420-kV system, single-phase (I_{k1TF}) and three-phase terminal fault currents (I_{k3TF})

9.2 EMTP simulation results

Tabulated values of line-side TRV parameters are given in Appendix B for various system characteristics: rated voltage (U_r), short-circuit current (I_{SC}), short-line faults, long-line faults, etc. The following section presents examples of line TRV waveshapes for source side short-circuit powers of 100% and 80% of the rated short-circuit current of the circuit-breaker. A Matlab script was developed to compare the IEC line TRV specifications and the line TRVs obtained by EMTP simulations, thus allowing instants of current interruption to be detected and TRVs of the three poles to be superimposed on the standard TRV envelopes of the actual IEC SLF test duties. Voltage translation and polarity change (if necessary) were also applied.

The graphs of the simulation results are presented in Figures 9.4 to 9.6. IEC TRV requirements are plotted in red: the line TRV as a dotted line and the total TRV across the circuit-breaker terminals as a solid line. In addition, each graph depicts the following simulation results:

- Line TRV for each pole following current interruption (1st pole: blue dotted line, 2nd pole: cyan solid line, 3rd pole: green solid line)
- First-pole total TRV across the circuit-breaker terminals as simulated by EMTP (blue solid line)

To see the first-pole line TRV discrepancy, the blue dotted line can be compared to the red dotted line, while for the total TRV across the circuit-breaker terminals, the blue and red solid lines are considered.

Figure 9.4a presents the simulation results for the following source parameters:

- Rated source voltage (U_r): 315 kV
- Rated short-circuit current (I_{SC}): 40 kA
- First-pole-to-clear factor (k_{pp}): 1.3
- Source TRV parameters: k_{af}= 1.4, RRRV= 2.0 kV/μs at I_{SC}= 40 kA.

The line parameters are:

- Line configuration: Single circuit line with 2 conductors per phase
- Line impedance: 450 Ω
- 3-phase SLF duty: L75 (75% of the rated I_{SC}= 40 kA)

For the EMTP simulation results presented in Figure 9.4b, the source I_{SC} for the EMTP model was reduced to 32 kA (i.e. 80% x rated I_{SC}= 40 kA). Based on the rated I_{SC} of 40 kA, it should be pointed out that the three-phase L90 (36 kA) is no longer relevant. On the other hand, since the source I_{SC} is reduced, the source TRV is increased to 2.5 kV/μs, which corresponds to linear interpolation between TRV slopes of 2 and 3 kV/ μs, respectively, for 100% and 60% of the rated I_{SC}. The line length for L75 (based on the rated I_{SC} of 40 kA) was adjusted to 1.081 km, giving a fault current of 30 kA.

Figures 9.5 and 9.6 gives similar EMTP simulation results with source and line parameters that have been modified as follows:

- Rated source voltage (U_r): 230 kV
- First-pole-to-clear factor (k_{pp}): 1.5
- Line configuration: Double circuit line with one conductor per phase
- 3-phase SLF duty for Fig. 9.5: L75
- 3-phase SLF duty for Fig. 9.6: L60

From these simulation results, it can be concluded that:

1) For a short-circuit power equal to 100% of the rated value (Figs 9.4a, 9.5a, 9.6a), the first-pole line TRV peak (blue dotted line) is greater than the IEC value (red dotted line) while the TRV slope is smaller since the simulated transmission line produces a surge impedance (Z_L) lower than 450 Ω. Note that the line TRV slope is equal to Z_L x (dI_{SC}/dt).
2) For a short-circuit power equal to 80% of the rated value (Figs 9.4b, 9.5b, 9.6b) **the line TRV peaks and slopes are lower** that the standard TRV envelope of the actual IEC SLF test duties while the line TRV amplitude for L60 (Fig. 9.6b) is closer to the IEC requirements than that for L75.

The curves plotted in the next section with the analytical expression provide a better understanding of the line TRV variations as a function of source short-circuit power and the IEC SLF test duty.

a)

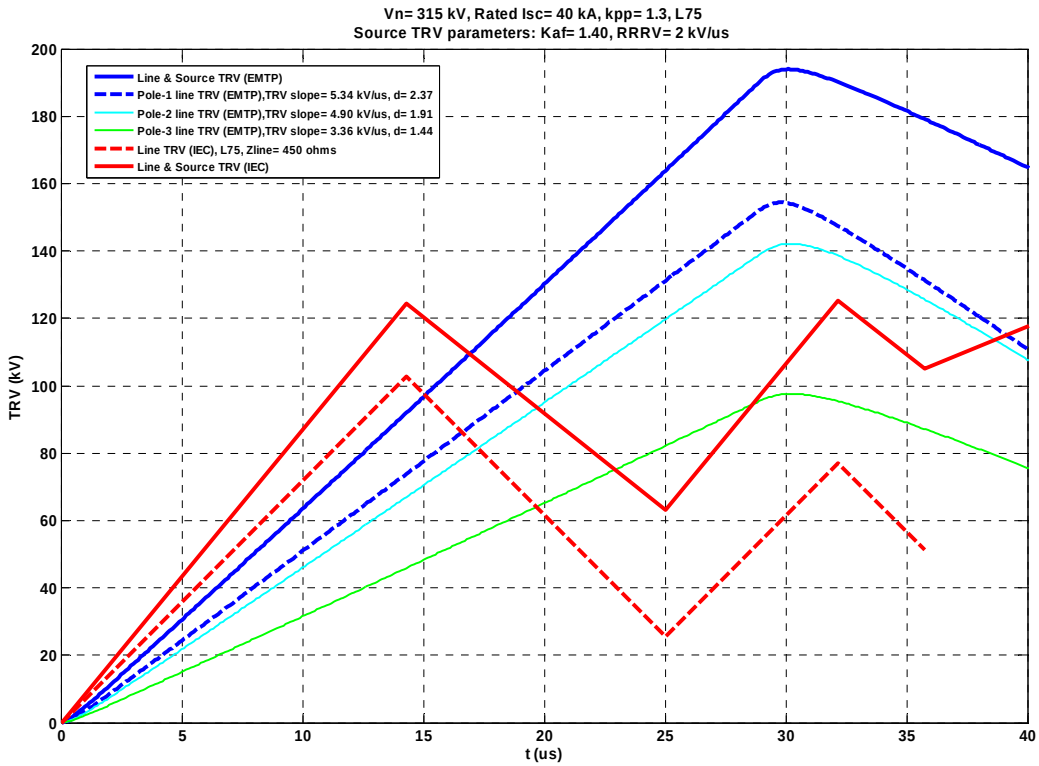

b)

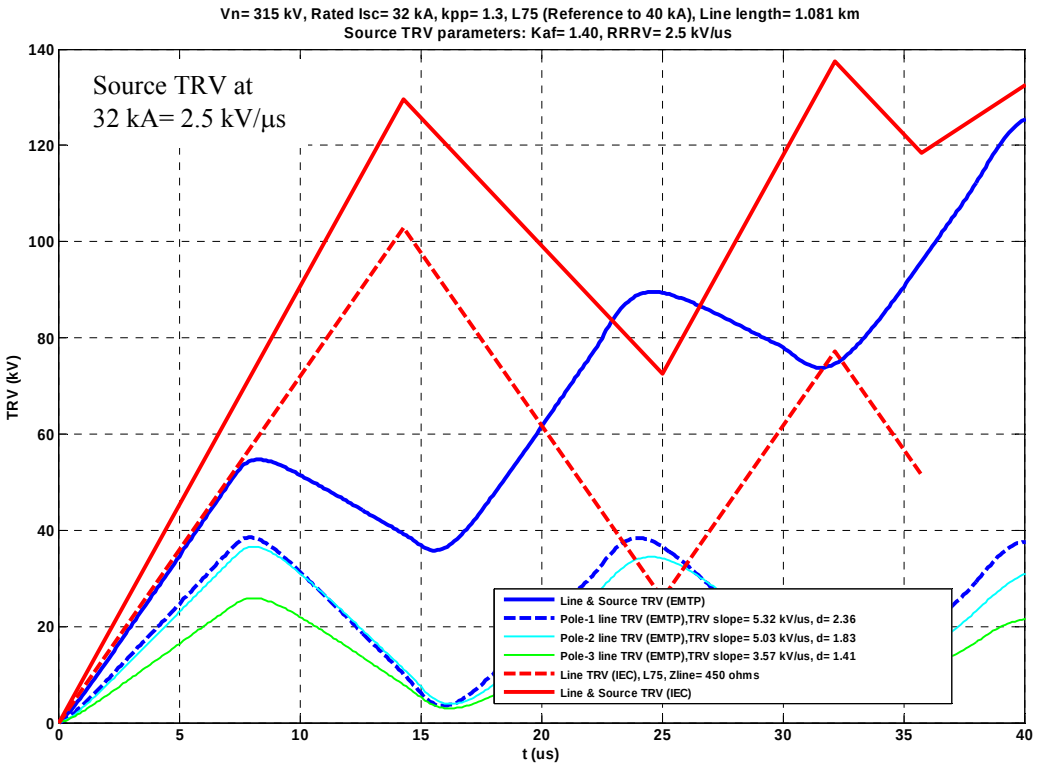

Figure 9.4: 3-phase SLF TRV amplitudes and slopes compared to IEC SLF test duties
a) 3-phase L75 vs IEC L75
b) 3-phase L75 (with reference to rated Isc= 40 kA) with reduced source Isc of 32 kA vs IEC L75

a)

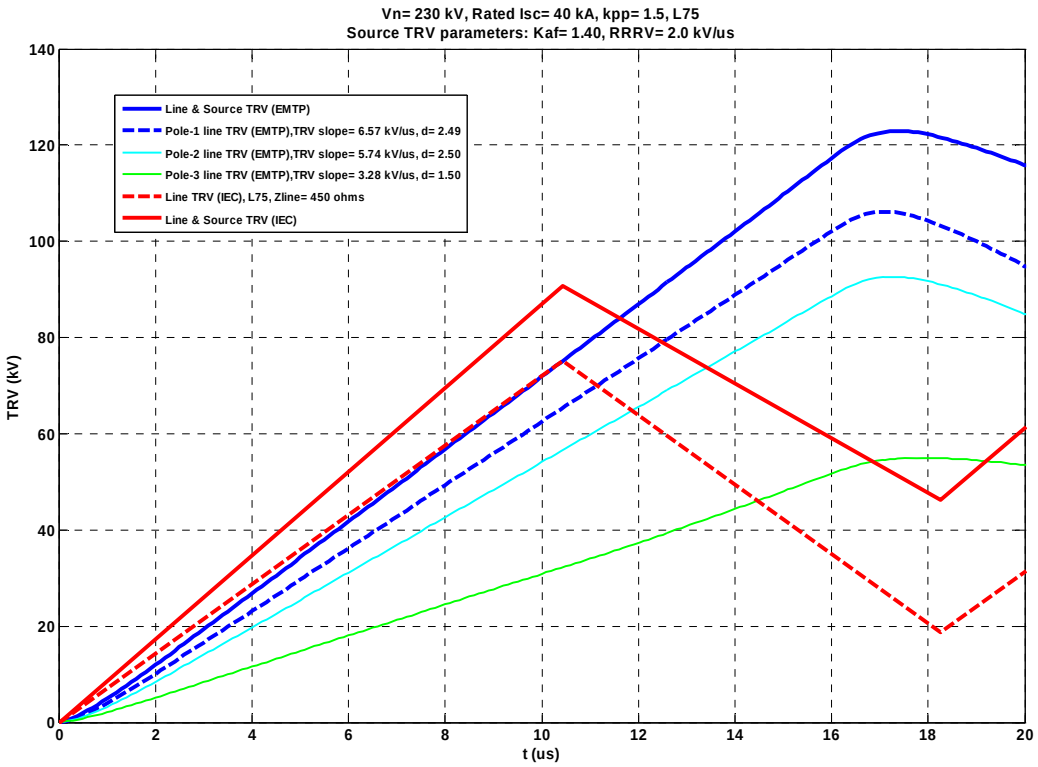

b)

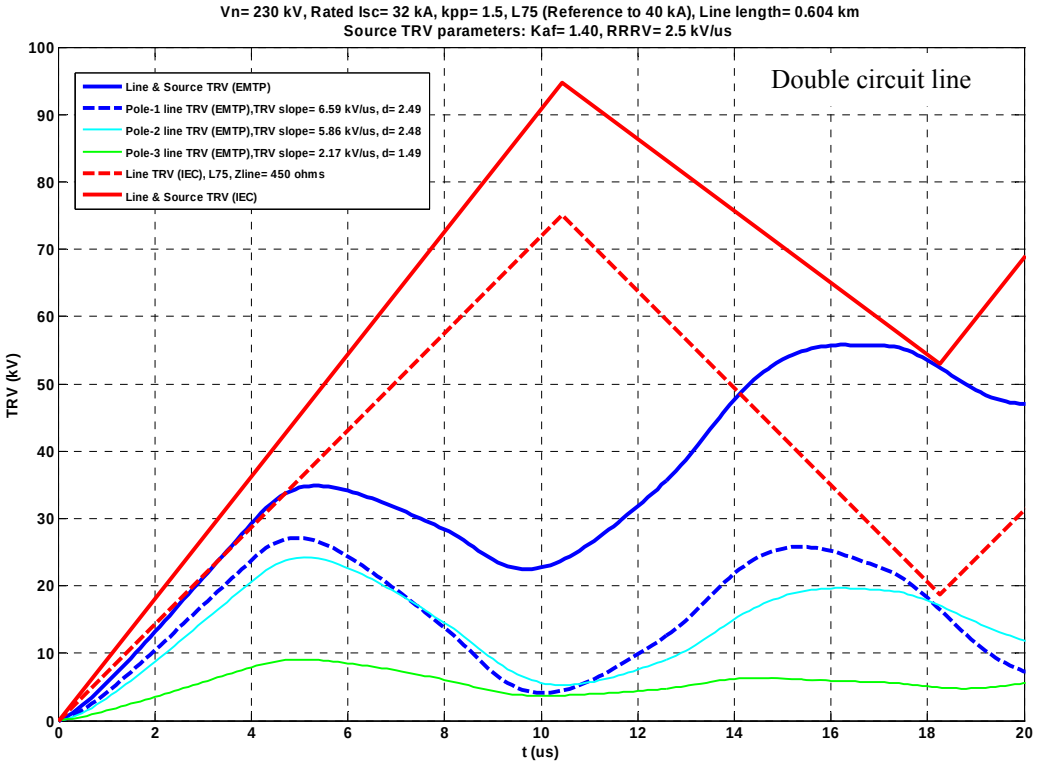

Figure 9.5: 3-phase SLF TRV amplitudes and slopes compared to IEC SLF test duties
a) 3-phase L75 vs IEC L75
b) 3-phase L75 (with reference to rated Isc= 40 kA) with reduced source Isc of 32 kA vs IEC L75

a)

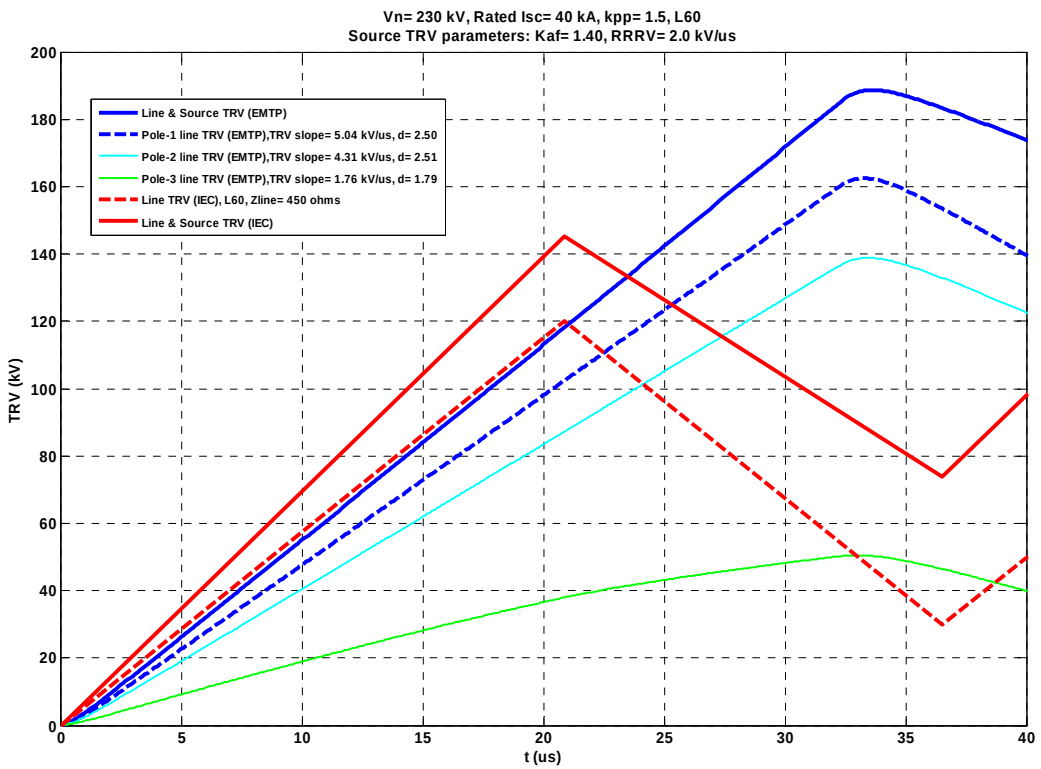

b)

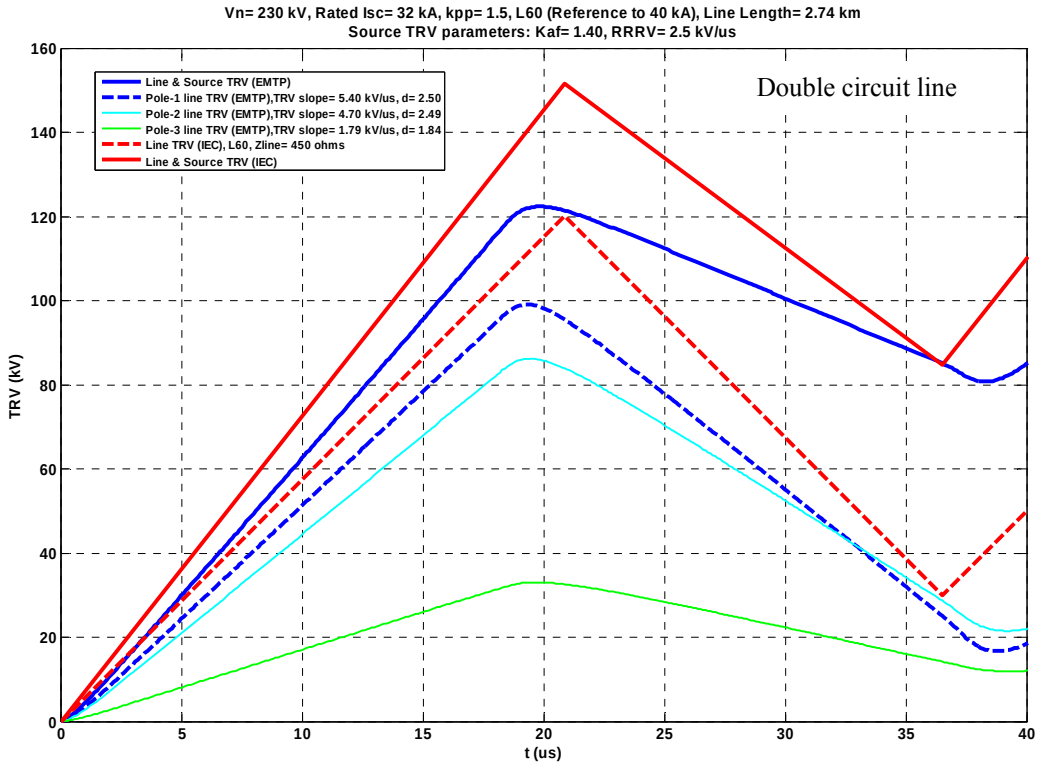

Figure 9.6: 3-phase SLF TRV amplitudes and slopes compared to IEC SLF test duties
a) 3-phase L60 vs IEC L60
b) 3-phase L60 (with reference to rated Isc= 40 kA) with reduced source Isc of 32 kA vs IEC L60

9.3 Analytical equation for assessing the line TRV peak and time-to-peak of the first-pole-to-clear

For the first-pole-to-clear of a three-phase short-line fault, a simple analytical expression (Eq. 9.7) was derived to evaluate the ratio of the three-phase line TRV peak (3ϕ $\hat{U}_L$) to the IEC line TRV peak (IEC $\hat{U}_L$) as a function of SLF test-duty percentage (Fsc) when the source short-circuit power (Fs in % of the rated I_{SC}) varies from 80% to 100%. Based on this equation, Figure 9.7 depicts the curves that were plotted for different values of the d factor: 2.3 (Fig. 9.7a), 2.4 (Fig. 9.7b) and 2.5 (Fig. 9.7c). The calculated $\hat{U}_L$ ratio values are in line with EMTP simulation results.

Assuming the following symbol definitions, Equations 9.1 to 9.13 can be written as follows:

IEC $\hat{U}_L$: IEC line TRV peak
IEC t_L: IEC line TRV time-to-peak
3ϕ $\hat{U}_L$: Line TRV peak of the 1st pole following a 3-phase SLF fault interruption
3ϕ t_L: Line TRV time-to-peak of the 1st pole following a 3-phase SLF fault interruption
F_{SC}: SLF test duty as a percentage of the rated I_{SC} (e.g. 90%, 75%, 60%)
F_S: Source short-circuit current in percentage of the rated I_{SC} (e.g. 80%, 90%)
U_r: Rated voltage
I_{SC}: Actual short-circuit current as limited by the source and line impedances
I_{SCr}: Rated short-circuit current (e.g. 40 kA)
L_{line}: Line inductance in μH
$L_{li/m}$: Line inductance in μH/m (typical value 1 μH/m)
l_{line}: Line length
S_L: Line TRV slope (dv/dt)
IEC Z_L: IEC line surge impedance = 450 Ω

$$\mathbf{IEC\ \hat{U}_L = (1 - F_{SC}) \times \frac{U_r}{\sqrt{3}} \times \sqrt{2} \times 1.6} \tag{9.1}$$

$$\mathbf{3\varphi\ \hat{U}_L = L_{line} \times \frac{dI_{SC}}{dt} \times d\ factor} \tag{9.2}$$

$$\mathbf{L_{line} = Total\ Inductance - Source\ Inductance = \frac{U_r/\sqrt{3}}{F_{SC} I_{SCr} \times 2\pi \times 60} - \frac{U_r/\sqrt{3}}{F_S I_{SCr} \times 2\pi \times 60}} \tag{9.3}$$

$$\mathbf{L_{line} = \frac{U_r}{\sqrt{3}} \times \frac{1}{I_{SCr} \times 2\pi \times 60} \times \left(\frac{1}{F_{SC}} - \frac{1}{F_S} \right)} \tag{9.4}$$

$$\mathbf{\frac{dI_{SC}}{dt} = I_{SC} \times \sqrt{2} \times 2\pi \times 60 \quad with\ I_{SC} = F_{SC} I_{SCr}} \tag{9.5}$$

Substituting L_{line} (Eq. 9.4) and dI_{SC}/dt (Eq. 9.5) in equation 9.2:

$$\mathbf{3\varphi\ \hat{U}_L = \frac{U_r}{\sqrt{3}} \times \sqrt{2} \times \left(\frac{F_S - F_{SC}}{F_S} \right) \times d\ factor} \tag{9.6}$$

To determine the line TRV peak ratio between a three-phase fault and the one specified by IEC (Eq. 9.7), the right-hand side of equation 9.6 can be divided by the right-hand side of equation 9.1.

$$\mathbf{\hat{U}_L\ ratio = \frac{3\varphi\ \hat{U}_L}{IEC\ \hat{U}_L} = \frac{\left(F_S - F_{SC}\right)}{F_S \times \left(1 - F_{SC}\right)} \times \frac{d\ factor}{1.6} \quad with\ F_S \geq F_{SC}} \tag{9.7}$$

As given by Eq. 9.7, $\hat{U}_L$ is function of the d factor. Using equation 9.7, the graphs of the line TRV peak ratio ($\hat{U}_L$ ratio, Fig. 9.7) are plotted for different F_S values as a function of F_{SC}. Moreover, these graphs establish clearly F_S and F_{SC} ranges for which the first-pole-to-clear line TRV is less severe than the IEC line TRV requirements (i.e. for $\hat{U}_L$ ratio < 1).

Similarly to the line TRV peak, for the first-pole-to-clear, a simple analytical expression (Eq. 9.12) was also derived for the ratio of the three-phase line TRV time-to-peak ($3\phi\ t_L$) to the IEC line TRV time-to-peak (IEC t_L) as a function of the SLF test-duty percentage (Fsc) when the source short-circuit power (Fs in % of the rated I_{SC}) varies from 80% to 100%. Based on Eq. 9.12 and for different F_S values, Figure 9.8 shows curves that were plotted as a function of F_{SC} (SLF duty percentage) for different values of $L_{li/m}$: 0.9 μH/m (Fig. 9.8a), 1.0 μH/m (Fig. 9.8b), 1.1 μH/m (Fig. 9.9a) and 1.2 μH/m (Fig. 9.9b).

$$\mathbf{IEC\ t_L = \frac{IEC\ \hat{U}_L}{S_L} = \frac{\left(U_r/\sqrt{3}\right) \times \sqrt{2} \times \left(1 - F_{SC}\right) \times 1.6}{450 \times F_{SC} \times I_{SCr} \times \sqrt{2} \times 2\pi \times 60}} \tag{9.8}$$

$$\mathbf{3\varphi\ t_L = \frac{2 \times l_{line}}{c} = \frac{2 \times l_{line}}{280}} \tag{9.9}$$

where c: propagation speed of the travelling waves (typical value= 280 m/μs)

$$\mathbf{l_{line} = \frac{L_{line}}{L_{li/m}}} \tag{9.10}$$

Substituting L_{line} (Eq. 9.4) and 1_{line} (Eq. 9.10) in equation 9.9:

$$\mathbf{3\varphi\ t_L = \frac{2 \times \left(U_r/\sqrt{3}\right)}{I_{SCr} \times 2\pi \times 60} \times \left(\frac{F_S - F_{SC}}{F_{SC} F_S} \right) \times \frac{1}{L_{li/m} \times 280}} \tag{9.11}$$

The line TRV time-to-peak ratio (t_L ratio) can be obtained by dividing the right-hand side of equation 9.11 over the right-hand side of equation 9.8. By simplifying and grouping the different terms, equation 9.12 can be written as follows:

$$\mathbf{t_L\ ratio} = \frac{\mathbf{3\varphi\ t_L}}{\mathbf{IEC\ t_L}} = \frac{\left(\mathbf{F_s - F_{SC}}\right)}{\mathbf{F_S\left(1 - F_{SC}\right)}} \times \frac{\mathbf{2}}{\mathbf{280}} \times \frac{\mathbf{450}}{\mathbf{1.6}} \times \frac{\mathbf{1}}{\mathbf{L_{li/m}}} \quad \mathbf{with\ F_S \geq F_{SC}} \tag{9.12}$$

The calculated t_L ratio values are in line with the simulation results.

Finally, by dividing Eq. 9.7 by Eq. 9.12, the line TRV slope ratio can be derived:

$$\mathbf{Line\ TRV\ slope\ ratio} = \frac{\mathbf{\hat{U}_L\ ratio}}{\mathbf{t_L\ ratio}} = \mathbf{d\ factor} \times \frac{\mathbf{280}}{\mathbf{450}} \times \frac{\mathbf{L_{li/m}}}{\mathbf{2}} \tag{9.13}$$

As given by Eq. 9.12, the line TRV slope ratio (3-phase SLF line TRV slope / IEC SLF line TRV slope) is directly proportional to the product of the d factor and the line inductance per unit length ($L_{li/m}$).

9.4 Final result analysis

Based on the graphs of Figs 9.7 to 9.9, Table 9.4 extracts the $\hat{U}_L$ and t_L ratios as a function of the relevant parameters: short-circuit power percentage (i.e. 80%-100%) and SLF duty percentage (60%-90%). For the selected parameters, it should be pointed out that the TRV slope ratio is always lower than one (Eq. 9.13). In principle, if the surge impedance remains unchanged for 3-phase SLF, this TRV slope ratio should be equal to 1. Note that the parameter $L_{li/m}$ is directly linked to the actual line surge impedance. Therefore, to conclude about the severity of the 3-phase SLF line TRV, only the $\hat{U}_L$ ratio value (Eq. 9.7) must be examined.

The values appearing in green color in Table 9.4 refer to a 3-phase SLF TRV severity lower than that of the single-phase IEC SLF since the $\hat{U}_L$ ratio is lower than 1. Based on this criterion, it can be deduced that, for the first-pole-to-clear, the 3-phase SLF is less severe than the IEC single-phase SLF for the following source short-circuit power (F_S in % of the rated I_{SC}) and SLF test-duty percentage (F_{SC}):

- F_S= 80% and F_{SC}= 60% (L60) and 75% (L75);
- F_S= 85% and F_{SC}= 75% (L75);
- F_S= 90% and F_{SC}= 75% (L75, except for d=2.5);
- F_S= 95% and F_{SC}= 90% (L90).

A source side short-circuit power of 80% of the rated value is required in order to get a lower severity of the 3-phase SLF both for L60 and L75 SLF test duties. For short-circuit power of 85% and 90% of the rated value, only the 3-phase L75 is less severe than the single-phase L75, except for 2.5.

In summary, for the three-phase SLF interruption and based on IEC standard requirements, it can be concluded that the source short-circuit power has a very significant effect on the severity of the first-pole-to-clear SLF TRV.

Table 9.4- $\hat{U}_L$ and t_L ratios as a function of source short-circuit power and IEC SLF test duties

Source short-circuit power (%)	SLF test duty (%)	$\hat{U}_L$ ratio			t_L ratio				TRV slope ratio (Eq. 9.13)	Highest SLF line TRV severity (3-phase or 1-phase)
		d=2.3	d=2.4	d=2.5	$L_{li/m}$= 0.9	$L_{li/m}$= 1.0	$L_{li/m}$= 1.1	$L_{li/m}$= 1.2		
80	**60**	**0.90**	**0.94**	**0.98**	**1.40**	**1.26**	**1.14**	**1.05**	0.644-0.933	1-phase SLF
	75	**0.36**	**0.38**	**0.39**	**0.56**	**0.50**	**0.46**	**0.42**		1-phase SLF
85	60	1.06	1.10	1.15	1.64	1.48	1.34	1.23		3-phase SLF
	75	**0.68**	**0.71**	**0.74**	**1.05**	**0.95**	**0.86**	**0.79**		1-phase SLF
90	60	1.20	1.25	1.30	1.86	1.67	1.52	1.40		3-phase SLF
	75	**0.96**	**1.00**	1.04	**1.49**	**1.34**	**1.22**	**1.12**		1-phase SLF, except for d=2.5
95	60	1.32	1.38	1.44	2.06	1.85	1.68	1.54		3-phase SLF
	75	1.21	1.26	1.32	1.88	1.69	1.54	1.41		3-phase SLF
	90	**0.76**	**0.79**	**0.82**	**1.18**	**1.06**	**0.96**	**0.88**		1-phase SLF
100	60	1.44	1.50	1.56	2.23	2.01	1.83	1.67		3-phase SLF
	75									
	90									

$L_{li/m}$: Line inductance (μH/m)
$\hat{U}_L$ ratio= 3ϕ $\hat{U}_L$ / IEC $\hat{U}_L$ (Eq. 9.7 and Fig. 9.7)
t_L ratio= 3ϕ t_L / IEC t_L (Eq. 9.12 and Figs 9.8 and 9.9)

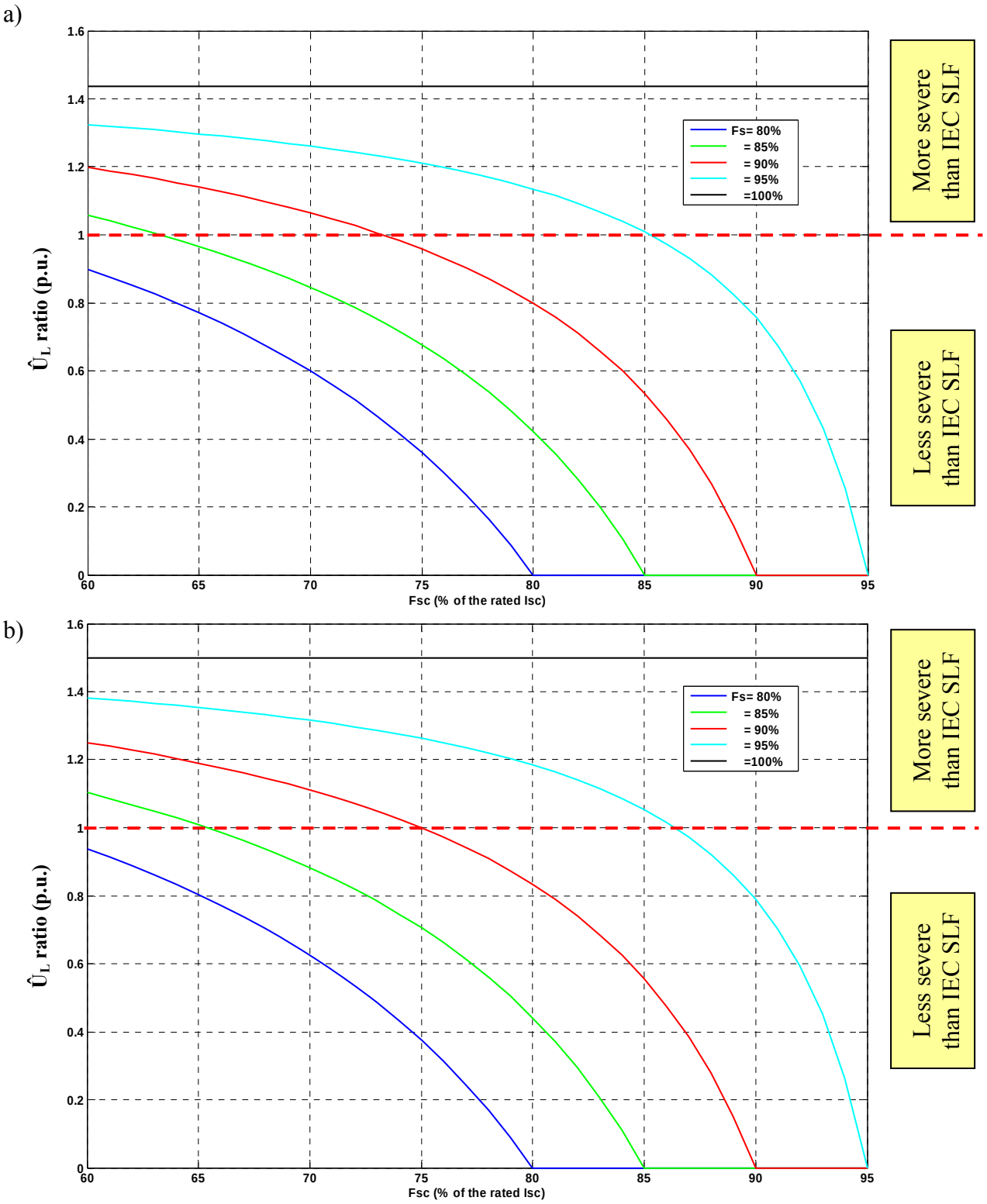

Figure 9.7: $\hat{U}_L$ ratio for source short-circuit power (F_S = 80-100% of the rated Isc) as a function of IEC SLF test duty (F_{SC}= 60-95% of the rated I_{SC})
a) d= 2.3
b) d= 2.4

c)

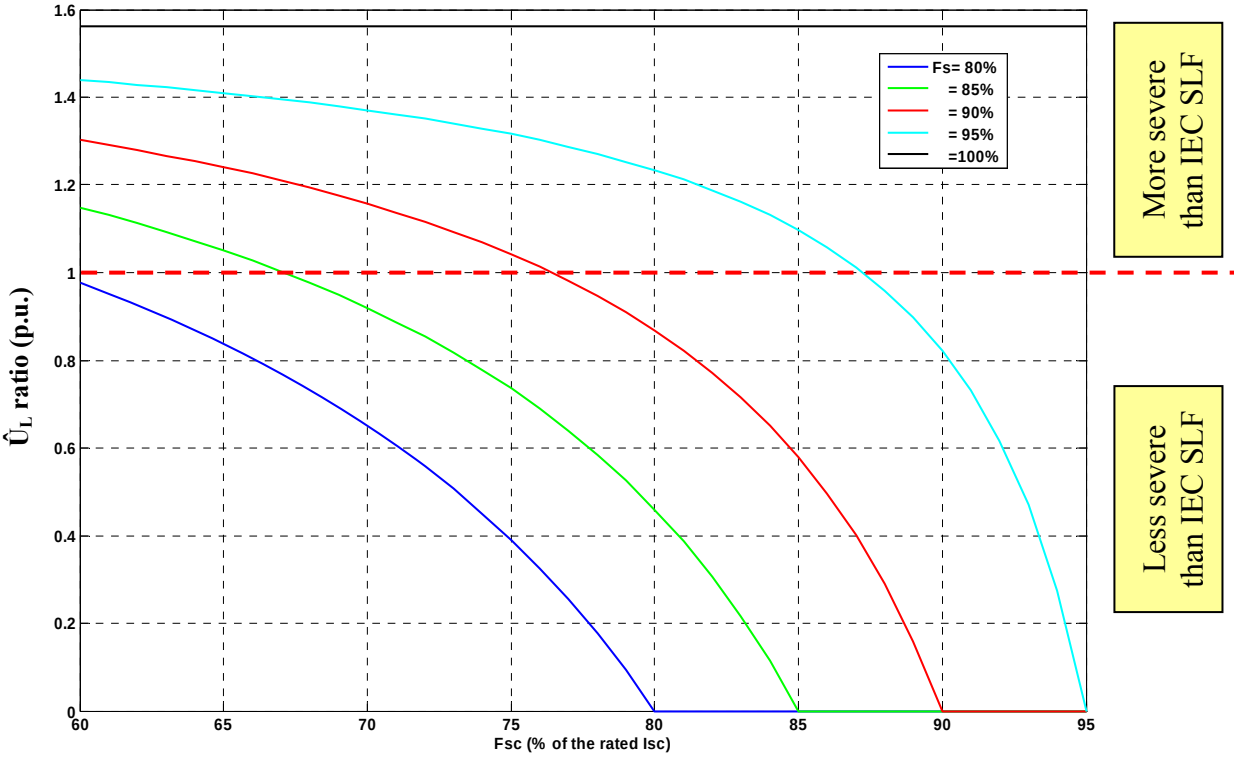

Figure 9.7: $\hat{U}_L$ ratio for source short-circuit power (F_S = 80-100% of the rated Isc) as a function of IEC SLF test duty (F_{SC}= 60-95% of the rated I_{SC})
c) d=2.5

a)

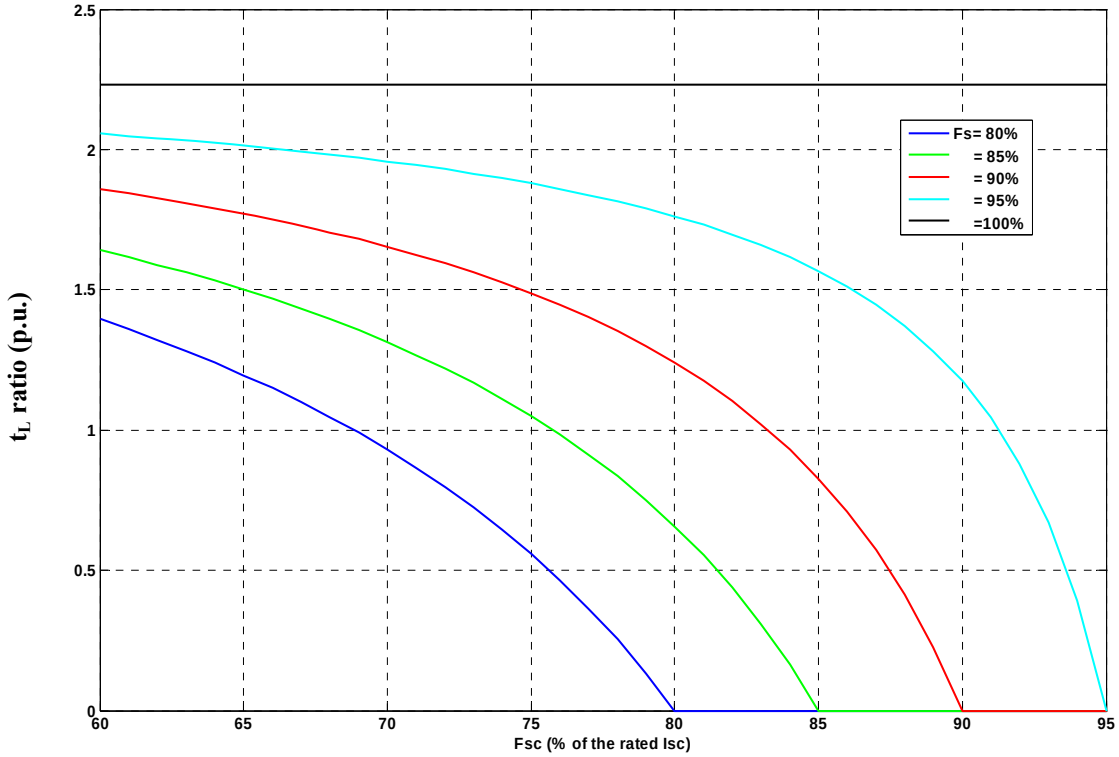

b)

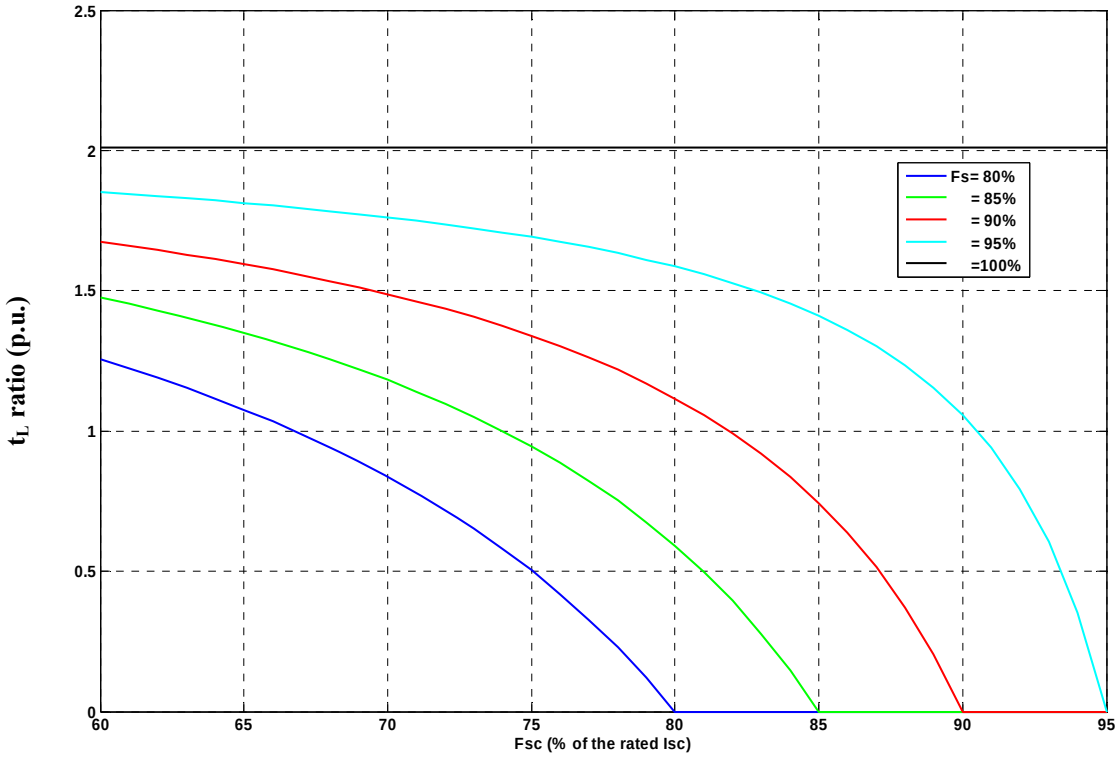

Figure 9.8: t_L ratio for source short-circuit power (F_S = 80-100% of the rated Isc) as a function of IEC SLF test duty (F_{SC}= 60-95% of the rated I_{SC})
a) $L_{li/m}$= 0.9 µH/m
b) $L_{li/m}$= 1.0 µH/m

c)

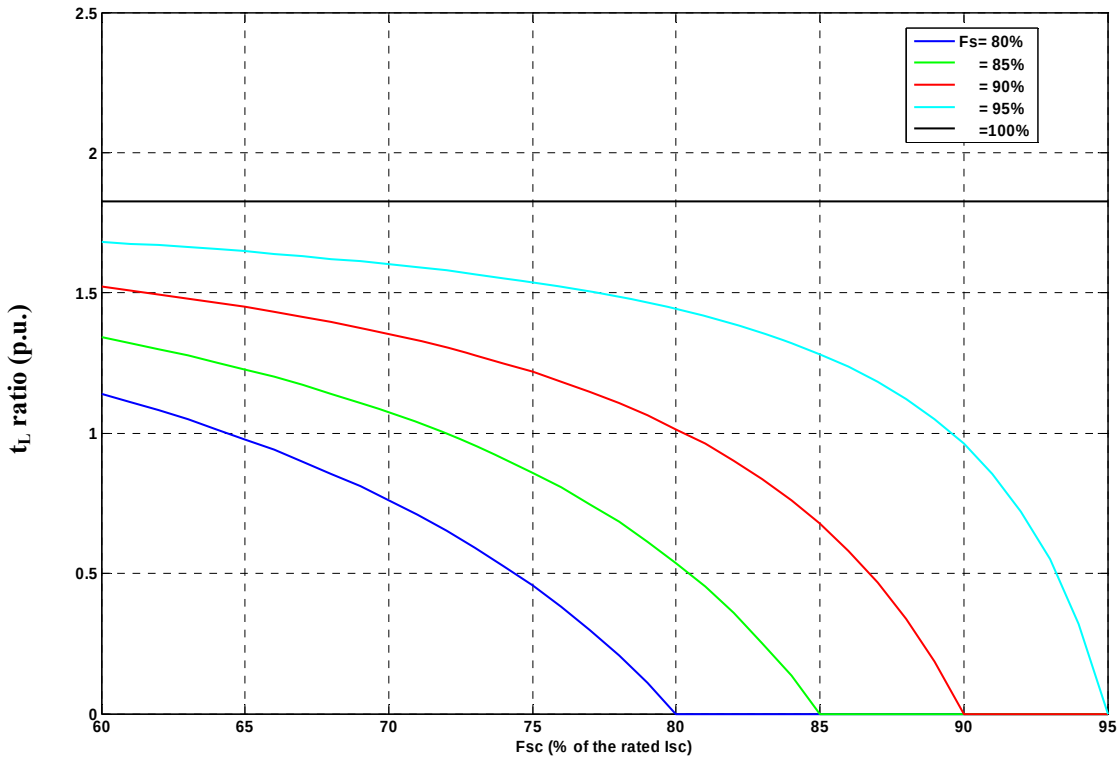

d)

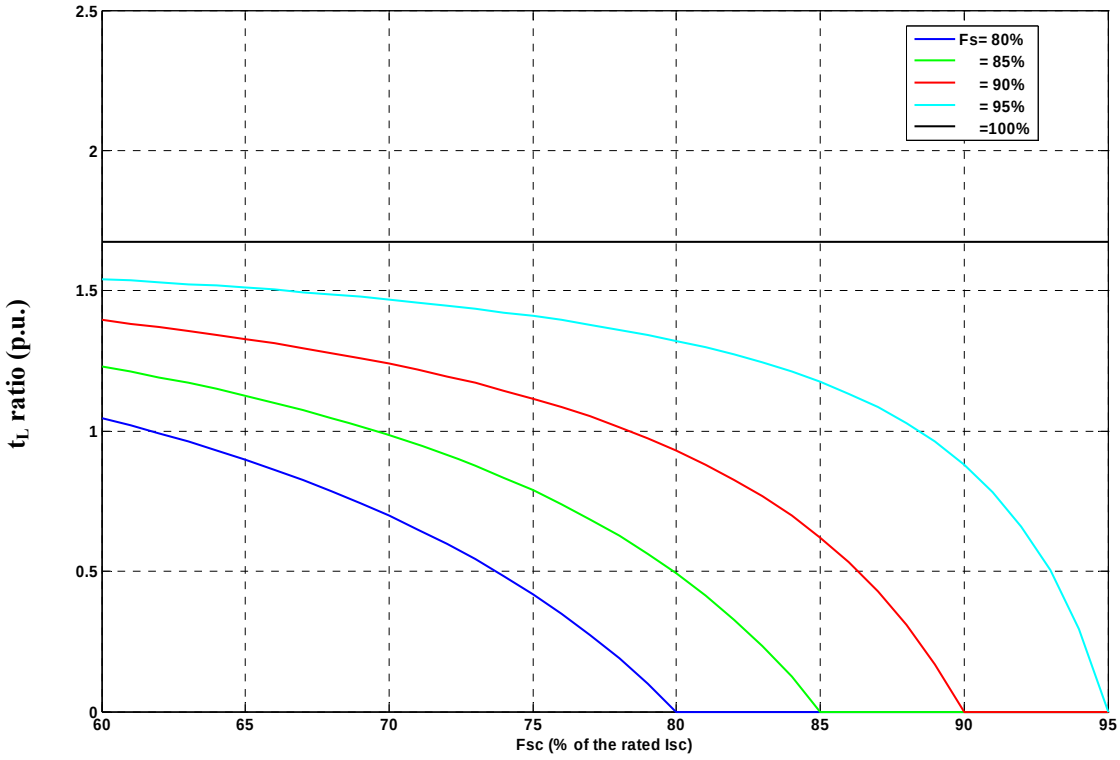

Figure 9.9: t_L ratio for source short-circuit power (F_S = 80-100% of the rated Isc) as a function of IEC SLF test duty (F_{SC}= 60-95% of the rated I_{SC})
a) $L_{li/m}$= 1.1 µH/m
b) $L_{li/m}$= 1.2 µH/m

10. Evidence from testing

10.1 Introduction

At the interruption of an electric current the following phenomena take place in a circuit-breaker. After contact separation the electric system will force an arc between the contacts to allow the current to keep flowing through the circuit. Modern high-voltage AC circuit-breaker technologies, like SF_6 gas and vacuum, need to wait for a current zero to extinguish the arc and thus clear the current. First, this chapter will deal with the dielectric performance of single pressure SF_6 gas circuit-breakers. At the end, attention will be given to vacuum circuit-breakers in this respect.

Within the first mucroseconds after reaching a current zero the power input into the arc is minimal, as the post-arc current is very small. To facilitate interruption, an attempt is made to reduce the arc conductivity fast enough to prevent the current from resumption, by cooling the remaining plasma adequately. The struggle between the cooling process (taking energy out of the arc) and the energy input into the arc (by the post-arc current) is called the thermal phase of the current interruption process. During the thermal phase, the initial part of the transient recovery voltage plays an important role, as some time delay (t_d) will help to limit the energy input, whilst a fast rise of the recovery voltage (RRRV) will increase the energy input by accelerating the plasma ions.

The duration of the thermal phase depends on the arc's thermal time constant, which, for SF_6 gas, is in the order of 0.3 to 0.4μs, leading to a thermally critical period of 1 to 2 μs [29]. If the gas blast is not sufficient to cool the arc and reduce its conductivity drastically, the current will resume and another attempt at current interruption will occur at the next current zero. As the circumstances may be more advantageous, since the gas flow and pressure may have increased, the circuit-breaker pole will have a better chance to be successful at this second attempt. But the circumstances may also become more severe, forcing the circuit-breaker to wait for a third current zero. At the end of the contact stroke, usually the circumstances are so bad that the circuit-breaker is not able to clear the current at all. In reality, for the severe test duties, the number of current zeros where the circuit-breaker pole may be successful in interrupting the current is very limited (one to two depending on the moment of current zero with respect to the contact separation).

As, in service, it is not known at which moment after contact separation the current zeros will appear, for a test duty it is required that the circuit-breaker pole is able to clear at a certain arcing time and every moment afterwards until half a cycle, so that at least the current zero falling into this period (the interrupting window) will lead to successfully clearing the current. The shortest arcing time that the circuit-breaker can handle is called the minimum arcing time. The time frame between the minimum arcing time and the longest arcing time the circuit-breaker can handle is called the interrupting window (under the condition that all arcing times in between will lead to successful clearings). Both minimum arcing time and interrupting window may vary for different test duties.

In this way, during the thermal phase it is determined at which current zero the circuit-breaker pole "wins the struggle" between energy input to the arc and output from the arc. It is the thermal performance of the design that determines also the minimum arcing time; i.e. the minimum contact gap at which the initial phase of current interruption is successful. After the thermal phase, the SF_6 gas plasma has disappeared and the insulating medium is a (very) hot SF_6 gas (i.e. several hundreds degree C to several thousands degree K [29]). The struggle around the arc is over, but the race between dielectric withstand strength and the dielectric

stress from the transient recovery voltage (TRV) takes over. As long as the dielectric withstand strength is larger than the dielectric stress the interruption will be successful. Otherwise a re-ignition will occur and current interruption may be attempted at the next current zero.

10.2 Basis for Short-line fault (SLF) requirements

The SLF test duties were introduced in international Standards to demonstrate the interrupting capability of high-voltage circuit-breakers in the thermal phase of interruption i.e. during the period of a few microseconds around the instant when current passes through zero and during which the evolution of arc resistance is governed by the energy balance in the arc [30].

A proven capability to interrupt short-line faults is required for circuit-breakers designed for direct connection to overhead lines (without intervening cable connections) and having a rated voltage of 15 kV and above and a rated short-circuit breaking current exceeding 12.5 kA. IEC 62271-100 [2] requires a single-phase test at phase-to-earth voltage to demonstrate the capability to interrupt all types of short-line faults (see sub-clauses 4.105 and L.3). IEEE C37.04 requires also the capability to interrupt single-phase SLF [31].

The choice of a single-phase SLF test is supported by the following considerations.

- The rate-of-rise-of-recovery-voltage (RRRV) is the main critical TRV parameter for SF_6 circuit-breakers. Single-phase SLF interruption produces the highest RRRV. Performing a single-phase SLF breaking test with the highest possible RRRV, determined either from the last pole to clear a three-phase SLF or the pole interrupting a single-phase SLF, covers also the 2-phase and 3-phase SLF conditions for all poles in the thermal phase of the current interruption.

  For SF_6 circuit-breakers, RRRV is the critical parameter in the thermal phase and the SLF capability is expressed by the maximum RRRV that can be withstood as function of the fault current derivative (di/dt) [29].

  Any decrease in the RRRV leads to an increase in the performance of an SF_6 circuit-breaker as can be seen with the following equation that gives the relation between the limit of the interrupted current (di/dt) and the RRRV [29]:

$$\mathbf{di/dt} = \frac{\mathbf{K}}{\mathbf{RRRV^a}} \qquad \text{with} \quad \mathbf{0.4 < a < 0.5} \qquad (10.1)$$

  Another characteristic of SF_6 circuit-breakers is that when the time to peak is at least five times the arc time constant (i.e. a time to peak higher than 1.5 to 2 μs), the limiting RRRV that can be withstood in the thermal phase is independent from the time to peak [6].

  Similar considerations apply to air-blast circuit-breakers that were found to be also most sensitive to the RRRV during the thermal phase of interruption.

  It is recognized that circuit-breakers using the vacuum or oil as interrupting media are not sensitive to the conditions of SLF in the thermal phase so that the interrupting capability is in practice covered by the terminal fault test duties, although SLF test duties are required for them as for other types of circuit-breakers.

- The surge impedance value of 450 Ω given in Table 8 of IEC 62271-100 and in IEEE C37.04 is such that RRRV for each pole to clear is covered in all cases.

- The single-phase short-line fault tests demonstrate an interrupting window of 180°-dα (dα being a small time interval defined as 18° in the standards) that covers the requirement for the multi-phase fault cases with effectively-earthed and non-effectively earthed systems (see section 4.6).

- The SLF test duties are defined for 90% of the rated short-circuit current (L90), 75% (L75) and 60% (L60). The idea is that the highest RRRV occurs at the highest percentage, but then the line-side peak value of the TRV is rather low. At 75% the RRRV is 17% lower, but the line-side peak is 2.5 times higher; at 60% the RRRV is 33% lower, but the line-side peak is 4 times higher. By the series L90, L75 and L60 both the highest RRRV and higher line-side peak values (triangular waveshapes) are covered.
- Experience indicates that L90 is the most severe test duty and that circuit-breakers are not really stressed by L60, unless they show a critical percentage below 90%. In recognition of this, L60 is only mandatory, when the minimum arcing time (t_{arc} min.) of L75 is a quarter of a cycle or more greater than t_{arc} min. for L90. Otherwise L90 and L75 are assumed to cover all possible SLF cases down to L60.

10.3 Circuit-breaker Dielectric Performance

For the thermal phase, the steepness of the recovery voltage (determined by RRRV and t_d) plays a critical role. During the dielectric phase, the peak value of the TRV is the most important stress factor, and of course the time to peak and the Standards define these aspects quite precisely in terms of two and four parameter TRV envelopes. Amongst other factors, the dielectric withstand strength depends on the contact gap and hence on the arcing time. With respect to the dielectric withstand strength, within the given interrupting window for a certain test duty, the minimum arcing time is expected to be the most critical one. Test duties with low currents, like capacitive currents, have no discernable thermal phase and very short arcing times are therefore possible leading to high dielectric stresses approximately one half cycle after current interruption. The dielectric strength after the interruption of such small currents is comparable with the cold dielectric withstand curve which is measured by stressing the circuit-breaker dielectrically without any current interruption involved [29].

However, the hot SF_6 gas after the thermal phase will have a lesser dielectric withstand strength than cold gas, due to the lower density of the gas and higher degree of dissociation at higher temperatures [29]. The higher the interrupted current, the higher the arc energy, the higher the SF_6 gas temperature during the dielectric phase will be. Arc duration and amplitude of the interrupted current are of influence to the blast pressure and to the cooling and refreshment of the hot SF_6 gas. Modern technology circuit-breakers are optimized for this cooling process, especially at L90 and T100.

Test duty T100 is performed at 100% of the rated short-circuit current and at TRV values higher than those of L90, but with a lower RRRV (2 kV/μs) and a larger t_d. L90 is a test duty with 90% of the rated short-circuit current, relatively low dielectric stresses, but a steep RRRV varying between 7 and 14 kV/μs (depending on rated short-circuit current and power frequency) and negligible t_d (in most circumstances). These characteristics typically lead to a larger minimum arcing time for L90 in comparison to T100, and thus a larger contact gap during the dielectric phase.

Table 10.1 offers the possibility to compare the data on the differences between minimum arcing times of L90 and T100s from four manufacturers. Knowing that the required arcing window varies from 6.1 to 7.5 ms (unearthed and earthed neutral networks) and from 7.5 to 9.0 ms for 60 and 50 Hz respectively, it is clear that there is a large overlap in the arcing windows of L90 and T100s. Knowing also that typical minimum arcing times are from 9 to 18ms, the total arcing-time difference between L90 and T100s is only a few percent, up to at

maximum of ten percent. Additionally the hot gas temperature will be less at L90 than that at T100, due to the lower interrupted current.

Table 10.1-Minimum-arcing-time differences between L90 and T100s test duties

Manufacturer	Voltage (kV)	Short-circuit current (kA)	Frequency (Hz)	t_{arc} min. (L90) - t_{arc} min. (T100s) (ms)
A	245	63	60	0.4
A	245	50	60	1.9
A	245	40	60	0.2
B	145	40	50	1.3
B	145	63	60	2.3
B	170	40	50	0.5
B	170	40	60	0.5
B	245	40	50	1.1
B	300	50	50	0.3
B	300	63	60	1.6
B	550	63	60	0.6
C	245	63	50	2.0
C	245	63	50	1.1
C	300	63	50	1.4
D	245	63	60	0.4
D	245	50	60	1.9
D	245	40	60	0.2
C	72.5	31.5	50	0.7
C	72.5	31.5	60	1.3
C	145	40	50	1.2
C	145	40	60	1.8

The minimum arcing time defines the smallest contact gap that has to withstand the dielectric stresses. Figure 10.1 shows schematically the dependence of the dielectric withstand strength as function of the contact separation (arcing time) for various test duties. Note that there will be some scattering around the linear characteristic, so that the lower 90% probability curve has to be used (not specifically shown in the figure). Figure 10.1 is indicative only, as the relationship between arcing time and contact gap is non-linear, but nevertheless gradually progressive, at least for T100s and L90 within a successful type test series as required by the Standards.

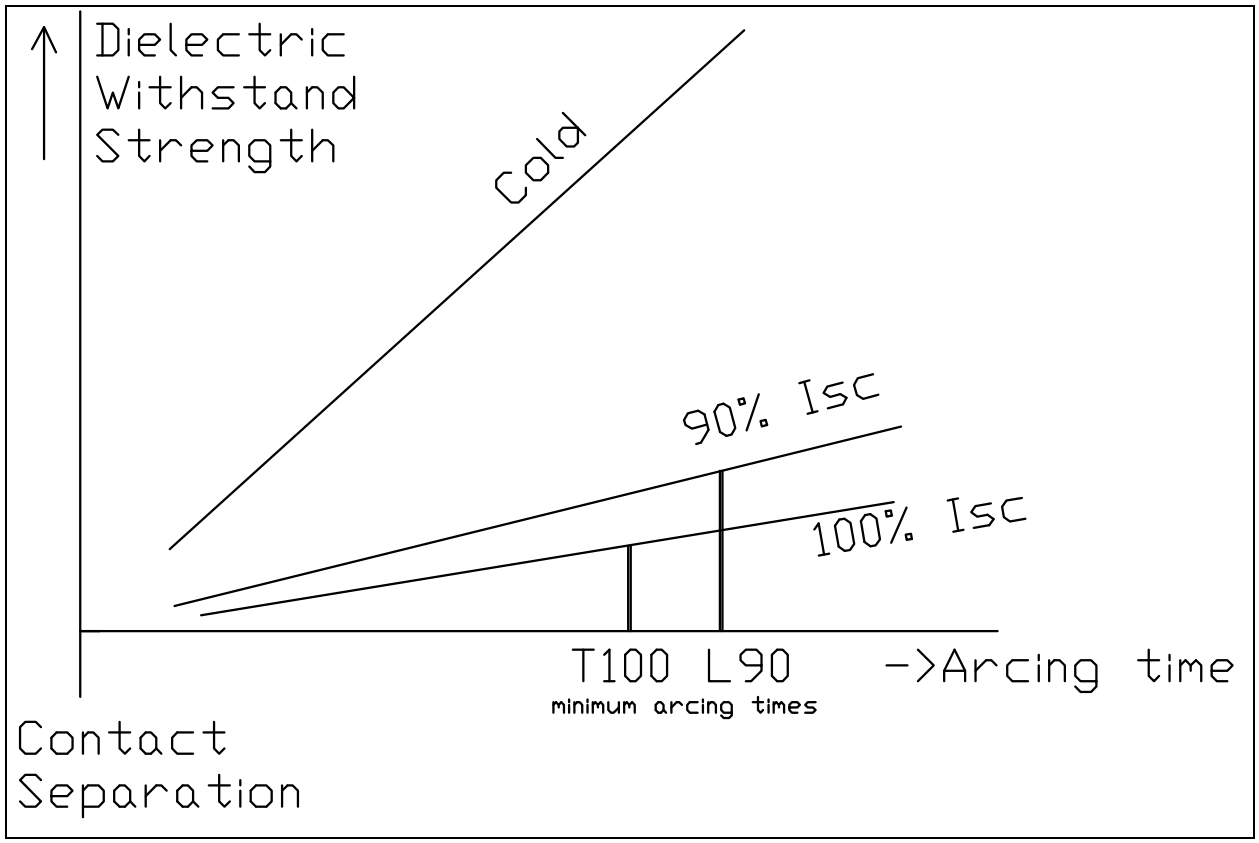

Figure 10.1: Dielectric withstand strength as a function of arcing time and short-circuit current amplitudes

The making and breaking type tests as specified in the Standards cover the different characteristics of the circuit-breaker, for instance:

- Thermal behaviour (the ability to show an interrupting window as large as required in the Standards) by L90 and L75 with longer minimum arcing times
- Dielectric behaviour with "hot gas" by T100, T60, T30, T10, OP with smaller minimum arcing times
- Dielectric behaviour with "cold gas" by capacitive current switching with very short minimum arcing times.

On the basis that a given circuit-breaker passes successfully the type tests (interrupting window long enough, no gaps in interrupting window, withstanding all dielectric stresses over the interrupting window), the above can be summarized as follows:

- RRRV and t_d determine the thermal stress immediately after current zero
- The thermal stress determines the minimum arcing time
- There is a non-linear, but gradually progressive relationship between the arcing time, the contact gap, and contact gap dielectric strength
- The minimum arcing time leads to the highest dielectric stresses within the interrupting window of any given test duty
- After the thermal phase, the dielectric withstand strength of the hot SF_6 gas is determined by its temperature/density
- The temperature is determined by arc energy and thus the amplitude of the interrupted current.

- The arcing time is less important for the temperature of the hot SF_6 gas, but plays a vital role in the pressure build-up used for the gas flow (cooling and refreshment of SF_6 gas).

By using the information on the minimum arcing time of T100s and knowing that typically a 2-parameter TRV ("steady" rise of 2kV/μs to U_c) cannot be withstood, whilst a 4-parameter TRV is required in the Standards ("steady" rise of 2kV/μs to U_1) an indication of the dielectric withstand curve can be given, as shown in figure 10.1, where at the minimum arcing time for T100s, the dielectric withstand strength curve will be just above U_1.

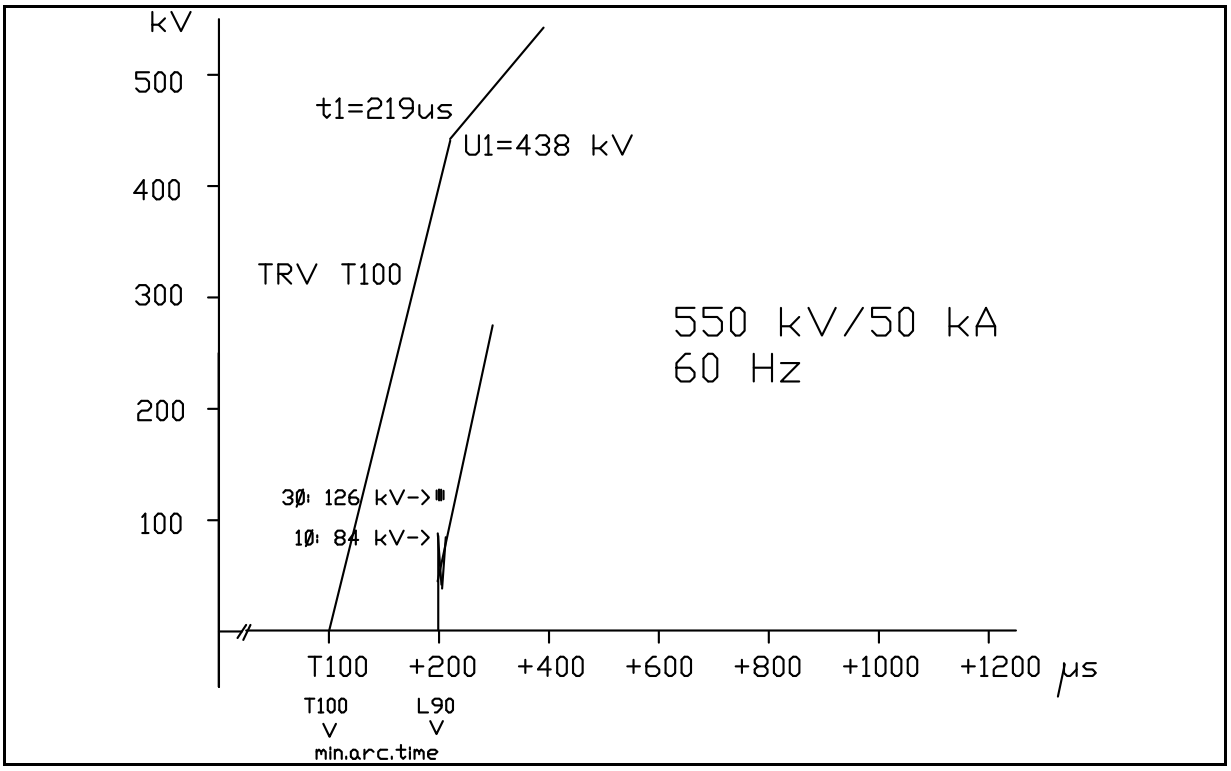

Figure10.2: Comparison of TRV peaks for T100s and single-phase/three-phase SLF L90 as a function of time, shifted for the minimum arcing time

Also shown in figure 10.1 is the minimum arcing time of L90 and the dielectric withstand strength at that moment, which anyway is larger than that of T100s at its minimum arcing time, due to the larger contact gap and due to the lower SF_6 gas temperature.

The following considerations are relevant to the rate at which the full dielectric strength of the contact gap is reached. It is well known from dielectric performance that the "cold" withstand strength is larger for fast phenomena (e.g. lightning impulse) than for slow phenomena (e.g. switching impulse) and this applies to hot gas as well. So, it is reasonable to conclude that the purely dielectric part of the L90 TRV could be steeper as long as it does not exceed the equivalent T100s TRV. Indeed, from SLF tests, it is well-known that circuit-breakers do not fail around the first peak of the line-side TRV wave-shape (see section 10.4). The key issue is not the dielectric withstand strength but the transition from the thermal phase into the dielectric phase.

In figure 10.2 the TRV envelopes of both T100 and L90 are given for a 550 kV/50 kA/60 Hz circuit-breaker, under the assumption of a difference in minimum arcing time of 0.2 ms, this being the minimum difference stated in table 10.1. The thermal phase determines the minimum arcing time, as shown on the X-axis, but is given no further consideration in the figure which deals with the dielectric phase. (Note that the total SLF-TRV of the single-phase fault is shown in figure 10.2, but on this time scale the triangular reflections at the line-side can hardly be seen.)

In figure 10.2, the 3-phase L90 case is also plotted which exhibits a similar minimum arcing time to the single-phase L90 and a roughly 50% higher dielectric stress, but this remains far below the expected dielectric withstand strength. That the hot SF_6 medium can withstand the steep RRRV is, apart from physics as discussed above, proven by the single-phase L90, where a higher RRRV than that of T100s has been withstood during the more difficult phase of recovery of the dielectric strength. Furthermore, testing evidence from several designs (different manufacturers) confirm this ability of single pressure SF_6 gas circuit-breakers.

For instance, a certain 245 kV design has been tested successfully for 50 kA/50 Hz and 40 kA/60 Hz ratings. This design has passed four SLF type tests according to IEC: L90 and L75 at both 50 and 60 Hz. SLF interrupting capability of SF_6 gas circuit-breakers depends on the current derivative before current zero (di/dt) and the RRRV that is proportional to the di/dt (except if capacitors are used). It follows that the maximum short-circuit current that can be interrupted is different for applications at 50 and 60 Hz. Taking the example above, the de-rating at 60 Hz is due to the fact that the di/dt would be 20% higher than at 50 Hz, when the rated short-circuit current remains unchanged.

The following example shows how type tests performed at 50 Hz to demonstrate a 50kA rating, can be used to demonstrate a three-phase SLF interrupting capability at 60 Hz (40kA rating) in some typical cases. SLF withstand values for both single-phase and three-phase SLF are shown in figure 10.3 for a 245-kV circuit-breaker.

Let assume the following conditions for single-phase SLF L75 and L90:

1 - 245 kV/50 kA/50 Hz

Test conditions of L75**:**

I_{SC} = 37.5 kA
U_L = 80 kV
du/dt_L = 7.5 kV/µs
First peak of TRV (including supply side contribution): **93** kV (point ①, Fig. 10.3)
RRRV = **8.7** kV/µs
Interrupting window required: 9 ms

2 –245 kV/40 kA/60 Hz

Test conditions for L90:

I_{SC} = 36 kA
U_L = 32 kV
du/dt_L = 8.64 kV/µs
First peak of TRV (including supply side contribution): **35** kV (point ②, Fig. 10.3)
RRRV = **9.45** kV/µs
Interrupting window required: 7.5 ms

For three-phase SLF L90:

3 –245 kV/40 kA/60 Hz

a) First example of a special specification based on a peak factor of 2.4 for the line side contribution to TRV and a surge impedance of 390Ω, both parameters being relative to the first pole to clear

Test conditions for L90**:**

I_{SC} = 36 kA
U_L = 48 kV
du/dt_L = 7.5 kV/µs
First peak of TRV: **55.9** kV
RRRV = **8.7** kV/µs
Interrupting window required for the first pole to clear: 2.5 ms

b) Second example where the surge impedance and the peak factor for the 3-phase fault are respectively 410Ω and 2.4

Test conditions for L90**:**

I_{SC} = 36 kA
U_L = 48 kV
du/dt_L = 7.87 kV/µs
First peak of TRV: **55.4** kV (point ③, Fig. 10.3)
RRRV = **9.1** kV/µs
Interrupting window required for the first pole to clear : 2.5 ms

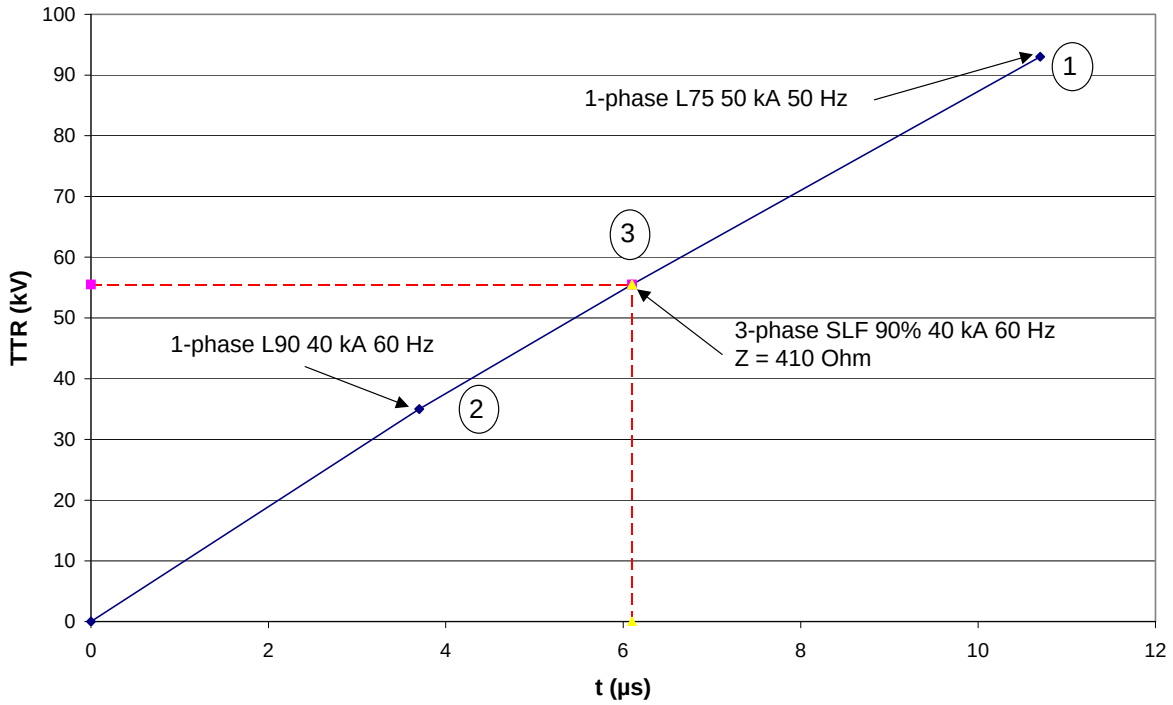

Figure 10.3: Comparison of withstand values for both single-phase and three-phase SLF for a 245 kV circuit-breaker

With respect to the difference in minimum arcing times for L90 and T100s, examples from different manufacturers are given in table 10.1 and lead to the conclusion that, as can be deduced from figure 10.2, enough margin is available, though often less than 1 ms. However, it should be noted that the accuracy of controlling the arcing time is limited: the Standards prescribe an accuracy of 0.5 ms. In any case, the experience with SF_6 high-voltage circuit-breakers is that the minimum arcing time for L90 is higher than the value obtained for T100s.

In a similar way, as shown in figure 10.2, L60 and T60 can be compared (figure 10.4), leading to the same conclusion, taking into account that the minimum arcing time of T60 will be less than, or at most equal to, that of T100s and the minimum arcing time of L60 will be about the same as that of L90.

From the above considerations, it can be concluded that for SF_6 gas circuit-breakers we might expect 3-phase SLF duties above 50% of the rated short-circuit current to be covered by the dielectric performance at T100/T60 and the thermal performance at single-phase L90 and L75 type tests.

It is known that vacuum circuit-breakers are not sensitive to high RRRVs and therefore SLF tests are not critical at all. Even in the event of a re-ignition, a second clearing attempt will be made at the next current zero under more favourable conditions. It is widely accepted that vacuum circuit-breakers are more sensitive to the dielectric stresses appearing at T100, especially Uc, which is much higher than the stresses occurring at L90 (both for the first and for the last clearing poles).

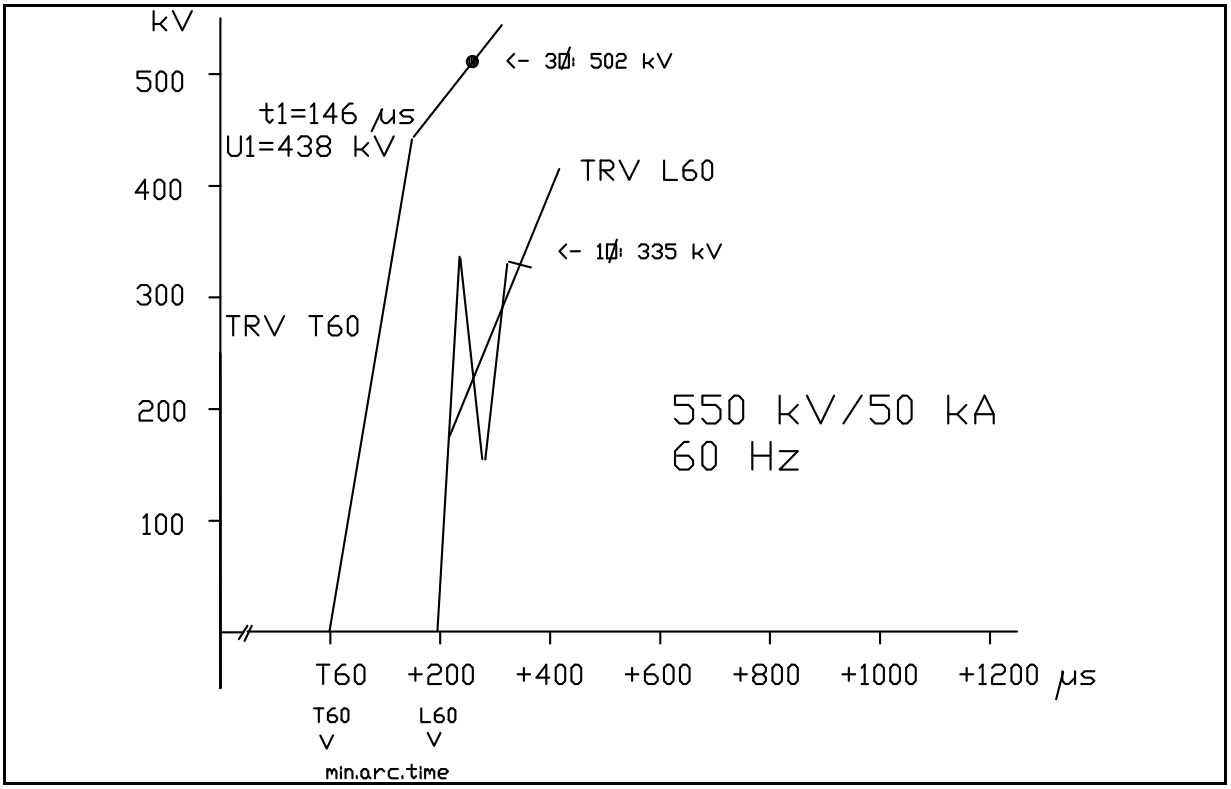

Figure 10.4: Comparison of TRV peaks for T60 and single-phase and three-phase SLF L60 as a function of the minimum arcing time

10.4 Results from SLF current zero measurements

The results of 743 SLF tests, performed in ten test stations in Europe, Asia and the USA, and covering thirty circuit-breaker designs from 72.5 to 550 kV have been analyzed on the basis of special current zero measurements. More than 90% of the tests have been conducted in accordance with IEC Standard 62271-100. The purpose of the investigations was to tune the simulation model for arc-circuit interaction in order to facilitate circuit-breaker design and to extrapolate test results to different circumstances. The arc model used is for the thermal interruption phase and not for the dielectric phase, but during testing the behaviour of the test object during the thermal phase as well as during the dielectric phase can be observed.

It is reported that from these 743 SLF tests, 432 resulted in a successful interruption. Of these the measurements show post-arc currents mostly less than 50mA, sometimes up to 100 mA and very rarely up to some hundreds of mA. The post-arc current normally decayed to zero long before the first line-side TRV peak is reached.

From the 311 re-ignitions, 291 cases occurred with a thermal re-ignition (i.e. under influence of the post arc current) with the moment of re-ignition being much earlier than the moment of the first inherent TRV peak. A further seven cases with a “dielectric” re-ignition have been reported before the TRV reached 50% of the first inherent peak value of the TRV (at the line-side) and two cases with a “dielectric” re-ignition between 50% and 100% of the first inherent peak value of the TRV (at the line side). This re-ignition mode is called a transition mode between the thermal phase and the dielectric phase of the interruption process.

There were 11 cases with a re-ignition long after the first line-side peak value of the TRV, usually near the crest value of the total TRV (Uc), a region where no thermal effects are involved.

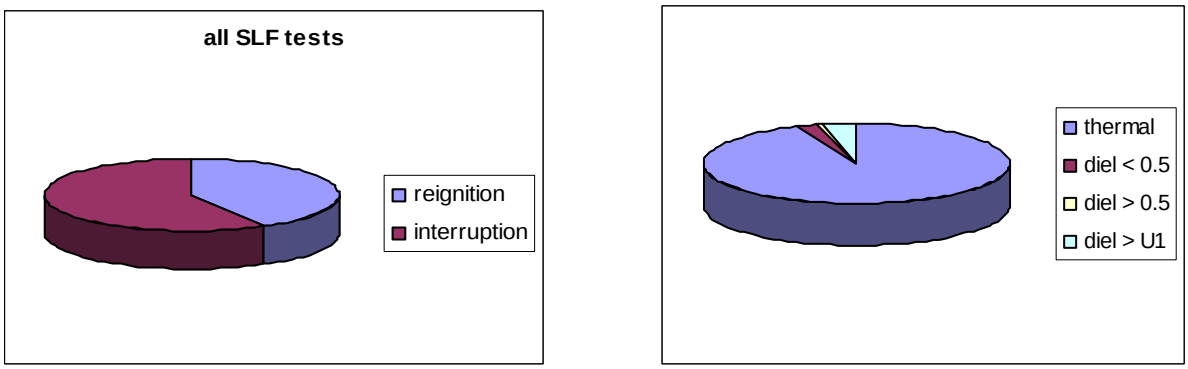

Figure 10.5: Distribution of re-ignitions versus interruptions and of re-ignition characteristics

Since the measurements were also performed to further improve the arcing models of the designs involved, additional SLF tests have been carried out at unrealistically short arcing times varying from 0 to over 25 ms. All dielectric re-ignitions were observed at tests with realistic arcing times.

Figure 10.5 shows the percentage of re-ignitions versus interruptions, as well as the subdivision of the re-ignitions.

Considering all of the SLF tests, 42% show a re-ignition, but a large percentage of tests have been performed at unrealistically short arcing times. This percentage is roughly 30% (of the thermal re-ignitions). When corrected for this 30%, it can be concluded that of the total amount of re-ignitions:

- ~ 5% are of a pure dielectric nature
- > 3% are of a transitional nature and occurred before 50% of the first line-side peak
- < 1% are between 50% and 100% of the line-side peak of the TRV.

It is to be expected that the re-ignitions with a pure dielectric nature would occur at terminal fault tests as well. This is important, as the considerations in the paragraph 10.3 were based on a design that successfully passed the regular type tests (with single-phase SLF tests) and its capability to handle a three-phase SLF was investigated. The considerations are not applicable to a design with a dielectric behaviour that is too weak to pass the regular tests.

So, excluding these 5% of the re-ignition cases from consideration, 96% of the re-ignitions are of a thermal nature and 4% are of a semi-dielectric nature mostly with a re-ignition at less than half of the first TRV peak value. For these SLF tests, the percentages of re-ignitions drop sharply with increasing TRV values, as shown in the figure 10.6. Where semi-dielectric re-ignitions are less than 5% of the total amount of re-ignitions, the amount above half of the first TRV peak is even less than 1% and can be disregarded.

As such the results from the current zero measurements support the view that SLF tests are critical during the thermal phase of the interruption process, whilst the dielectric phase is not critical.

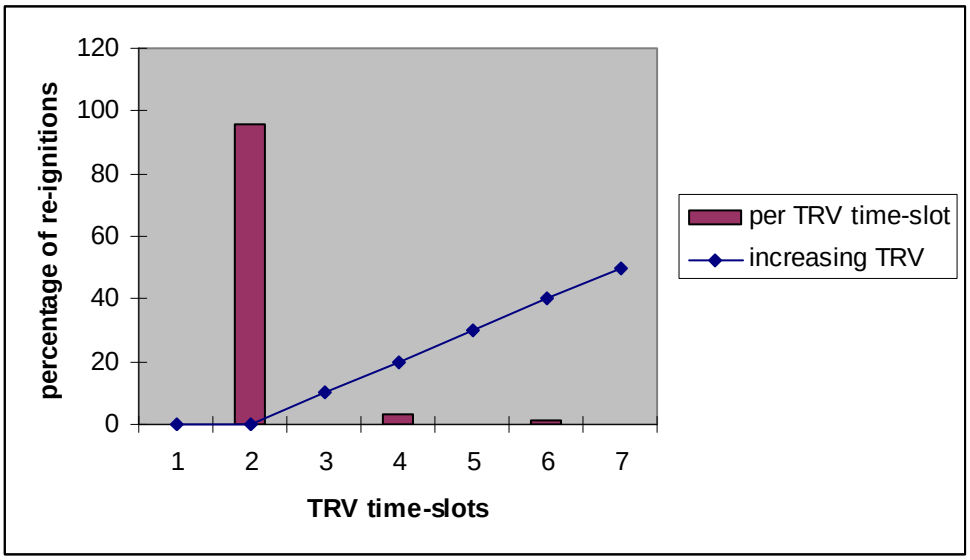

Figure 10.6: Distribution of re-ignitions versus line-side TRV (complete first ramp of line-side triangular waveshape is shown) (3 time slots: thermal, < 50%, > 50%)

10.5 Further considerations

- It is not necessarily true that L90 gives a larger minimum arcing time than T100s. The application case being given most consideration in the 3 phase line fault study is 550 kV for which modern circuit-breakers typically have two arcing chambers. With two equally graded arcing chambers, the thermal stresses are divided by approximately two and the time delay is increased by typically 0.2μs to 0.5μs, depending on the magnitude of the grading capacitors used. On this basis, the thermal stress from SLF is greatly reduced in comparison to single interrupter applications and the terminal fault duty (T100s) may actually determine the minimum arcing time. However, in such cases it can be argued that the design is over-dimensioned with respect to the SLF capability and that the higher peak value at 3-phase SLF will be covered automatically. In practice, manufacturers will aim to optimize their design for T100 as well as SLF, taking advantage of a longer time delay; an optimization that leads again to slightly larger arcing times for L90 in comparison to T100s.

- The contact gap is not the only determinant of TRV withstand performance since circuit-breakers have very complex relationships between contact parting time, contact gap, current phase at contact part time, pressure build up from current/ablation effects, and the resulting gas mass flow and nozzle arc zone flushing and rinsing. The mass flow and resulting flushing phenomenon are very important for TRV withstand performance. Notwithstanding this, the vast majority of experience shows that the dielectric withstand capability increases progressively with the contact gap (see also chapter 5 of [32]). Indeed, Standards are based on the awareness of the existence of a minimum arcing time after which the dielectric capability has at least to be maintained during the interrupting window. The highest TRV peak that has to be withstood during a three-phase SLF is only be experienced by the first clearing pole and the interrupting window for this pole is only 42º (see table 4.2). During test duty T100s, the dielectric withstand capability is demonstrated for 132° or 162°.

11. Risk Tolerance

About 40 years ago, CIGRÉ SC 3 recommended to IEC Subcommittee 17A to consider single-line to ground faults only, in order to avoid unjustified increases in circuit costs which would be required to address extremely unlikely conditions; namely three-phase short-line faults at the critical distance, with 100% short-circuit capacity on the supply side. Despite the fact that, from a technical point of view, the original position remains valid, the risk of a circuit-breaker failing as a result of such a rare duty resides with the user of the equipment. Indeed, some utilities are subject to legislation and regulations that may prevent them from taking probabilistic arguments into consideration for issues of this nature. These utilities are held liable for extreme conditions that could have been foreseen. Since three-phase faults do occur, utilities have to take them into consideration in some form, in order to satisfy the requirements of society.

Whilst utilities cannot simple disregard three-phase faults, the degree of special provision made to cater for them varies widely. Today's utilities are more business focussed than their predecessors and many have introduced the asset owner – asset manager – service provider models to tune the organisation better to the business values and business objectives the company has in mind. Risk management as a tool to balance financial, technical and societal aspects and to define the company's risk appetite is now widely accepted. Risk is defined in terms of the probability and the consequence of an event. However, the perception of risk is generally not linear, in that, for risks with major consequences the risk appetite requires a far lower probability than might be expected form a simple "probability × consequence = constant" [33] approach. As such utilities may not accept that a three-phase fault current cannot be interrupted, despite the very low probability of occurrence, and therefore they may adapt their specifications to cover all prevailing three-phase faults.

Risk management is a valuable tool for balancing the various risks faced by the utility It can be used to compare risks such as those of not tripping a three-phase fault, those of not clearing, for instance, at an out-of-phase condition or those of not clearing any particular condition due to inadequate specification and testing of old circuit-breakers. The main difference between taking three-phase faults into consideration for liability reasons or for risk management reasons is this balancing the possible risks.

There is always a risk associated that a circuit-breaker may not clear a three-phase short line fault with a higher peak value of the line-side TRV than specified in the Standards. As discussed previously, and according to the logic of IEC Standard 62271-100, such a risk is considered to be too low to be covered by separate or adapted type tests. In case a utility considers that the risk as unacceptable, special type tests (termed application tests in IEc 62271-100) can be specified to address the specific concerns of the utility.

Whether such a test is necessary or whether the capability of the circuit-breaker can be adequately proven by extrapolation of other test results remains an issue for agreement between user and manufacturer.

Part III

Implications for long-line faults

12. Long Line Faults

At the CIGRÉ SC A3 Session in 2006, Report A3-303 [18] from Japan was presented which describes high TRV peak values that exceed the Japanese Electrical Committee (JEC) Standard. Special duties were specified to cover these cases, for example T30-A and T30-B as described in the figure 12.1 below. The mechanism of the high TRV generation is related to LLF interruption. However, the high peak values mainly depend on the operating voltage condition of 600 kV which is 10% higher than the rated voltage of 550 kV in the IEC and JEC Standards.

The T30 prospective TRV in JEC and in previous IEC Standards with four parameters cannot cover the first peak voltage of the TRV due to LLF under such conditions, and additional test duties in Report A3-303 [18] have been specified. It is noted that the TRV specified in the latest IEC almost covers the expected TRVs due to LLF at 600 kV.

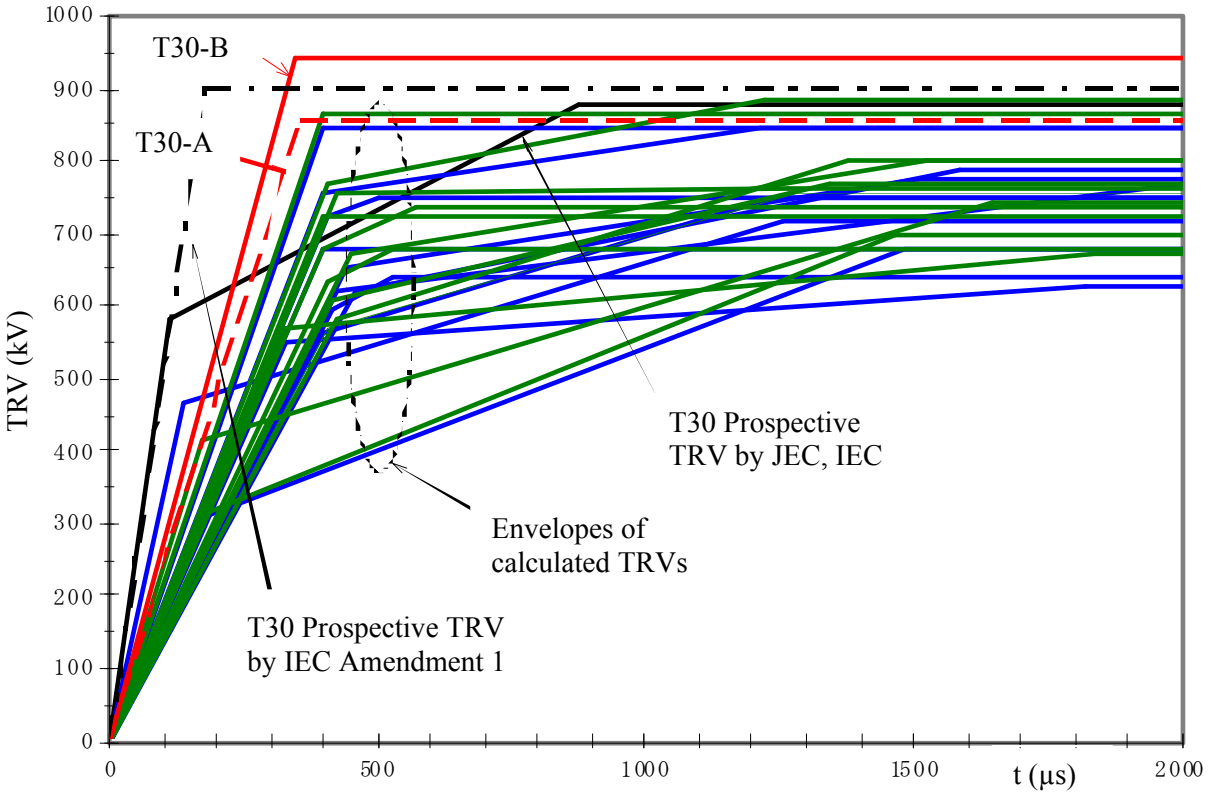

Figure 12.1: from CIGRÉ Report A3-303 (2006)

Oppositely, in the next figures, the situation is elaborated where the operating voltage (735 kV with maximum 765 kV) is less than the rated voltage (800 kV) which forms the basis for the TRV specifications. Figures 12.2 and 12.3 show the TRVs for the first pole clearing a three-phase L30 and L10 in comparison to the last clearing pole.

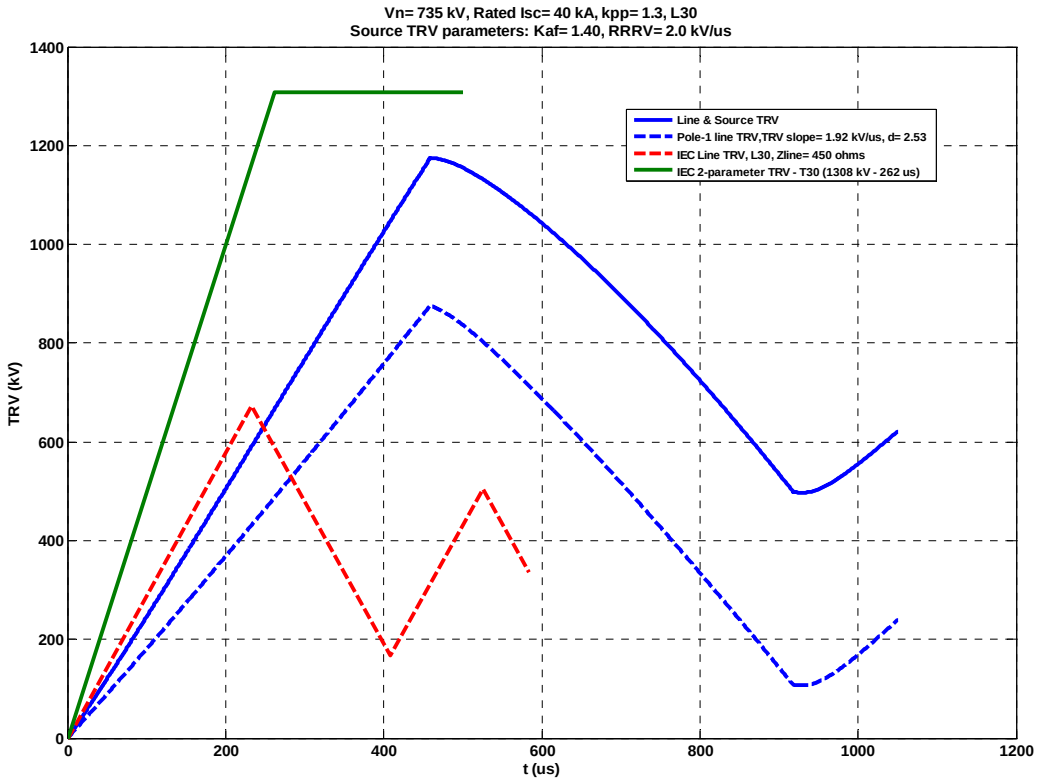

Figure 12.2: Comparison of 735 kV/40 kA first (blue) and last (red) clearing pole TRVs for three-phase L30, with total TRV for first pole (blue)

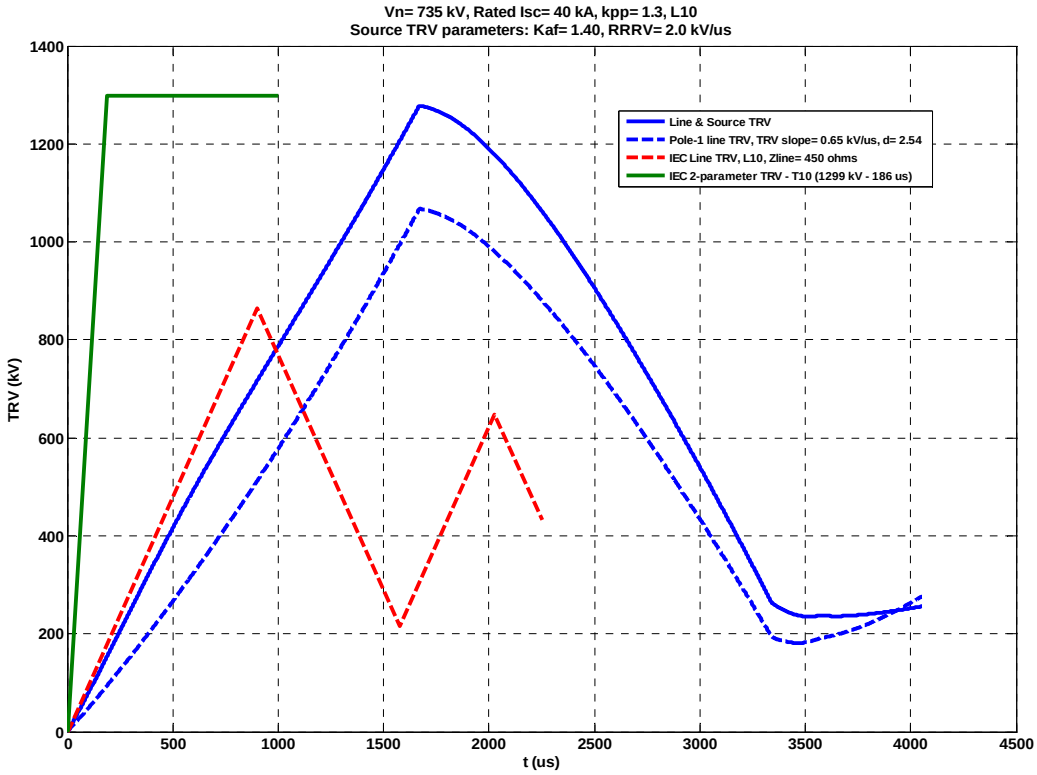

Figure 12.3: Comparison of 735 kV/40 kA first (blue) and last (red) clearing pole for three-phase L10, with total TRV for first pole (blue)

The green lines in figures 12.2 and 12.3 represent the TRV envelopes for T30 and T10 based on 800 kV. Extrapolating the simulation results calculated with 735 kV to 800 kV reveals that a three-phase LLF with 30% of the rated short-circuit current is just covered by T30, whilst a three-phase LLF with 10% is not covered by T10. The envelope for T10, as shown in figure 12.3, is based on a first pole-to-clear-factor of 1.3, but for T10 the latest edition of IEC Standard 62271-100 has introduced again the old first pole-to-clear-factor of 1.5. With the new factor leading to a peak value of 1499 kV, the three-phase LLF at 10% is therefore also covered.

LLFs correspond to short-circuit currents as specified for the test duties T30 and T10. As the test duties for out-of-phase switching are based on currents that are 25% and 5% of the rated short-circuit currents, the TRV parameters for OP can be taken into consideration also. In many cases the results from straight-forward calculations and simulations show that LLF can be considered as covered, assuming that for the OP test duty the minimum time to peak will be applied and that for T10 the first-pole-to-clear factor will be adapted to 1.5 instead of 1.3.

The LLF case, as described in [18], combines the travelling wave phenomena with an operating voltage higher than the rated operating voltage. Since operating voltages higher than rated voltages are outside the scope of the studies of WG A3.19, this aspect will not be considered and it can be concluded that generally LLF is covered by T30, T10 and OP.

Similar travelling wave phenomena as described for LLF can be experienced with out-of-phase switching, when the equilibrium point (the virtual short-circuit point) is on a long overhead line [19][20]. Figure 12.4 is taken from [20] as an example of a simulated out-of-phase condition on a long 1100kV line.

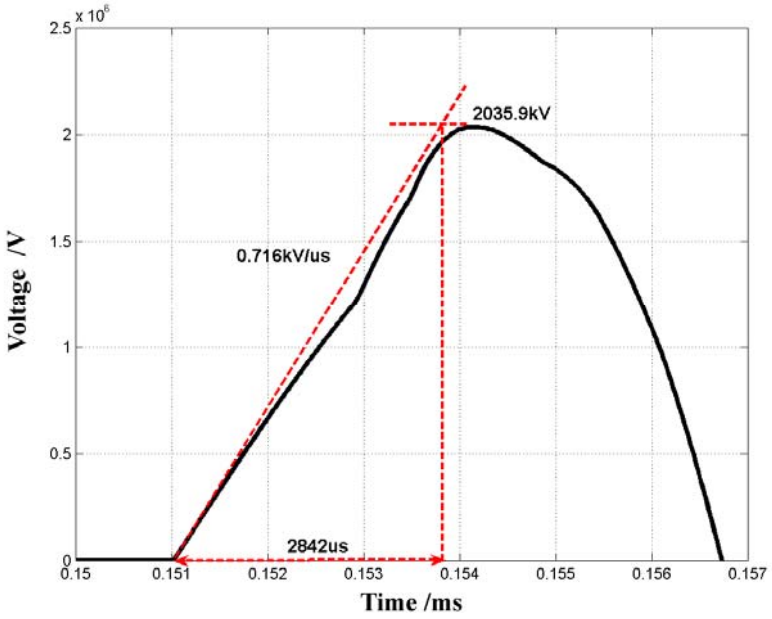

Figure 12.4: TRV waveform of Nanyang CB during out-of-phase condition while the oscillation center is in Jing-Nan line

Another phenomenon related to LLF has to be mentioned as well. In case of a LLF in a system with two circuits in parallel, the switching overvoltage caused by the circuit-breaker at the other side of the faulty line, will appear at the busbar of the substation with the circuit-breaker under study. When the circuit-breakers at both sides of the faulty line receive a

tripping command at the same time, as is usually the case with modern protection schemes, the timing of arrival of the traveling wave from this switching overvoltage may coincide with the timing of the TRV of the circuit-breaker under study. At the busbar terminal a traveling wave from the opposite side may arrive during the time frame of the first ramp from the traveling waves on the line. Together, these waves may cause a rather severe TRV waveshape with a peak value more severe than considered so far. Such a coincidence of traveling wave phenomena should not be overlooked in networks with a rather simple topology, like for 1100 kV. However, for meshed networks the traveling waves from the switching overvoltage will damp rather fast due to reflections at the substation of the sending end (and behind that point) and at the receiving end (and behind). Therefore, generally speaking, it can be neglected.

12.3 Conclusions

- Single-phase LLF cases are considered as covered by T30 and T10.
- TRV calculations show that at clearing three-phase long line faults the TRV waveshapes give higher peak values at the line side than for single-phase faults.
- Under certain circumstances the peak values for three-phase long line faults are slightly beyond the TRV envelope as specified in the Standards for the terminal fault test duty T30 (Chapter 6).
- Lower short-circuit currents are covered by the newly specified TRV envelope for T10 ($k_{pp} = 1.5$), and the envelope for the out-of-phase test duty OP, when the shortest time to peak is specified.
- The influence of a lower short-circuit power at the busbar is only marginal.

Conclusions

13. General conclusions

1. Circuit-breaker standards do not specify testing which explicitly covers all conceivable combinations of network conditions. Interpolation and/or extrapolation of the specified tests is necessary to demonstrate the full performance envelope of the tested equipment. The present standards use this approach to justify that all line fault interruption conditions are covered by the presently specified tests.
2. It is widely recognized that, with low probability, system conditions can exist which exceed standardised test values. It is not appropriate to base standardised values on these conditions but they must be recognised and catered for by users. Special customised tests or other means to prove the performance may be required in some cases.
3. Circuit-breaker standards are not truly technology independent however they treat known interrupting technologies equally. Specification of the type test regime and interpolation and/or extrapolation of test results require knowledge of the tested technology and particularly of its critical sensitivities. Without such knowledge, decisions regarding which particular tests to specify are impossible.
4. The process of standardisation and the interpolation and/or extrapolation of test results incorporates a level of risk assessment and risk management. This is an integral part of the standards making process where a balance must be struck between eliminating all risk (testing everything) and specifying an acceptable test regime.
5. Users should be aware of the assumptions and levels of risk embodied within circuit-breaker standards to ensure that operational risk falls within acceptable levels. Should the risks, when quantified, be considered excessive, also in a wider application, the standardisation bodies should be addressed regarding improvements to the standards.

Detailed conclusions on line fault phenomena are given in the summary.

References

[1] *Severe Duties on High-Voltage Circuit-Breakers observed in Recent Power Systems*
H. Hamada, Y. Kasahara, T. Shimato, K. Hirasawa, K. Suzuki, T. Yoshizumi
CIGRÉ SC 13 Session 2002, Report 13-103

[2] IEC Standard 62271-100, Edition 1.1 (May 2002)
Part 100 : High-voltage alternating-current circuit-breakers

[3] IEC document 17A/815/FDIS, Final Draft International Standard
IEC 62271-100 Ed.2: High-voltage switchgear and controlgear - Part 100 : High-voltage alternating-current circuit-breakers

[4] *Analysis of Circuit-breaker Transient Recovery Voltages Resulting from Transmission Line Faults*
Anders L. Johnson
Thesis for the degree of Master of Science at the University of Washington (2003)

[5] IEC document 17A(CIGRE)1, September 1963
Preliminary conclusions concerning short-line faults in three-phase systems
Communication dated 19th August 1963 to the Central Office of IEC from
Dr. H. Meyer, Chairman of CIGRE Study Committee3

[6] *Extremely short line fault tests of a puffer-type gas circuit-breaker by direct and synthetic test methods*
S. Tominaga, e.a.
IEEE Transactions on Power Apparatus and Systems, Vol. PAS-100, N02, Feb.1981

[7] IEC Standard 62271-100, Edition 1.2 (July 2006)
Part 100 : High-voltage alternating-current circuit-breakers

[8] *Surge Impedance of Overhead Lines with Bundle Conductors during Short-Line Faults*
CIGRÉ WG 13.01
Électra 17 (1971), pp. 113 - 122

[9] *Overhead-line parameters for circuit-breaker application*
E. Bolton, D. Birtwhistle, P. Bownes, M.G. Dwek, G.W. Routledge
Proc. IEE, Vol. 120, No. 5, May 1973, pp. 561 - 573

[10] *Transient Recovery Voltage in the Short Line Fault Regime*
M. B. Humphries
Proceedings of Symposium "Current interruption in HV networks", Baden 1977, published as book by Plenum Press, ISBN 0-306-40007-3

[11] *An Investigation of the Forces on Bundle Conductor Spacers under Fault Condition*
C. Manuzio
IEEE PAS, Vol. 86, No. 2 (Feb. 1967), pp. 166

[12] *fault and Load Current testing of a Bundle Conductor Spacer*
R. L. Retallack, T.R. Fry, C.A. Popeck
AIEE Transaction, pt.III, Vol. 82 (Oct. 1963), pp. 724

[13] *Electrocdynamic Studies of Bundled Conductor Spacers*
J. R. Ruhlman, R.A. Eucker, R.L. Swart
AIEE Transaction, pt III, Vol. 82 (Oct. 1963), pp. 750

[14] *Horizontal Bundle Spacers*
R. J. Mather, A.R. Hard
AIEE Transaction, pt III, Vol. 77 (Oct. 1958), pp. 823

[15] *Design on Bundled Conductor Spacer for Large Capacity Power Transmission Lines (Part I)*
R. Kashimura, N. Momose, T. Kasahara, T. Hirai
Showa-densen review, Vol. 21, No.3, (1971)
[16] IEEE Std. C37.011 (2005) *Application Guide for Transient Recovery Voltage for AC High-Voltage Circuit-breakers*
[17] CIGRÉ Technical Brochure 305, October 2006
Guide for the Application of IEC 62271-100 and IEC 62271-1, Part 2: Making and Breaking Tests
[18] *Severe Stresses on Switching Equipment of 500 kV Transmission System in Japan*
T. Shirato, K. Yokotsu, H. Yonezawa, J. Kida, T. Yokota, T. Sugiyama
CIGRÉ SC A3 Session 2006, Report A3-303
[19] CIGRÉ Technical Brochure 336, December 2007
Changing Network Conditions and System Requirements, Part II: The impact of long distance transmission on HV equipment
[20] *The Transient Characteristics of 1100 kV Circuit-breakers*
Lin Jiming, e.a.
IEC/CIGRÉ UHV Symposium Beijing, July 2007, Report 2-4-4
[21] *An International Survey on Electrical Stresses on High Voltage Circuit-breakers in Service*
CIGRÉ document 13-97 (SC)31 IWD, 13-97(WG08)69 IWD
A.L.J Janssen, W. Lanz, on behalf of CIGRÉ WG 13.08
[22] *Life-Management of Circuit-Breakers - A Summary of the Studies of CIGRE WG 13.08*
A.L.J. Janssen W. Lanz D.F. Peelo G. de Radiguès D. Makareinis
CIGRÉ SC 13 Session 2000, Report 13-104
[23] *Studies on Life Managaement of Circuit-Breakers*
A.L.J. Janssen Y. Yamagata W. Lanz G. Aldrovandi W. Degen
CIGRÉ SC 13 Session 1998, Report 13-204
[24] *Reliability end Electrical Stress Survey on High Voltage Circuit-breaker In Japan*
Y. Nakada, I.Takagi, M. Shin, J. Kida, M. Toyoda, H. Ito
CIGRÉ SC A3 Session 2006, Report A3-205
[25] *Stress of HV Circuit-Breakers during Operation in the Networks – German Utilities' Experience*
C. Neumann, G.Balzer, J. Becker, R. Meister, V.Rees, C.E. Sölver
CIGRÉ SC 13 Session 2002, Report 13-304
[26] IEC Technical Report 62271-310, April 2004
Electrical endurance testing for circuit-breakers of rated voltage 72.5 kV and above
[27] CIGRÉ Technical Brochure 165, August 2000
Life Management of Circuit-Breakers
[28] IEC 17A/MT40 document
Hydro-Québec Data 1980-2002 provided by Y. Filion
[29] CIGRÉ Technical Brochure 135, December 1998
State of the Art of Circuit-Breaker Modelling
[30] *A new concept in post arc analysis applied to power circuit-breakers*
Guy St Jean, Michel Landry, Marc Leclerc, André Chénier
IEEE Transactions on Power Delivery, Volume 3, N°3, July 1988
[31] IEEE Standard C37.04-1999
IEEE Standard Rating Structure for AC High-Voltage Circuit-breakers

[32] *Simulations and Calculations as Verification Tools for Design and Performance of High-Voltage Equipment*
M.K. Kriegel, e.a.
CIGRÉ SC A3 Session 2008, Report A3-210
[33] CIGRÉ Technical Brochure 309, December 2006
Asset Management of Transmission Systems and Associated CIGRÉ Activities

Appendix A: ATP simulation results of 3-phase line faults giving d-factor values for the 1st, 2nd and 3rd poles.

ATP simulation results of 3-phase line faults

I_{sc} = 63 kA, U_r = 420 kV, f_r = 50 Hz, RRRV = 2.0 kV/µs, k_{af} = 1.4 p.u., X_0/X_1 = 1.0

U_r [kV]	I_{SC} [kA]	Line length [km]	Line TRV parameters for the 3 phases					TRV (line + source) of 1st peak of FPTC			di/dt	Z_L calculated
			u_0 [kV]	$\hat{U}_L$ [kV]	t_L [µs]	d [p.u.]	S_L [kV/µs]	u_p [kV]	t_{LS} [µs]	S_{LS} [kV/µs]	[A/µs]	[Ω]
420	6.3 (L10)	136	307	-455	920	2.48	0.83	788	920	0.85	2.81	295
			-307	410	920	2.34	0.78				2.54	307
			318	-203	920	1.64	0.56	540	920		1.70	329
	18.9 (L30)	35.5	240	-359	241	2.50	2.49	727	241	3.02	8.40	296
			-244	318	241	2.30	2.33				7.00	330
			277	-170	241	1.61	1.83	548	241		5.05	362
	37.8 (L60)	10.2	137	-208	69	2.52	5.00	429	69	6.21	16.8	298
			-152	183	69	2.20	4.86				15.0	324
			189	-109	69	1.58	4.32				12.0	360
	47.3 (L75)	5.1	85.5	-128	35	2.47	6.04	265	35	7.57	21.0	287
			-103	105	35	2.02	5.94				19.0	313
			131	-71.1	35	1.54	5.77				17.0	340
	56.7 (L90)	1.7	34.4	-51.5	12	2.50	7.16	107	12	8.91	25.2	284
			-45.1	41.9	12	1.93	7.20				24.1	300
			57.4	-33.2	12	1.58	7.55				23.4	322

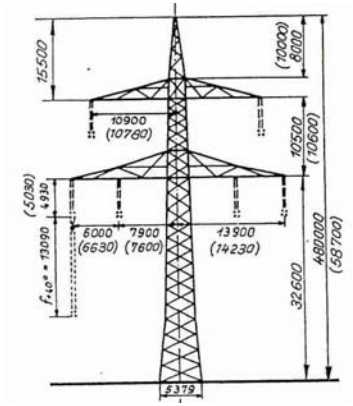

Appendix B: Simulation results of the first-pole-to-clear line TRV parameters for typical HV overhead lines

B1 Typical tower shapes of HV overhead lines in Germany

In the following pages, simulation results are presented for the German 145, 245 and 420-kV overhead lines, while the impact of the variations in the source impedances (80% and 100%) is given for 145 and 420 kV. TRV parameters have been assessed for k_{pp} of 1.0 and 1.5.

Voltage level: 123 / 145 kV	
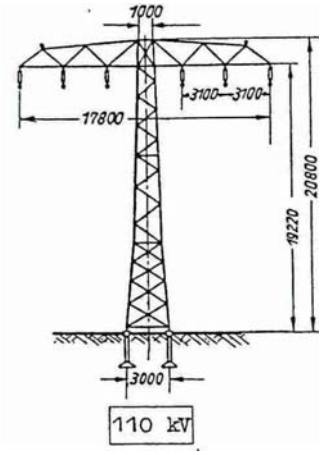	**Conductors:** 1 x Al/St 240/40 Outer diameter: 2.1 cm Inner diameter: 0.8 cm Resistance: 0.12 Ω/km **Ground wires:** 2 x St 50 Diameter: 0.9 cm Resistance: 3.6 Ω/km Minimum height at mid span 6 m
Voltage level:245 kV	
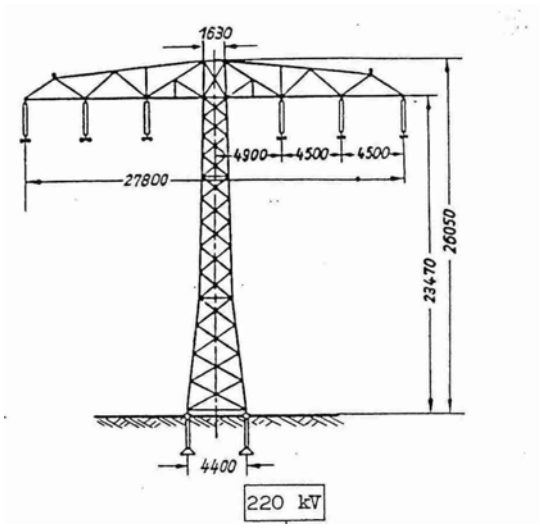	**Conductors:** 2 x Al/St 240/40 Space between conductors: 40 cm Outer diameter: 2.1 cm Inner diameter: 0.8 cm Resistance: 0.12 Ω/km **Ground wires:** 2 x Al/St 240/40 Outer diameter: 2.1 cm Inner diameter: 0.8 cm Resistance of one conductor: 0.12 Ω/km Minimum height at mid span 8 m

Voltage level 420 kV

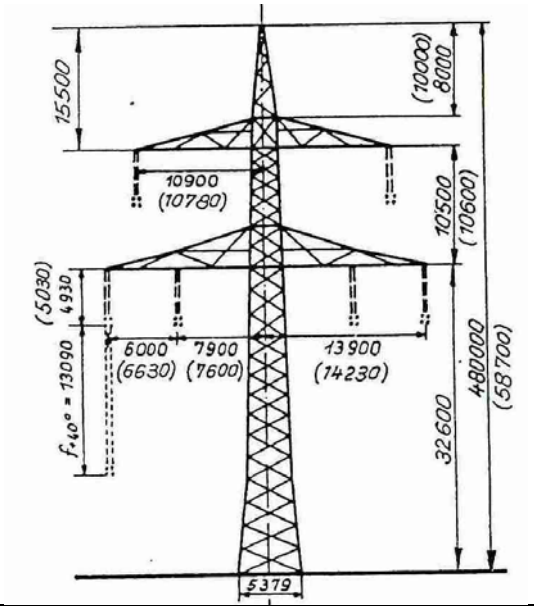

Conductors:
4 x Al/St 240/40
Space between conductors: 40 cm
Outer diameter: 2.1 cm
Inner diameter: 0.8 cm
Resistance of one conductor: 0.12 Ω/km

Ground wires:
1 x Al/St 240/40
Outer diameter: 2.1 cm
Inner diameter: 0.8 cm
Resistance: 0.12 Ω/km

Minimum height at mid span 8 m

ATP simulation results of 3-phase line faults

f_r = 50 Hz, Source TRV parameters: RRRV = 2.0 kV/µs, k_{af} = 1.4 p.u., k_{pp}= 1.5

U_r [kV]	I_{SC} [kA]	Line length [km]	Line TRV parameters for the first-pole-to-clear					TRV (line + source) of 1st peak of FPTC			di/dt	Z_L calculated
			u_0 [kV]	$\hat{U}_L$ [kV]	t_L [µs]	d [p.u.]	S_L [kV/µs]	u_p [kV]	t_{LS} [µs]	S_{LS} [kV/µs]	[A/µs]	[Ω]
145 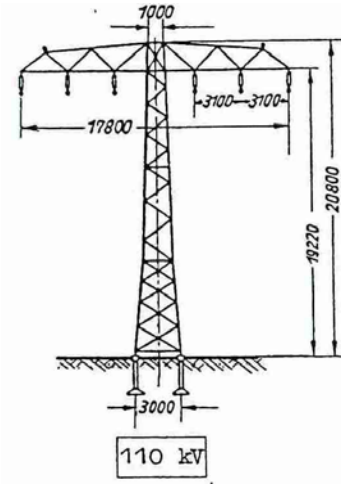	**I_{SC}= 100 % of the rated I_{SC}= 40 kA**											
	4.0 (L10)	46.0	102	-118	312	**2.16**	-0.71	270	312	0.87	1.76	401
	12.0 (L30)	12.0	82.0	-98.3	82	**2.20**	-2.20	228	82	2.78	5.33	413
	24.0 (L60)	3.6	47.2	-60.1	24	**2.27**	-4.47	135	24	5.62	10.7	418
	30.0 (L75)	1.8	29.5	-38.0	12	**2.29**	-5.63	85.3	12	7.11	13.3	423
	36.0 (L90)	0.6	11.7	-15.2	4.3	**2.30**	-6.67	34.3	4.3	8.24	16.0	417
	I_{SC}= 80 % of the rated I_{SC}= 32 kA											
	4.0 (L10)	44.5	99.5	-109	300	**2.10**	-0.70	277	300	0.92	1.78	393
	12.0 (L30)	10.5	70.4	-87.0	71	**2.24**	-2.22	223	71	3.14	5.33	416
	24.0 (L60)	2.3	30.1	-38.7	16	**2.29**	-4.41	97.4	16	6.09	10.7	412
	30.0 (L75)	0.42	6.9	-8.9	3.1	**2.29**	-5.71	22.8	3.1	7.16	13.3	429

Note: For 80% of the rated I_{SC}, L90 is not longer applicable

ATP simulation results of 3-phase line faults

f_r = 50 Hz, Source TRV paramerters: RRRV = 2.0 kV/µs, k_{af} = 1.4 p.u., X_0/X_1 = 1.0 (k_{pp} = 1.0)

U_r [kV]	I_{SC} [kA]	Line length [km]	Line TRV parameters for the first-pole-to-clear					TRV (line + source) of 1st peak of FPTC			di/dt [A/µs]	Z_L calculated [Ω]
			u_0 [kV]	$\hat{U}_L$ [kV]	t_L [µs]	d [p.u.]	S_L [kV/µs]	u_p [kV]	t_{LS} [µs]	S_{LS} [kV/µs]		
245	**I_{SC}= 100 % of the rated I_{SC}= 40 kA**											
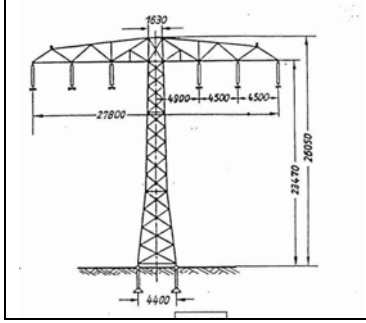	4.0 (L10)	114.8	173.8	-261.0	770	**2.50**	-0.56	462	770	0.60	1.80	311
	12.0 (L30)	29.1	135.7	-204.0	198	**2.50**	-1.72	426	198	2.15	4.76	360
	24.0 (L60)	8.55	79.7	-119.3	58.0	**2.50**	-3.40	271	58.0	4.57	10.34	328
	30.0 (L75)	4.20	49.6	-71.8	29.0	**2.45**	-4.22	165	29.0	5.73	13.33	317
	36.0 (L90)	1.67	19.9	-31.9	12.0	**2.60**	-4.69	72.2	12.0	6.02	16.00	293

ATP simulation results of 3-phase line faults

f_r = 50 Hz, Source TRV parameters: RRRV = 2.0 kV/µs, k_{af} = 1.4 p.u., X_0/X_1 = 1.0 (k_{pp}= 1.0)

U_r [kV]	I_{SC} [kA]	Line length [km]	Line TRV parameters for the first-pole-to-clear					TRV (line + source) of 1st peak of FPTC			di/dt [A/µs]	Z_L calculated [Ω]
			u_0 [kV]	$\hat{U}_L$ [kV]	t_L [µs]	d [p.u.]	S_L [kV/µs]	u_p [kV]	t_{LS} [µs]	S_{LS} [kV/µs]		
420 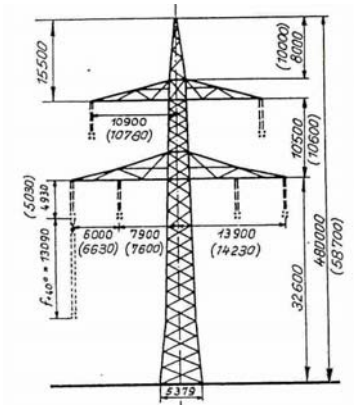	**I_{SC}= 100 % of the rated I_{SC}= 63 kA**											
	6.3 (L10)	136	307	-455	920	**2.48**	-0.83	788	920	0.85	2.81	295
	18.9 (L30)	35.5	240	-359	241	**2.50**	-2.49	727	241	3.02	8.40	296
	37.8 (L60)	10.2	137	-208	69	**2.52**	-5.00	429	69	6.21	16.8	298
	47.3 (L75)	5.1	85.5	-128	35	**2.47**	-6.04	265	35	7.57	21.0	287
	56.7 (L90)	1.7	34.4	-51.5	12	**2.50**	-7.16	107	12	8.91	25.2	284
	I_{SC}= 80 % of the rated I_{SC}= 50.4 kA											
	6.3 (L10)	132	298	-443	896	**2.49**	-0.83	782	896	0.87	2.80	295
	18.9 (L30)	31.5	211	-328	212	**2.55**	-2.54	710	212	3.35	8.40	303
	37.8 (L60)	6.4	84.4	-133	43	**2.57**	-5.06	300	43	7.00	16.8	300
	47.3 (L75)	1.28	21.6	-32.8	10	**2.51**	-6.15	75.1	10	8.33	21.0	293

Note: For 80% of the rated I_{SC}, L90 is not longer applicable

B2 Typical tower shapes of HV overhead lines in Canada

In the following pages, simulation results are presented for the Canadian 120, 161, 230, 315 and 735-kV overhead lines, while the impact of the variations in the source impedances (80% and 100%) is given for 230 kV. TRV parameters have been assessed for k_{pp} of 1.3 and 1.5.

<table>
<tr><td colspan="2">Voltage level: 120 kV</td></tr>
<tr><td>Single circuit line
(Dimensions in meters):
 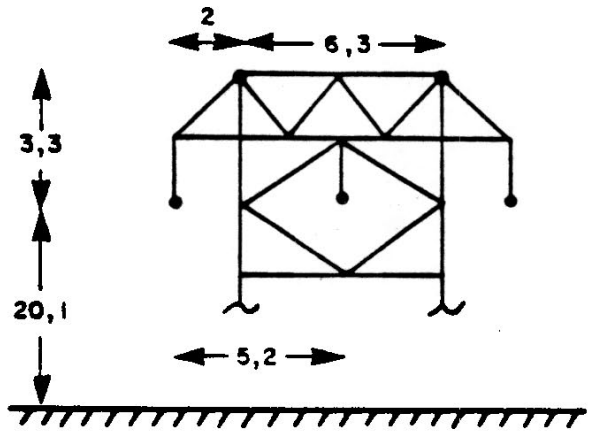
</td><td>Conductors:
One conductor per phase
DC resistance/conductor: 0.0741 Ω/km
Outside diameter: 2.774 cm

Ground wires:
DC resistance/conductor: 3.41 Ω/km
Outside diameter: 0.95 cm</td></tr>
<tr><td>Double circuit line
(Dimensions in meters):
 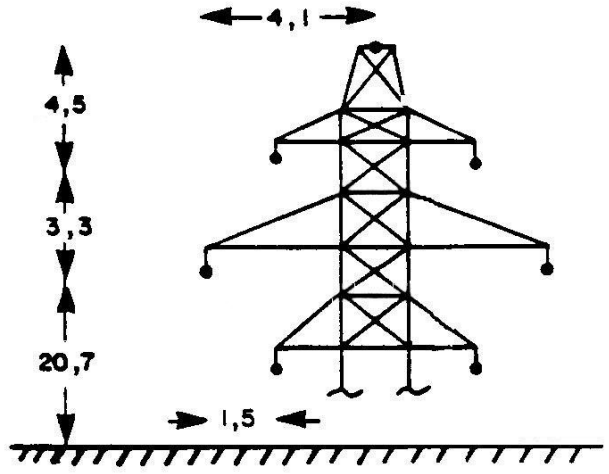
</td><td>Conductors:
One conductor per phase
DC resistance/conductor: 0.0741 Ω/km
Outside diameter: 2.774 cm

Ground wires:
DC resistance/conductor: 3.41 Ω/km
Outside diameter: 1.1 cm</td></tr>
</table>

Voltage level: 161 kV	
Single circuit line (Dimensions in meters): 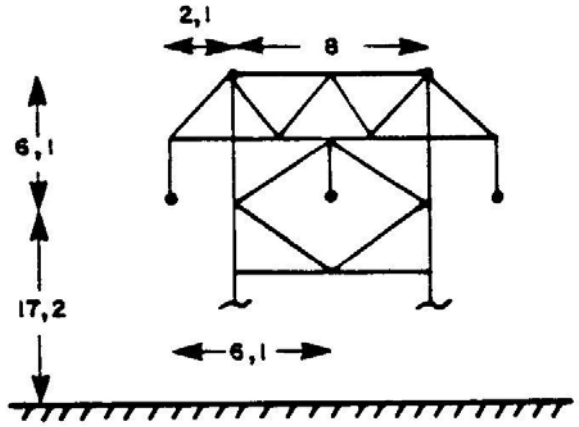 	**Conductors:** One conductor per phase DC resistance/conductor: 0.0741 Ω/km Outside diameter: 2.774 cm **Ground wires:** DC resistance/conductor: 4.20 Ω/km Outside diameter: 0.95 cm
Double circuit line (Dimensions in meters): 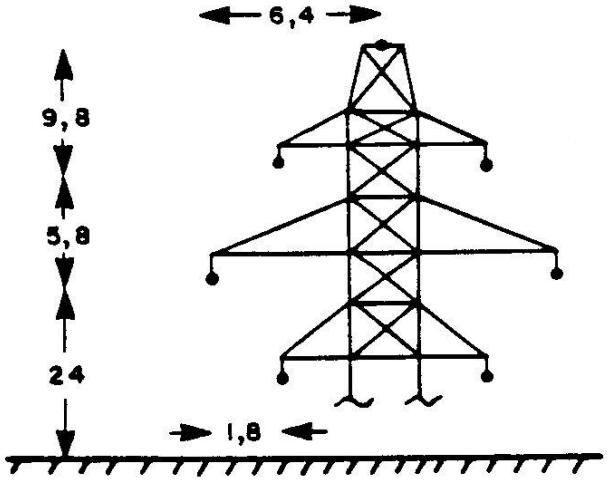 	**Conductors:** One conductor per phase DC resistance/conductor: 0.0741 Ω/km Outside diameter: 2.774 cm **Ground wires:** DC resistance/conductor: 3.41 Ω/km Outside diameter: 1.111 cm

Voltage level: 230 kV	
Single circuit line (Dimensions in meters): 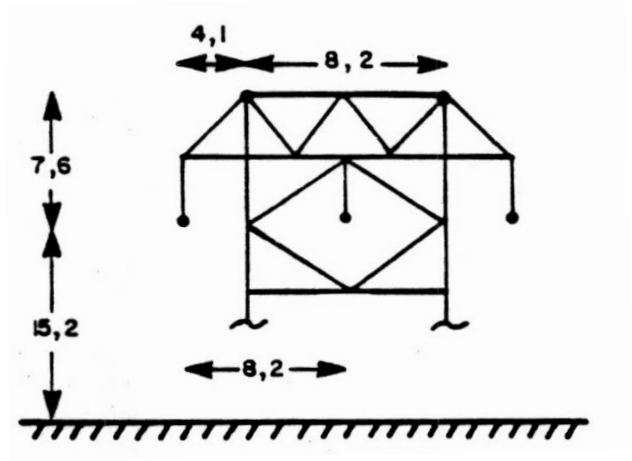 	**Conductors:** One conductor per phase DC resistance/conductor: 0.0574 Ω/km Outside diameter: 3.162 cm **Ground wires:** DC resistance/conductor: 4.20 Ω/km Outside diameter: 0.953 cm
Double circuit line (Dimensions in meters): 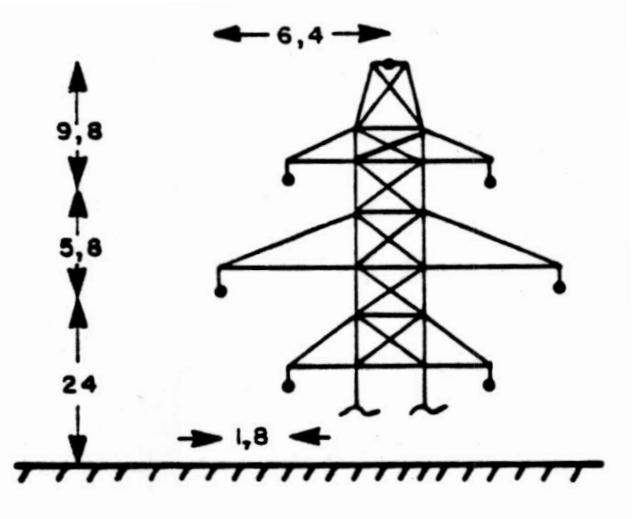 	**Conductors:** One conductor per phase DC resistance/conductor: 0.0574 Ω/km Outside diameter: 3.162 cm **Ground wires:** DC resistance/conductor: 3.41 Ω/km Outside diameter: 1.111 cm

<table>
<tr><td colspan="2">Voltage level: 315 kV</td></tr>
<tr><td><u>Single circuit line</u>
(Dimensions in meters):
 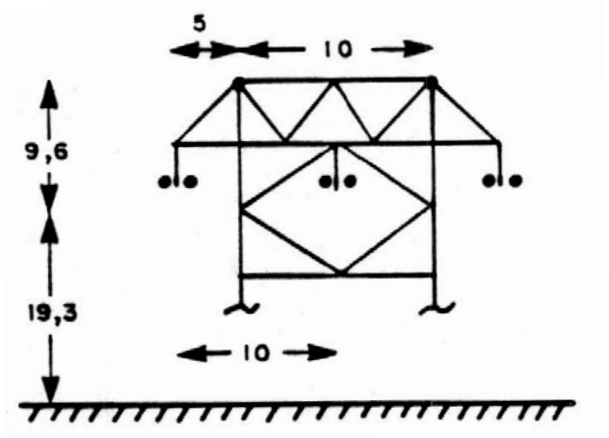
</td><td>Conductors:
Bundle of 2 conductors per phase
Bundle conductor distance: 41 cm
DC resistance/conductor: 0.0457 Ω/km
Outside diameter: 3.556 cm

Ground wires:
DC resistance/conductor: 3.41 Ω/km
Outside diameter: 1.111 cm</td></tr>
<tr><td><u>Double circuit line</u>
(Dimensions in meters):
 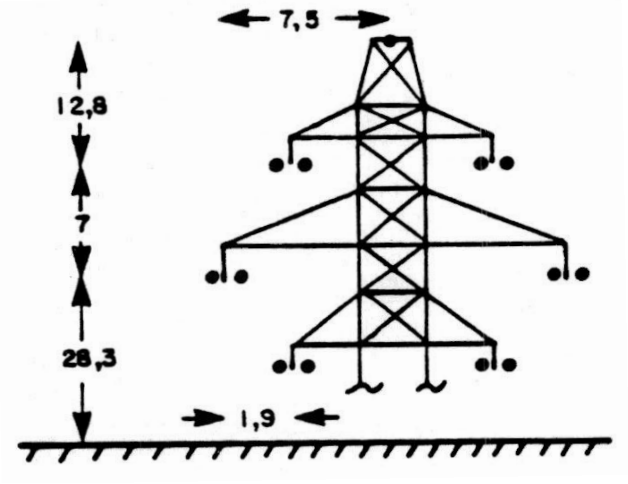
</td><td>Conductors:
Bundle of 2 conductors per phase
Bundle conductor distance: 41 cm
DC resistance/conductor: 0.0574 Ω/km
Outside diameter: 3.162 cm

Ground wires:
DC resistance/conductor: 3.41 Ω/km
Outside diameter: 1.111 cm</td></tr>
</table>

Voltage level: 735kV	
Rigid metallic tower (Dimensions in meters): 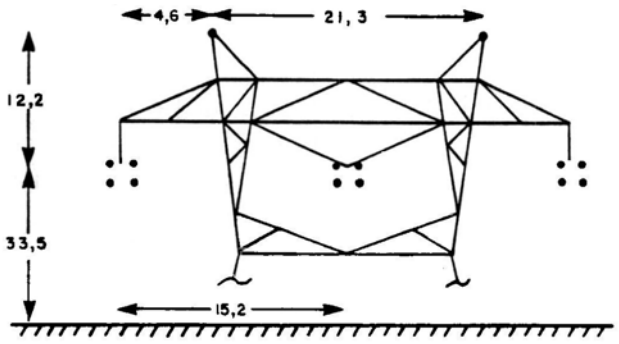 	**Conductors:** Bundle of 4 conductors per phase Bundle conductor distance: 46 cm DC resistance/conductor: 0.0457 Ω/km Outside diameter: 3.556 cm **Ground wires:** DC resistance/conductor: 3.41 Ω/km Outside diameter: 1.27 cm
Guyed metallic tower (Dimensions in meters): 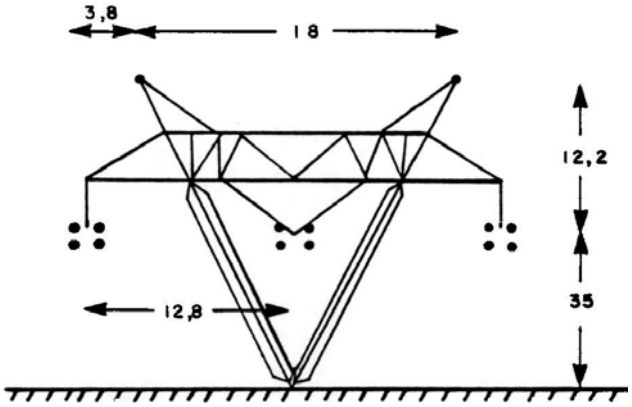 	**Conductors:** Bundle of 4 conductors per phase Bundle conductor distance: 46 cm DC resistance/conductor: 0.0457 Ω/km Outside diameter: 3.556 cm **Ground wires:** DC resistance/conductor: 3.41 Ω/km Outside diameter: 1.27 cm

EMTP simulation results of 3-phase line faults
f_r= 60 Hz, Source TRV parameters: RRRV = 2 kV/µs, K_{af} = 1.40

U_r [kV]	I_{SC} [kA]	Line length [km]	Line TRV parameters for the first-pole-to-clear					TRV (line + source) of 1st peak of FPTC			di/dt [A/µs]	Z_L calculated [Ω]
			u_0 [kV]	$\hat{U}_L$ [kV]	t_L [µs]	d [p.u.]	S_L [kV/µs]	u_p [kV]	t_{LS} [µs]	S_{LS} [kV/µs]		
120 kV (Single circuit line) 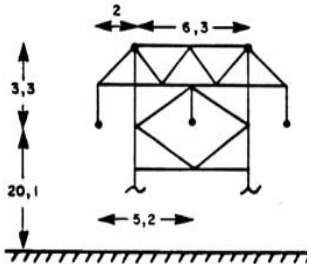	**I_{SC}= 100 % of the rated I_{SC}= 40 kA, k_{pp}= 1.5**											
	24 (L60)	2.566	39.37	-50.33	18.0	**2.28**	-5.23	108.88	18.2	6.29	12.79	410
	30 (L75)	1.283	24.63	-31.22	9.5	**2.27**	-6.52	67.79	9.7	7.77	15.99	408
	36(L90)	0.428	9.86	-12.29	3.7	**2.25**	-7.57	27.59	3.9	9.04	19.19	394
	38(L95)	0.203	4.93	-6.06	2.2	**2.23**	-7.15	14.40	2.3	8.64	20.25	353
	I_{SC}= 100 % of the rated I_{SC}= 40 kA, k_{pp}= 1.3											
	24 (L60)	2.566	39.21	-50.48	18.0	**2.29**	-5.23	109.60	18.3	6.33	12.79	409
	30 (L75)	1.283	24.57	-31.28	9.5	**2.27**	-6.52	68.31	9.7	7.82	15.99	408
	36(L90)	0.428	9.85	-12.28	3.7	**2.25**	-7.54	27.85	3.9	9.08	19.19	393
	38(L95)	0.203	4.93	-6.08	2.1	**2.23**	-7.09	14.59	2.3	8.75	20.25	350

EMTP simulation results of 3-phase line faults
f_r= 60 Hz, Source TRV parameters: RRRV = 2 kV/µs, K_{af} = 1.40

U_r [kV]	I_{SC} [kA]	Line length [km]	Line TRV parameters for the first-pole-to-clear					TRV (line + source) of 1st peak of FPTC			di/dt [A/µs]	Z_L calculated [Ω]
			u_0 [kV]	$\hat{U}_L$ [kV]	t_L [µs]	d [p.u.]	S_L [kV/µs]	u_p [kV]	t_{LS} [µs]	S_{LS} [kV/µs]		
120 kV (Double circuit line) 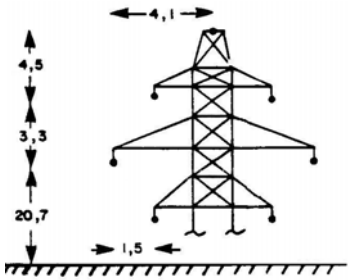	**I_{SC}= 100 % of the rated I_{SC}= 40 kA, k_{pp}= 1.5**											
	24 (L60)	2.671	38.93	-52.83	18.8	**2.36**	-5.13	107.15	19.1	5.93	12.79	401
	30 (L75)	1.339	24.41	-33.00	9.9	**2.35**	-6.40	67.30	10.1	7.36	15.99	400
	36(L90)	0.447	9.79	-13.15	3.9	**2.34**	-7.49	27.76	4.1	8.62	19.19	390
	38(L95)	0.211	4.88	-6.57	2.2	**2.35**	-7.23	14.64	2.5	8.41	20.25	357
	I_{SC}= 100 % of the rated I_{SC}= 40 kA, k_{pp}= 1.3											
	24 (L60)	2.655	38.59	-52.70	18.7	**2.37**	-5.14	107.12	19.0	5.97	12.79	402
	30 (L75)	1.331	24.23	-32.87	9.8	**2.36**	-6.41	67.32	10.1	7.40	15.99	401
	36(L90)	0.445	9.73	-13.10	3.9	**2.35**	-7.47	27.84	4.1	8.65	19.19	389
	38(L95)	0.211	4.88	-6.56	2.3	**2.34**	-7.10	14.77	2.5	8.43	20.25	351

EMTP simulation results of 3-phase line faults
f_r= 60 Hz, Source TRV parameters: RRRV = 2 kV/μs, K_{af} = 1.40

U_r [kV]	I_{SC} [kA]	Line length [km]	Line TRV parameters for the first-pole-to-clear					TRV (line + source) of 1st peak of FPTC			di/dt [A/μs]	Z_L calculated [Ω]
			u_0 [kV]	$\hat{U}_L$ [kV]	t_L [μs]	d [p.u.]	S_L [kV/μs]	u_p [kV]	t_{LS} [μs]	S_{LS} [kV/μs]		
161 kV (Single circuit line) 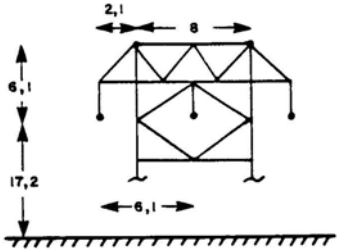	**I_{SC}= 100 % of the rated I_{SC}= 40 kA, k_{pp}= 1.5**											
	24 (L60)	3.371	53.43	-68.67	23.5	**2.29**	-5.42	146.94	23.7	6.47	12.79	424
	30 (L75)	1.686	33.45	-42.68	12.2	**2.28**	-6.75	91.45	12.4	8.00	15.99	422
	36(L90)	0.562	13.39	-16.80	4.6	**2.25**	-7.96	36.97	4.8	9.40	19.19	415
	38(L95)	0.266	6.68	-8.26	2.6	**2.24**	-7.78	19.04	2.8	9.36	20.25	384
	I_{SC}= 100 % of the rated I_{SC}= 40 kA, k_{pp}= 1.3											
	24 (L60)	3.347	52.82	-68.60	23.3	**2.30**	-5.43	147.01	23.6	6.52	12.79	425
	30 (L75)	1.674	33.12	-42.55	12.1	**2.28**	-6.76	91.54	12.3	8.06	15.99	423
	36(L90)	0.558	13.27	-16.69	4.6	**2.26**	-7.95	37.02	4.8	9.46	19.19	414
	38(L95)	0.264	6.65	-8.21	2.6	**2.23**	-7.81	19.11	2.8	9.46	20.25	386

EMTP simulation results of 3-phase line faults
f_r= 60 Hz, Source TRV parameters: RRRV = 2 kV/μs, K_{af} = 1.40

U_r [kV]	I_{SC} [kA]	Line length [km]	Line TRV parameters for the first-pole-to-clear					TRV (line + source) of 1st peak of FPTC			di/dt [A/μs]	Z_L calculated [Ω]
			u_0 [kV]	$\hat{U}_L$ [kV]	t_L [μs]	d [p.u.]	S_L [kV/μs]	u_p [kV]	t_{LS} [μs]	S_{LS} [kV/μs]		
161 kV (Double circuit line) 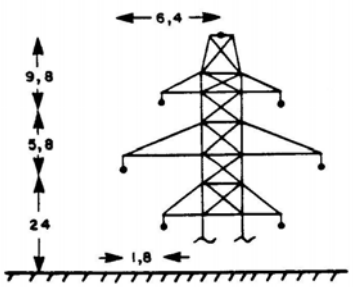	**I_{SC}= 100 % of the rated I_{SC}= 40 kA, k_{pp}= 1.5**											
	24 (L60)	3.324	51.83	-69.97	23.3	**2.35**	-5.48	140.89	23.6	6.26	12.79	428
	30 (L75)	1.664	32.37	-43.75	12.1	**2.35**	-6.83	88.23	12.3	7.79	15.99	427
	36(L90)	0.555	12.94	-17.39	4.7	**2.34**	-8.05	36.07	4.9	9.18	19.19	420
	38(L95)	0.263	6.50	-8.68	2.6	**2.34**	-7.93	18.86	2.9	9.17	20.25	392
	I_{SC}= 100 % of the rated I_{SC}= 40 kA, k_{pp}= 1.3											
	24 (L60)	3.313	51.64	-69.86	23.2	**2.35**	-5.48	141.14	23.5	6.31	12.79	428
	30 (L75)	1.659	32.37	-43.53	12.1	**2.34**	-6.83	88.44	12.4	7.83	15.99	427
	36(L90)	0.555	12.95	-17.42	4.6	**2.35**	-8.06	36.33	4.8	9.24	19.19	420
	38(L95)	0.263	6.50	-8.68	2.6	**2.34**	-7.90	19.03	2.9	9.22	20.25	390

EMTP simulation results of 3-phase line faults
f_r= 60 Hz, Source TRV parameters: RRRV = 2 kV/µs, K_{af} = 1.40

U_r [kV]	I_{SC} [kA]	Line length [km]	Line TRV parameters for the first-pole-to-clear					TRV (line + source) of 1st peak of FPTC			di/dt [A/µs]	Z_L calculated [Ω]
			u_0 [kV]	$\hat{U}_L$ [kV]	t_L [µs]	d [p.u.]	S_L [kV/µs]	u_p [kV]	t_{LS} [µs]	S_{LS} [kV/µs]		
230 kV (Single circuit line) 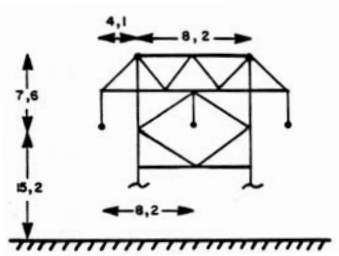	**I_{SC}= 100 % of the rated I_{SC}= 40 kA, k_{pp}= 1.5**											
	24 (L60)	4.698	76.15	-95.45	32.5	**2.25**	-5.46	205.86	32.8	6.52	12.79	427
	30 (L75)	2.349	47.61	-59.36	16.7	**2.25**	-6.80	127.86	16.9	8.05	15.99	425
	36(L90)	0.783	19.06	-23.35	6.2	**2.23**	-8.07	51.32	6.4	9.50	19.19	421
	38(L95)	0.371	9.53	-11.51	3.3	**2.21**	-8.06	26.18	3.5	9.68	20.25	398
	I_{SC}= 100 % of the rated I_{SC}= 40 kA, k_{pp}= 1.3											
	24 (L60)	4.674	75.49	-95.44	32.4	**2.26**	-5.47	206.27	32.7	6.56	12.79	428
	30 (L75)	2.337	47.26	-59.22	16.6	**2.25**	-6.81	128.15	16.9	8.10	15.99	426
	36(L90)	0.779	18.95	-23.26	6.1	**2.23**	-8.07	51.48	6.3	9.56	19.19	421
	38(L95)	0.369	9.48	-11.46	3.3	**2.21**	-8.14	26.30	3.5	9.75	20.25	402

EMTP simulation results of 3-phase line faults
f_r= 60 Hz, Source TRV parameters: RRRV = 2 kV/μs, K_{af} = 1.40

U_r [kV]	I_{SC} [kA]	Line length [km]	Line TRV parameters for the first-pole-to-clear					TRV (line + source) of 1st peak of FPTC			di/dt [A/μs]	Z_L calculated [Ω]
			u_0 [kV]	$\hat{U}_L$ [kV]	t_L [μs]	d [p.u.]	S_L [kV/μs]	u_p [kV]	t_{LS} [μs]	S_{LS} [kV/μs]		
230 kV (Double circuit line) 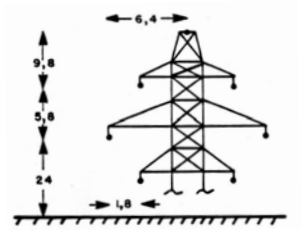	**I_{SC}= 100 % of the rated I_{SC}= 40 kA, k_{pp}= 1.5**											
	24 (L60)	4.818	68.77	-88.79	33.7	**2.29**	-4.85	182.00	34.1	5.56	12.79	379
	30 (L75)	2.412	45.83	-59.07	17.4	**2.29**	-6.43	120.92	17.7	7.32	15.99	402
	36(L90)	0.804	18.57	-24.72	6.3	**2.33**	-8.01	50.84	6.5	9.13	19.19	417
	38(L95)	0.381	9.29	-12.29	3.4	**2.32**	-8.06	26.16	3.7	9.35	20.25	398

EMTP simulation results of 3-phase line faults
f_r= 60 Hz, Source TRV parameters: RRRV = 2 kV/µs, K_{af} = 1.40

U_r [kV]	I_{SC} [kA]	Line length [km]	Line TRV parameters for the first-pole-to-clear					TRV (line + source) of 1st peak of FPTC			di/dt [A/µs]	Z_L calculated [Ω]
			u_0 [kV]	$\hat{U}_L$ [kV]	t_L [µs]	d [p.u.]	S_L [kV/µs]	u_p [kV]	t_{LS} [µs]	S_{LS} [kV/µs]		
230 kV (Double circuit line) 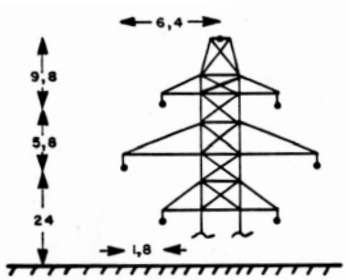	**I_{SC}= 100 % of the rated I_{SC}= 40 kA, k_{pp}= 1.3**											
	4 (L10)	46.000	110.27	-166.07	308.80	**2.51**	-0.90	319.40	309.3	1.16	2.13	423
	12 (L30)	12.800	92.30	-139.69	86.8	**2.51**	-2.71	**298.40 273.40**	**262.8 87.4**	3.21	6.40	423
	24 (L60)	4.799	73.86	-99.38	33.1	**2.35**	-5.40	201.03	33.5	6.23	12.79	422
	30 (L75)	2.403	46.25	-62.01	17.0	**2.34**	-6.73	125.67	17.3	7.72	15.99	421
	36(L90)	0.801	18.53	-24.59	6.3	**2.33**	-8.01	50.93	6.5	9.17	19.19	417
	I_{SC}= 80 % of the rated I_{SC}= 32 kA, k_{pp}= 1.3											
	12 (L10)	44.800	107.68	-161.73	300.95	**2.50**	0.90	316.30	301.8	1.04	2.13	423
	12 (L30)	11.740	84.41	-127.18	79.7	**2.51**	2.70	**305.30 264.20**	**240.7 80.8**	3.59	6.40	422
	24 (L60)	2.720	39.37	-58.93	19.2	**2.50**	5.40	121.8	19.7	6.58	12.79	422
	30 (L75)	0.595	10.74	-15.98	4.92	**2.49**	6.58	34.54	5.35	8.00	15.99	412

Note 1: For L30, two TRV coordinates are given: the second crest (highest peak) and the first crest (lower peak value)
Note 2: For 80% of the rated I_{SC}, L90 is not longer applicable

EMTP simulation results of 3-phase line faults
f_r= 60 Hz, Source TRV parameters: RRRV = 2 kV/µs, K_{af} = 1.40

U_r [kV]	I_{SC} [kA]	Line length [km]	Line TRV parameters for the first-pole-to-clear					TRV (line + source) of 1st peak of FPTC			di/dt [A/µs]	Z_L calculated [Ω]
			u_0 [kV]	$\hat{U}_L$ [kV]	t_L [µs]	d [p.u.]	S_L [kV/µs]	u_p [kV]	t_{LS} [µs]	S_{LS} [kV/µs]		
315 kV (Single circuit line) 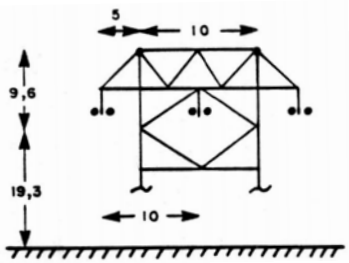	**I_{SC}= 100 % of the rated I_{SC}= 40 kA, k_{pp}= 1.5**											
	24 (L60)	8.716	105.23	-143.82	59.1	**2.37**	-4.28	312.80	59.6	5.37	12.79	335
	30 (L75)	4.358	65.79	-89.50	30.0	**2.36**	-5.34	193.28	30.3	6.60	15.99	334
	36(L90)	1.453	26.32	-35.43	10.4	**2.35**	-6.36	76.88	10.6	7.79	19.19	331
	38(L95)	0.688	13.16	-17.54	5.3	**2.33**	-6.62	38.73	5.5	8.15	20.25	327
	I_{SC}= 100 % of the rated I_{SC}= 40 kA, k_{pp}= 1.3											
	24 (L60)	8.656	103.83	-143.97	58.7	**2.39**	-4.29	313.66	59.2	5.42	12.79	335
	30 (L75)	4.328	65.06	-89.35	29.8	**2.37**	-5.34	193.35	30.1	6.67	15.99	334
	36(L90)	1.443	26.10	-35.31	10.3	**2.35**	-6.36	77.20	10.6	7.87	19.19	331
	38(L95)	0.684	13.06	-17.49	5.2	**2.34**	-6.67	38.97	5.4	8.23	20.25	329

EMTP simulation results of 3-phase line faults
f_r= 60 Hz, Source TRV parameters: RRRV = 2 kV/μs, K_{af} = 1.40

U_r [kV]	I_{SC} [kA]	Line length [km]	Line TRV parameters for the first-pole-to-clear					TRV (line + source) of 1st peak of FPTC			di/dt [A/μs]	Z_L calculated [Ω]
			u_0 [kV]	$\hat{U}_L$ [kV]	t_L [μs]	d [p.u.]	S_L [kV/μs]	u_p [kV]	t_{LS} [μs]	S_{LS} [kV/μs]		
315 kV (Double circuit line) 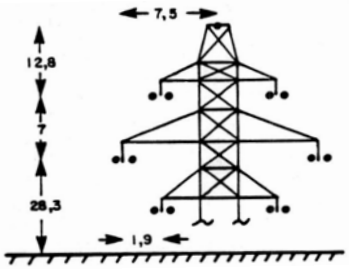	**I_{SC}= 100 % of the rated I_{SC}= 40 kA, k_{pp}= 1.5**											
	24 (L60)	8.833	100.53	-145.95	59.9	**2.45**	-4.18	292.76	60.4	4.95	12.79	327
	30 (L75)	4.421	62.89	-91.33	30.3	**2.45**	-5.22	182.43	30.7	6.13	15.99	327
	36(L90)	1.474	25.16	-36.43	10.6	**2.45**	-6.25	73.25	10.9	7.30	19.19	326
	38(L95)	0.698	12.51	-18.21	5.4	**2.46**	-6.53	37.17	5.7	7.66	20.25	322
	I_{SC}= 100 % of the rated I_{SC}= 40 kA, k_{pp}= 1.3											
	24 (L60)	8.790	99.80	-145.91	59.6	**2.46**	-4.19	293.23	60.1	4.98	12.79	328
	30 (L75)	4.400	62.52	-91.10	30.2	**2.46**	-5.22	182.75	30.6	6.17	15.99	327
	36(L90)	1.466	25.05	-36.28	10.5	**2.45**	-6.25	73.40	10.8	7.34	19.19	326
	38(L95)	0.695	12.52	-18.42	5.4	**2.47**	-6.65	39.54	5.6	8.21	20.25	328

EMTP simulation results of 3-phase line faults
f_r= 60 Hz, Source TRV parameters: RRRV = 2 kV/μs, K_{af} = 1.40

U_r [kV]	I_{SC} [kA]	Line length [km]	Line TRV parameters for the first-pole-to-clear					TRV (line + source) of 1st peak of FPTC			di/dt [A/μs]	Z_L calculated [Ω]
			u_0 [kV]	$\hat{U}_L$ [kV]	t_L [μs]	d [p.u.]	S_L [kV/μs]	u_p [kV]	t_{LS} [μs]	S_{LS} [kV/μs]		
735 kV (Rigid metallic tower) 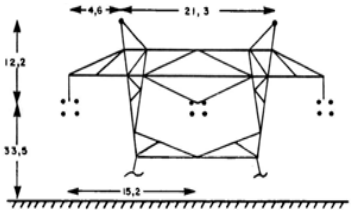	**I_{SC}= 100 % of the rated I_{SC}= 40 kA, k_{pp}= 1.3**											
	24 (L60)	23.155	246.16	-353.50	155.3	**2.44**	-3.89	774.73	156.0	5.03	12.79	304
	30 (L75)	11.578	154.52	-218.65	78.1	**2.42**	-4.83	477.28	78.5	6.17	15.99	302
	36(L90)	3.860	62.09	-86.24	26.5	**2.39**	-5.76	188.40	26.8	7.26	19.19	300
	38(L95)	1.829	31.11	-42.77	12.9	**2.38**	-6.05	94.14	13.1	7.61	20.25	299
735 kV (Guyed metallic tower) 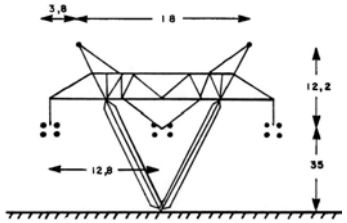	**I_{SC}= 100 % of the rated I_{SC}= 40 kA, k_{pp}= 1.3**											
	24 (L60)	24.175	246.14	-365.20	162.1	**2.48**	-3.80	794.27	162.7	4.94	12.79	297
	30 (L75)	12.088	154.48	-226.24	81.5	**2.46**	-4.72	489.55	81.9	6.06	15.99	295
	36(L90)	4.030	62.10	-89.25	27.6	**2.44**	-5.63	193.14	27.9	7.13	19.19	293
	38(L95)	1.909	31.11	-44.26	13.4	**2.42**	-5.92	96.45	13.6	7.47	20.25	292

Appendix C: Driving influences of ground resistivity on the d factor in the case of single-phase line fault

High-Level Summary of Takeaways

- It was demonstrated in ATP analysis that the ground resistivity, through its impact on the self and mutual impedance of the transmission line, has a significant impact on the d-factor.
- Through simulation, it was shown that d-factors greater or lower than 1.6 can be obtained by varying the ground resistivity.
- Power-point animations were created for single-phase short-line faults (SLF) for comparison of those to be constructed for the three-phase line fault case.

Description of Analysis

Based on the minutes of the last CIGRE WG A3.19 meeting in Zurich, Switzerland, there is a need to obtain animations of travelling waves initiated by both single-line-to-ground faults (SLGF) and three-phase grounded faults (3PGF). The focus is to monitor travelling waves for SLGF and 3PGF and the impacts on the resulting amplitude factor (d-factor).

The purpose of the analysis described here is to examine the driving phenomena for traveling waves associated with SLGF for comparison to travelling waves associated with 3PGF. This analysis will also serve as a basis for the next phase of the CIGRE WG analysis, which involves creating animated plots of travelling waves for 3PGF, similar to the animation for SLGF that can be found in references [i] and [ii] and included power-point files "SLF_1P_ANIM_001.ppt" and "SLF_1P_ANIM_001a.ppt" constructed in parallel with this memo. This analysis also provides description for the impacts of ground resistivity on the self and mutual impedances of a transmission line and thereby the travelling waves associated with a SLGF through use of the Alternative Transients Program (ATP).

Figure C1 shows that for SLGF, the travelling voltage waves on the line-side of the circuit-breaker exhibit the highest d-factor for simulations with a near zero ground resistivity for the transmission line (note lowest ground resistivity of 0.1 μΩ-m examined here), whereas for increasing ground resistivities, the d-factor decreases. A near zero ground resistivity minimizes Carson's earth-return correction factor added to the self and mutual impedances of the transmission line. For the near-zero ground resistivity case, the d-factor was 1.96 (nearly 2.0) and for the case with a ground resistivity of 10.0 Ω-m, the d-factor was 1.625, which is close to the d-factor of 1.6 recommended by ANSI/IEEE Standards [iii]. This can also be learnt from the formula $\mathbf{d = 0.4\{2+L_L0(hf)/L_L1(lf)\}}$, where for near-zero ground resistivity $\mathbf{L_L0(hf)}$ is equal to $\mathbf{L_L0(lf)}$ and thus about 3-times larger than $\mathbf{L_L1(lf)}$ and for higher resistivities the ratio tends towards 2-times $\mathbf{L_L1(lf)}$, as $\mathbf{L_L1(lf)}$ increases. Figure C1 shows the formula used to calculate the d-factor, based on the initial peak and the 1st peak of the line-side voltage component at the circuit-breaker terminals. All parameters for the simulations (Fig. C1) were held constant except for the ground resistivity. Because of the different ground resistivities examined, the line length was changed to tune the fault current to within ~1 % of 90% SLF current, and with increasing ground resistivities the current zero was shifted, causing the line-side voltage components to be initiated at different instances in time driven by the ground resistivity, degree of tuning, and line length. It was determined by simulation that this tuning had a negligible impact on the resulting d-factor.

Figure C2 shows the ATP circuit used for the simulation of the waves in Fig. C1. The circuit in Fig. C1 has the following parameters:

- 550 kV 50 kA rated source at 100%
- $X_0/X_1 = 1.0$
- Phase A opening time: 10 ms, Phase B/C opening time: 15 ms
- 90% SLF corresponding to line length of 0.9 mi for $\rho = 1.0$ Ω-m applied at $t = 0^-$

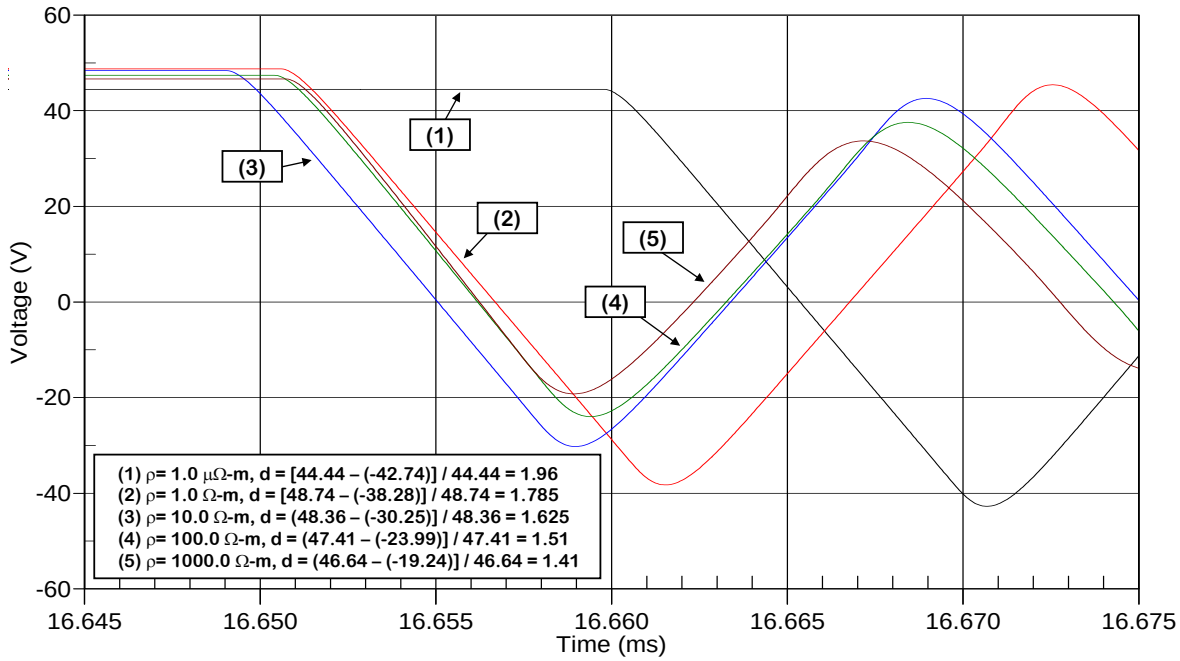

Figure C1. Line-side voltage components at circuit-breaker terminals and d-factors for various ground resistivities from 1.0 μΩ-m to 1000 Ω-m.

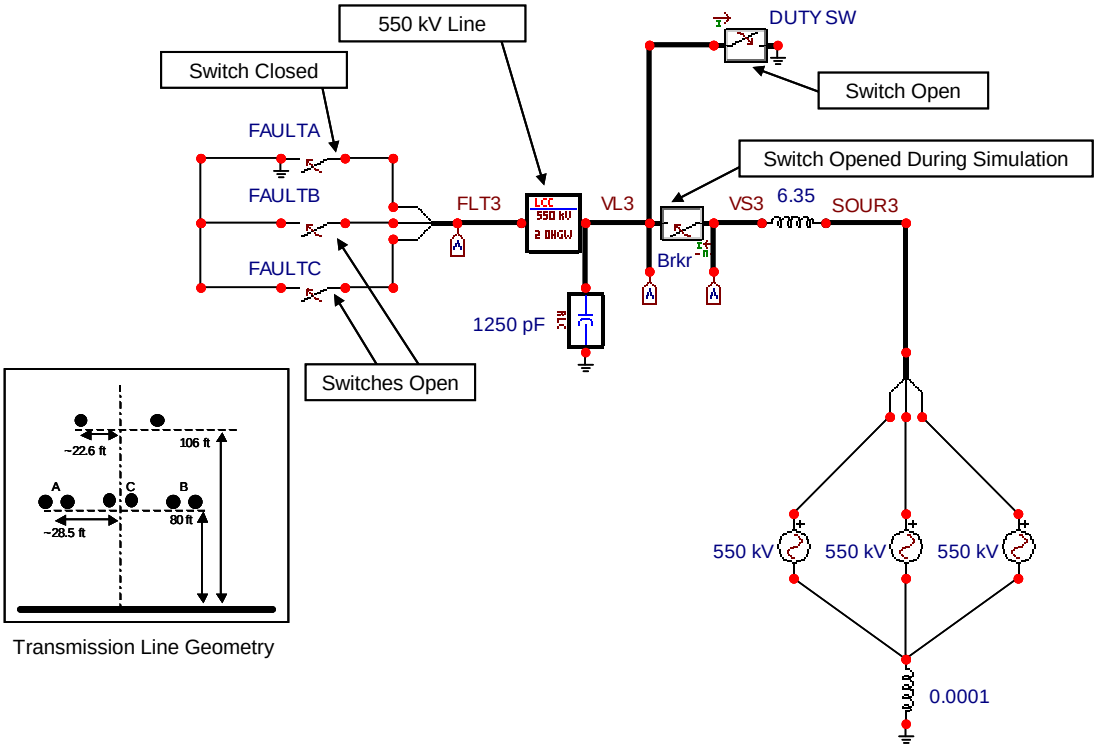

Figure C2. ATP circuit used to obtain voltage waves shown in Fig. C1.

Based on the voltage waves shown in Fig. C1, for ground resistivities ranging from 1.0 μΩ-m to 1000.0 Ω-m, it is evident that the ground resistivity plays a major role in the d-factor for short-line fault (SLF) phenomena.

A wide-range of ground resistivities was examined here for tutorial purposes. The following lists typical ranges for actual ground resistivities based on reference [ii]:

- General average: $\rho = 100$ Ω-m
- Sea water: $\rho = 0.01\text{-}1.0$ Ω-m
- Swampy ground: $\rho = 10\text{-}100$ Ω-m
- Dry earth: $\rho = 1000$ Ω-m
- Pure slate: $\rho = 10^7$ Ω-m
- Sandstone $\rho = 10^8$ Ω-m

Reference [iv] also provides information on the typical resistivity of common soil types, listed as follows:

- Filled land, ashes, and salt marsh
  - Average: 24 Ω-m
  - Minimum: 6 Ω-m
  - Maximum: 70 Ω-m
- Top soils, loam
  - Average: 41 Ω-m
  - Minimum: 3.4 Ω-m
  - Maximum: 160 Ω-m
- Hybrid soils
  - Average: 60 Ω-m
  - Minimum: 10 Ω-m
  - Maximum: 1350 Ω-m
- Sand and gravel
  - Average: 900 Ω-m
  - Minimum: 600 Ω-m
  - Maximum: 4600 Ω-m

To provide more insight into the driving phenomena for the d-factor from a travelling wave point-of-view, the transmission line in Fig. C2 was divided into 10 equal sections to allow monitoring of the travelling voltage wave as the wave travelled along the line. For each case, the length of each line section was 1/10 of the total line length from the original case. Figure C3 shows the resulting line-side voltage components at each 1/10 increment, where the initial peak voltage at the circuit-breaker terminals can be traced along the transmission line to the short-circuit. It can be observed that the negative peak reaches a much lesser negative peak magnitude for the $\rho = 10.0$ Ω-m compared to the case where $\rho = 0.1$ μΩ-m. Note that for clarity reasons the red curves for $\rho = 10.0$ Ω-m are shifted in time with respect to the black curves, that belong to $\rho = 0.1$ μΩ-m. Further the red TRV curves have a similar waveshape as the black curves, as stressed by the remark in the figure C3.

It was observed that for cases with the transmission line divided into 10 equal sections compared to cases with the transmission line modelled as 1-section for ground resistivities of 0.1 μΩ-m and 1.0 μΩ-m, the d-factor for the cases with the transmission line divided into 10 equal sections was less than for cases with the transmission line modelled as 1-section (e.g.,

1.91 compared to 1.96). The opposite trend was observed for cases with higher ground resistivities (i.e., 1.0 Ω-m to 1000 Ω-m), where the d-factor increased (by ~3-5%) for the cases with 10 equal sections compared to cases with the transmission line modelled as 1-section for the same ground resistivity. Figure C4 shows an example for comparison of cases for ρ = 0.1 μΩ-m/section for 10 sections and ρ = 0.1 μΩ-m for 1-section. Most probably this phenomenon is related to the simulation model and not to physical parameters in real life.

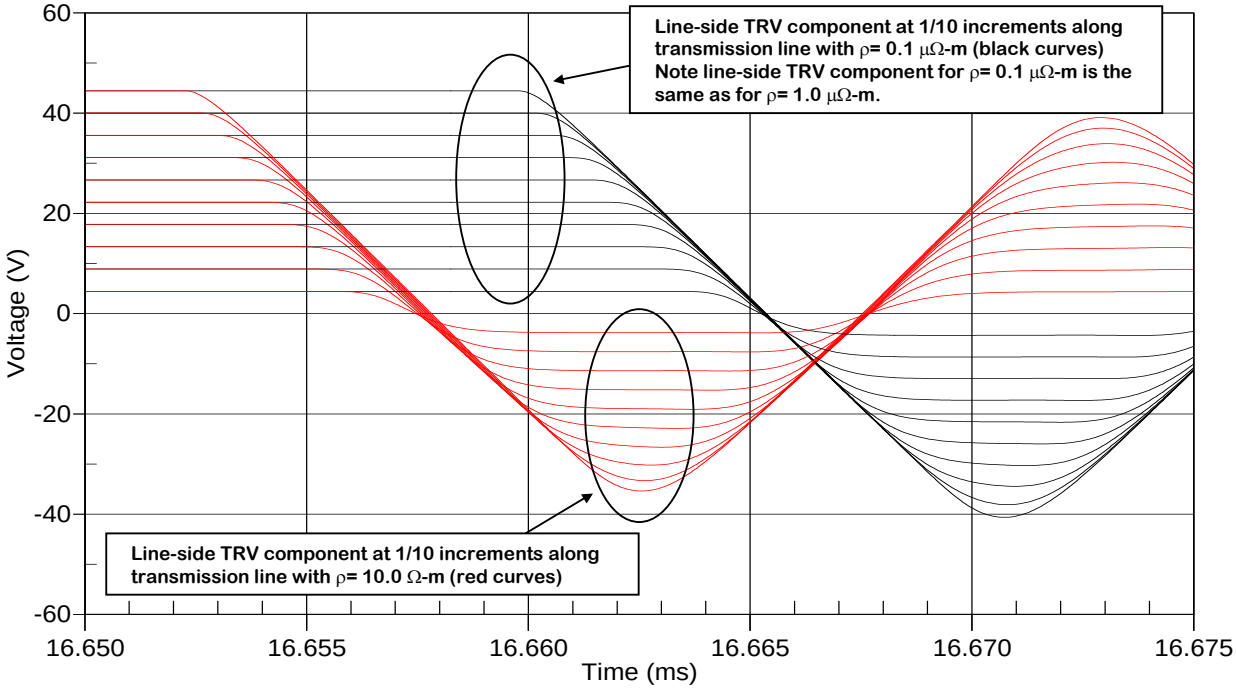

Figure C3. Simulation results for cases with the transmission line divided into 10 equal sections for ρ = 0.1 μΩ-m and ρ = 10.0 Ω-m with fault current tuned to 45.0 kA RMS.

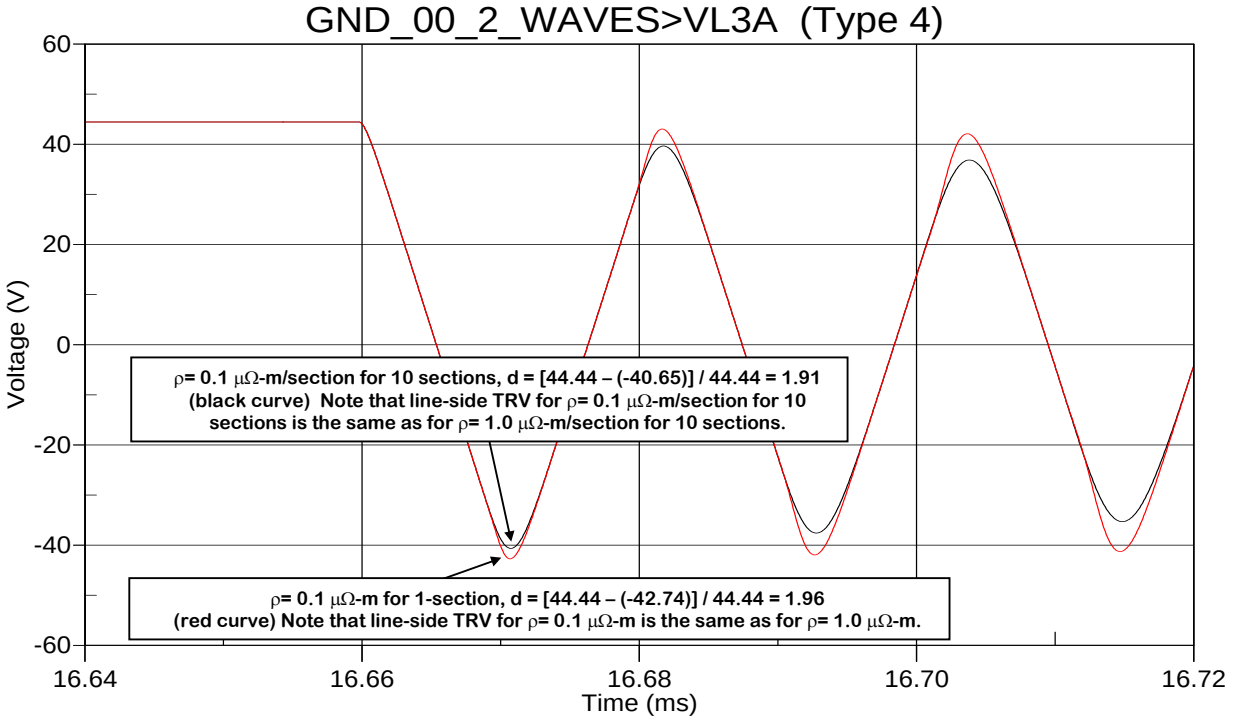

FigureC4. Simulation results for cases with ρ = 0.1 μΩ-m/section for 10 sections (d-factor = 1.91) and with ρ = 0.1 μΩ for 1-section of line (d-factor = 1.96).

In an attempt to determine where the energy from the traveling wave is going, causing the varying d-factors for the ground resistivities examined in Fig. C1, sensitivity cases were simulated as summarized in Table C1. Table C1 lists the d-factor associated with phase A at the line-side of the circuit-breaker observed for each sensitivity case. Figures C5 and C6 show diagrams of the key sensitivities listed in Table C1. Note that sensitivity cases were performed with phase B and phase C of the circuit-breaker opened throughout the entire simulation, and a few cases were simulated to verify that the results did not change with the circuit-breaker initially closed and phases B and C opening after phase A.

The impacts of the effects of coupling between the phases and shielding wires and the faulted phase were bounded through the magnitude of the resulting d-factor. The following lists observations based on interpretation of the results listed in Table 1 with respect to the impacts of moving the phase conductors and shield wires either vertically and/or horizontally about the original electro-geometric configuration:

- Overall, it was observed that "tighter" horizontal line configurations resulted in lower d-factors than "wider" line configurations. Also, shorter vertical line configurations resulted in lower d-factors than higher vertical line configurations.
- It was observed that the electro-geometric configuration (e.g., vertical or horizontal spacing of the phase conductors and shield wires) of the transmission line could cause at most a 3 to 5% increase in the d-factors in addition to the effects of the ground resistivity on the d-factor.
    - Higher ground resistivities cause the electro-geometric configuration to have a greater impact on the d-factor.
    - For cases with ground resistivities near zero (e.g., 0.1 μΩ-m and 1.0 μΩ-m examined here), changes to the electro-geometric configuration had a negligible impact on the d-factor.
    - Changes to the vertical spacing had similar effects compared to changes to the horizontal spacing.
- It was observed that the location of the shield wires relative to the position of each phase conductor impact the d-factor.
    - When the phase conductors were moved without the shield wires, the d-factor did not vary significantly, and decreased a few percent for each case for ρ = 1.0 Ω or greater.
    - When the phase conductors were moved with the shield wire, the d-factor increased by a few to approximately 5%.

The following are the overall observations based on the analysis:

- For conditions with a near zero ground resistivity (ρ = 0.1 μΩ-m or ρ = 1.0 μΩ-m), the d-factor was observed to be near its theoretical maximum of 2.0.
- It was observed that for the range of ground resistivities examined, which was 0.1 μΩ-m to 1000 Ω-m, the d-factor varied from near 2.0 to 1.4.
    - For a range of ground resistivities from 1.0 Ω-m to 100 Ω-m, the d-factor varied from 1.5 to 1.8.
    - It was observed that the electro-geometric configuration (e.g., vertical or horizontal spacing of phase conductors and shield wires) of the transmission line could cause at most a 3 to 5% increase in the d-factors in addition to the effects of the ground resistivity.

- The ground resistivity appears to have a first-order effect on the traveling waves, causing d-factors ranging from near 2.0 to 1.4 at the line-side of the circuit-breaker for ground resistivities of ρ = 0.1 $\mu\Omega$-m to 1000 Ω-m.
- For a near zero ground resistivity (e.g., ρ = 0.1 $\mu\Omega$-m or ρ = 1.0 $\mu\Omega$-m), changes in the electro-geomagnetic characteristics of the transmission line do not significantly impact the d-factor, which is almost 2.0 for near zero ground resistivity cases.

Takeaways

- It was demonstrated in ATP analysis that the ground resistivity, through its impact on the self and mutual impedance of the transmission line, has a significant impact on the d-factor. Refer to the next subsection for more information on the impacts of changes in the ground resistivity on the self and mutual impedance of a transmission line through ATP simulation.
    - Decreased (or increased) ground resistivity causes decreased (or increased) self and mutual impedance and correspondingly increased (or decreased) d-factor. Thus, the d-factor has an inverse proportional relationship to the ground resistivity.
        - It is anticipated that the decreased (or increased) self and mutual impedance impacts the d-factor in two ways in ATP simulation:
            - Changes standard linear distribution of charge at breaker opening where maximum is at breaker terminals and minimum is at fault by increasing (or decreasing) the self and mutual impedance of the circuit. Thus, traveling wave components no longer solely bounce between an open and short-circuit, and are increasingly (or decreasingly) influenced by self (i.e., physically, driven by location of conductor and characteristics of ground and shield wires) and mutual impedance (i.e., physically, driven by location of conductor and characteristics of ground and shield wires, and location and characteristics of other phase conductors) through Carson's earth-return correction factor.
            - Decreased (or increased) modal characteristic surge impedance, primarily for mode 0.
            - Further investigation may be warranted to determine the extent of each of the effects described above. This analysis concentrated on the combined effects and impacts on d-factor.
- Through simulation, it was shown that d-factors greater or lower than 1.6 can be obtained by varying the ground resistivity.

The next subsection provides background on applicable assumptions for Carson's theory, a description of the behavior of traveling waves taken from reference [ii], and Carson's earth-return correction equations for reference purposes along with above takeaways.

Description of Impacts of Ground Resistivity on Traveling Wave Phenomena

This subsection provides a description of the impact of ground resistivity on traveling wave phenomena through ATP simulation, which can account for the impact of different ground resistivities on self and mutual impedances of a transmission line through a method based on Carson's earth-return correction equations [v]. It should be noted that Carson's formula is based on the following assumptions as described in reference [v], where error can be introduced when not all of the assumptions are met fully:

(a) The conductors are perfectly horizontal above ground, and are long enough so that three-dimensional effects can be neglected (this makes the field problem two-dimensional). The sag is taken into account indirectly by using an average height above ground.

(b) The aerial space is homogeneous without loss, with permeability μ_0 and permittivity ε_0.

(c) The earth is homogeneous with uniform resistivity ρ, permeability μ_0 and permittivity ε_0, and is bounded by a flat plane with infinite extent, to which the conductors are parallel. The earth behaves as a conductor, i.e., $1/\rho >> w\varepsilon_0$, and hence the displacement current may be neglected. Above the critical frequency $f_{critical} = 1/(2\pi\varepsilon_0\rho)$, other formulas must be used (for ρ = 10 000 Ω-m in rocky ground, $f_{critical}$ = 1.8 MHz, which is still on the high side for most EMTP line models).

(d) The spacing between conductors is at least one order of magnitude larger than the radius of the conductors, so that proximity effects (current distribution within one conductor influenced by current in an adjacent conductor) can be ignored.

Thus, it must be remembered that the ground resistivity in ATP/EMTP employs correction factors to the self and mutual impedances, based on certain assumptions and estimations, and are not meant to be an exact representation of the ground plane and its impacts.

Reference [ii] describes short-line faults as follows:

> *"At current zero, when the circuit-breaker interrupts, the generated voltage will be near its peak. Therefore the line, now served from the system, momentarily has on it a charge distribution which is a maximum at the circuit-breaker and declines more or less linearly to zero at the fault. It was shown in Section 9.2 that an unbound distribution of charge on a line will not remain static but will travel, or attempt to do so, in both directions along the line. In this particular instance the charge is somewhat confined, in that a travelling wave cannot proceed into the source since it is blocked by the open circuit-breaker, nor can the charge propagate as a wave beyond the fault, assuming that the fault is a short circuit…"*

The impact of the ground resistivity on the phenomena described above is accounted for in ATP/EMTP through its impact on the self and mutual impedances of the transmission line. Examination of Carson's earth-return correction equations below provides a basic understanding for these impacts:

$$L_{ii-e} = \frac{\mu_0}{2\pi}\ln\frac{1}{GMR_i} + \frac{L_e}{3}[H/m] \qquad (1)$$

$$\mathrm{L_{ij\text{-}e}} = \frac{\mu_0}{2\pi}\ln\frac{1}{d_{ij}} + \frac{L_e}{3}[H/m] \qquad (2)$$

with :

$$\frac{L_e}{3} = \frac{\mu_0}{2\pi}\ln(85.06\sqrt{\rho_3}\,[H/m] \qquad (3)$$

Example for $\rho = 100\,\Omega\mathrm{m}$:

$$\frac{L_e}{3} = 0.2 \text{ x } \ln 850.6 = 1.3492\,[uH/m]$$

The equations above show that the self and mutual impedance is proportionally related to the ground resistivity. An increase (or decrease) in the ground resistivity will lead to an increase (or decrease) in the self and mutual impedance of the transmission line. Attached is an example of 500 kV transmission line input data and output parameters for a case where $\rho = 1$ and $\rho = 1000$ for reference purposes, illustrating the change in the phase matrices and modal parameters driven by the ground resistivity.

REFERENCES

[i] R.W. Alexander, D. Dufournet, "Tutorial on Transient Recovery Voltage (TRV) for High-Voltage Circuit-breakers."

[ii] Allan Greenwood, *Electrical Transients in Power Systems*, 2nd Ed., John Wiley and Sons, Inc., New York: 1991, pp. 265, 478.

[iii] IEEE Std C37.04-200x "IEEE Standard Rating Structure for AC High-Voltage Circuit-breakers" (draft) as referenced in IEEE PC37.011/D15 (draft).

[iv] Richard C. Dorf, *CRC Handbook of Engineering Tables*, CRC Press, Boca Raton: 2004, p. 1-8.

[v] Electromagnetic Transients Program Reference Manual (EMTP Theory Book) prepared by Hermann W. Dommel, August 1986.

Table C1- d-factor for various sensitivities on transmission line electro-geometric configurations

	Base Sensitivities						Other Sensitivities Performed For Reference							
	Base-Case	*Case 0*	*Case 1-a*	*Case 1-b*	*Case 1-c*	*Case 1-d*	*Case 1*	*Case 2*	*Case 3*	*Case 4*	*Case 5*	*Case 6*	*Case 7*	*Case 8*
Resistivity	**D-Factor Given Electro-Geometric Configuration**	**D-Factor Given Configuarion Length Modeled in 10 Sections**	**D-Factor B/C Phase Conductor & Shield Wires Spacing Halved (Horizontal)**	**D-Factor B/C Phase Conductor & Shield Wires Spacing Halved (Horizontal) Vertical Spacing Reduced by 1.6x**	**D-Factor B/C Phase Conductor & Shield Wires Spacing Doubled (Horizontal)**	**D-Factor A/B/C Phase Conductor & Shield Wires +50 ft (Vertical)**	**D-Factor B/C Phase Conductor +50 ft (Horizontal)**	**D-Factor B/C Phase Conductor & Shield Wires +50 ft (Horizontal)**	**D-Factor B/C Phase Conductor +200 ft (Horizontal)**	**D-Factor B/C Phase Conductor & Shield Wires +200 ft (Horizontal)**	**D-Factor B/C Phase Conductor +1000 ft (Horizontal)**	**D-Factor B/C Phase Conductor & Shield Wires +1000 ft (Horizontal)**	**D-Factor A/B/C Phase Conductor & Shield Wires +500 ft (Vertical)**	**D-Factor B/C Phase Conductor & Shield Wires +500 ft (Vertical)**
0.1 μΩ-m	1.96	1.91	1.95	1.95	1.97	1.96	1.98	1.97	1.975	1.975	1.975	1.975	1.96	1.97
1.0 μΩ-m	1.96	1.91	1.95	1.95	1.97	1.96	1.98	1.97	1.975	1.975	1.975	1.975	1.96	1.97
1.0 Ω-m	1.785	1.80	1.81	1.74	1.80	1.855	1.76	1.85	1.76	1.86	1.81	1.81	1.94	1.85
10.0 Ω-m	1.625	1.72	1.63	1.565	1.63	1.72	1.60	1.695	1.56	1.72	1.67	1.66	1.90	1.725
100.0 Ω-m	1.51	1.56	1.52	1.38	1.43	1.58	1.44	1.56	1.48	1.79	1.51	1.55	1.80	1.73
1000.0 Ω-m	1.41	1.50	1.46	1.40	1.41	1.50	1.40	1.46	1.35	1.61	1.45	1.58	1.68	1.61

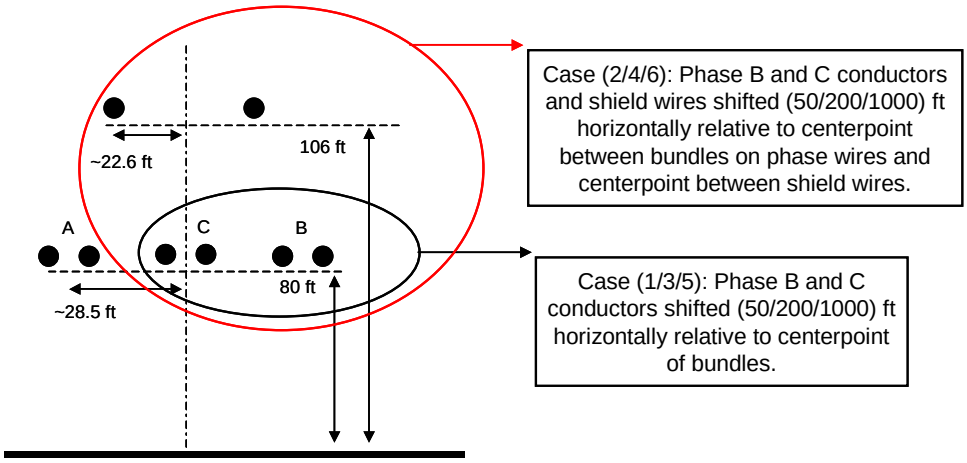

Figure C5. Diagram for Cases 1 through 6.

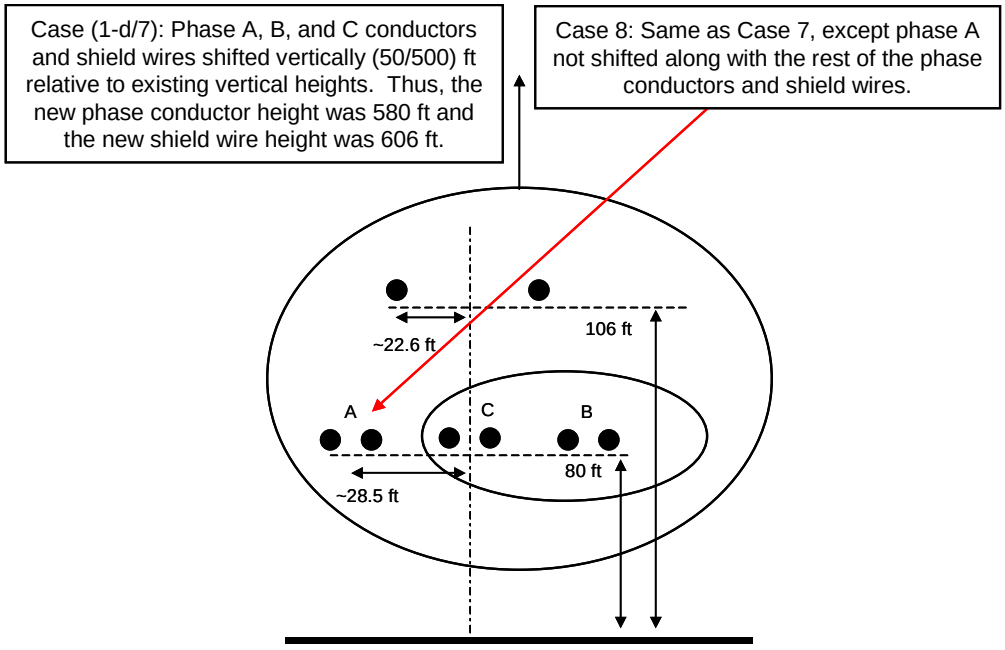

Figure C6. Diagram for Cases 1-d, 7, and 8.